

**VEGF FAMILY MEMBERS –
MODULATORS OF
TUMOR ANGIOGENESIS AND LYMPHANGIOGENESIS**

Inauguraldissertation

zur

Erlangung der Würde eines Doktors der Philosophie
vorgelegt der
Philosophisch-Naturwissenschaftlichen Fakultät
der Universität Basel

von

Lucie Kopfstein
aus Freienbach SZ

Basel, 2006

Genehmigt von der Philosophisch-Naturwissenschaftlichen Fakultät
auf Antrag von Prof. G. Christofori, Prof. C. Rüegg, Prof. C. Dehio

Basel, den 2.5.2006

Prof. Dr. Hans-Peter Hauri

The Median Isn't The Message
Stephen Jay Gould

Table of Contents

Table of Contents	I
List of Figures	IV
List of Tables	VI
Zusammenfassung	1
Summary	3
1. General Introduction	6
1.1. The two vascular systems	6
1.1.1. The cardiovascular system	6
1.1.2. The lymphatic system	6
1.2. Molecular players of vascular development	9
1.2.1. Early blood vascular development	9
1.2.2. Specification of blood vessels into arteries and veins	10
1.2.3. Maturation of blood vessels	11
1.2.4. Lymphatic vessel development	12
1.3. VEGF family members and their receptors	13
1.3.1. VEGFs	13
1.3.2. VEGFRs	16
1.3.3. Neuropilins	18
1.4. The role of VEGF family members in tumor angiogenesis and lymphangiogenesis	20
1.4.1. VEGFs and VEGFRs in tumor angiogenesis	20
1.4.2. VEGFs and VEGFRs in tumor-associated lymphangiogenesis	21
1.5. The Rip1Tag2 transgenic mouse tumor model	23
1.6. Aim of the study	24
2. General Materials and Methods	25
Mouse tissue processing	25
Histopathological analysis	25
Lectin Perfusion	27
Tumor grading	27
Collagen Gel Assay	27
Electron microscopy	27
Corrosion cast analysis	28
3. Generation and analysis of transgenic mice expressing lymphangiogenic VEGF family members during Rip1Tag2 tumorigenesis	29
3.1. Distinct Roles of Vascular Endothelial Growth Factor-D in Lymphangiogenesis and Metastasis	29
3.1.1. Abstract	30
3.1.2. Introduction	30
3.1.3. Materials and Methods	31
Transgenic Mouse Lines	31
Glucose measurements	31
Immunoblotting	32
Cell culture	32

	ELISA	32
3.1.4.	Results.....	33
	Peri-insular lymphangiogenesis in Rip1VEGF-D transgenic mice	33
	Repressed islet angiogenesis and reduced islet size in Rip1VEGF-D transgenic mice	38
	VEGF-D promotes peri- and intra-tumoral lymphangiogenesis.....	40
	Impaired tumor angiogenesis and reduced tumor growth in Rip1Tag2;Rip1VEGF-D mice	43
	VEGF-D promotes metastasis to regional lymph nodes and the lungs	45
	Human VEGF-D does not elicit an immune response in non-transgenic mice.....	47
	The tumor microenvironment modulates VEGF-D-elicited effects	49
3.1.5.	Discussion	51
3.2.	Activation of VEGFR-3 is sufficient to promote lymphogenous metastasis.....	55
3.2.1.	Abstract	56
3.2.2.	Introduction.....	56
3.2.3.	Materials and Methods	57
	Cloning of the Rip1VEGF-C156Sdel36 construct.....	57
	Generation of Rip1VEGF-C156S Transgenic Mice.....	58
3.2.4.	Results.....	59
	Generation of Rip1VEGF-C156S transgenic mice	59
	VEGF-C156S induces peri-insular lymphangiogenesis in Rip1VEGF-C156S transgenic mice	60
	VEGF-C156S promotes peri- and intra-tumoral lymphangiogenesis.....	62
	VEGF-C156S promotes regional lymph node metastasis.....	63
3.2.5.	Discussion	65
4.	Generation and analysis of transgenic mice expressing angiogenic VEGF family members during Rip1Tag2 tumorigenesis	67
4.1.	PIGF-1 Inhibits Tumor Growth in a Transgenic Mouse Model of Insulinoma	67
4.1.1.	Abstract	68
4.1.2.	Introduction.....	68
4.1.3.	Methods.....	70
	Cloning of the Rip1PIGF-1 construct	70
	Generation of Rip1PIGF-1 transgenic mice	70
	RT-PCR analysis of PIGF-1 expression	71
4.1.4.	Results.....	71
	Generation of Rip1PIGF-1 transgenic mice	71
	Dilated islet blood vessels in Rip1PIGF-1 transgenic mice	72
	Transgenic PIGF-1 represses tumor growth in Rip1Tag2;Rip1PIGF-1 mice.....	76
4.1.5.	Discussion	77
4.2.	VEGF-B₁₆₇ Promotes Tumor Angiogenesis in a Mouse Model of Pancreatic β-cell Carcinogenesis	80
4.2.1.	Abstract	81
4.2.2.	Introduction.....	81
4.2.3.	Materials and Methods	83
	Generation of Rip1VEGF-B ₁₆₇ transgenic Mice.....	83

4.2.4.	Results.....	83
	Generation of Rip1VEGF-B ₁₆₇ transgenic mice.....	83
	The islet blood vessel architecture of Rip1VEGF-B ₁₆₇ transgenic mice.....	84
	Transgenic VEGF-B ₁₆₇ promotes tumor angiogenesis but not tumor growth in Rip1Tag2;Rip1VEGF-B ₁₆₇ mice (preliminary data).....	86
	Expression of VEGFB ₁₆₇ does not affect tumor invasiveness in Rip1Tag2;Rip1VEGF-B ₁₆₇ mice (preliminary data).....	88
4.2.5.	Discussion.....	90
4.3.	Generation of a Transgenic Mouse Model for the Study of VEGFR-2-specific Functions.....	93
4.3.1.	Abstract.....	94
4.3.2.	Introduction.....	94
4.3.3.	Materials and Methods.....	96
	Cloning of the Rip1VEGF-E _{D1701} construct.....	96
	Generation of Rip1VEGF-E _{D1701} transgenic mice.....	96
	RT-PCR analysis of of Rip1VEGF-E _{D1701} transgenic mice for VEGF-E expression.....	96
4.3.4.	Results.....	97
	Generation of Rip1VEGF-E _{D1701} transgenic mice.....	97
	Analysis of transgenic VEGF-E _{D170} expression.....	98
4.3.5.	Discussion.....	99
5.	Conclusion and Outlook.....	100
6.	References.....	101
7.	Curriculum Vitae.....	115
8.	Conferences.....	116
9.	Publications.....	116
10.	Acknowledgements.....	117
11.	Declaration of Independence.....	118

List of Figures*General Introduction*

Figure 1. The blood and the lymphatic vascular systems.....	8
Figure 2. Involvement of VEGF family members in blood and lymphatic vessel development.....	10
Figure 3. VEGFs and VEGF receptors	14
Figure 4. Processing of VEGF-C and VEGF-D	15
Figure 5. Schematic representation of the VEGFR-2 structure.....	17
Figure 6. Schematic representation of the NP-1 structure.....	19
Figure 7. Multistep β -cell carcinogenesis in Rip1Tag2 transgenic mice.....	24

Distinct Roles of Vascular Endothelial Growth Factor-D in Lymphangiogenesis and Metastasis

Figure 1. Cloning of the Rip1VEGF-D construct for generation of Rip1VEGF-D transgenic mice	33
Figure 2. Histological analysis of pancreata from C57BL/6 control and transgenic Rip1VEGF-D mice	34
Figure 3. Intra-lymphatic immune cell accumulations in Rip1VEGF-D mice.....	35
Figure 4. Islet-associated immune cells, intra-peritoneal glucose tolerance tests of Rip1VEGF-D transgenic founderlines B12, E2 and J97, and intra-lymphatic hemorrhage in Rip1VEGF-D mice	36
Figure 5. Peri-insular hemorrhage and blood-lymphatic vessel shunts in Rip1VEGF-D mice	38
Figure 6. Collagen gel assay with Rip1VEGF-D islets.....	39
Figure 7. Expression of VEGF-D in Rip1Tag2 control and Rip1Tag2;Rip1VEGF-D tumors and Rip1VEGF-D islets.....	41
Figure 8. Peri-tumoral lymphangiogenesis in Rip1Tag2 and Rip1Tag2;Rip1VEGF-D mice.....	42
Figure 9. Hemorrhage in lymphatic vessels associated with Rip1Tag2;Rip1VEGF-D tumors.....	43
Figure 10. Pericyte-coating of intra-tumoral blood vessels and angiogenic activity of Rip1Tag2;Rip1VEGF-D tumors	45
Figure 11. Regional lymph node and distant lung metastases in 12 week-old Rip1Tag2;Rip1VEGF-D double transgenic mice.....	46
Figure 12. Immune cell accumulations in lymphatic lacunae surrounding Rip1Tag2;Rip1VEGF-D tumors	47
Figure 13. Subcutaneous injection of Rip1Tag2 and Rip1Tag2;Rip1VEGF-D tumor cells into Rip1Tag2 mice.....	49
Figure 14. Angiogenesis and lymphangiogenesis in ectopic subcutaneous Rip1Tag2 and Rip1Tag2;Rip1VEGF-D insulinomas.....	50

Activation of VEGFR-3 is sufficient to promote lymphogenous metastasis

Figure 1. Modification of the Rip1 VEGF-C156S construct for generation of Rip1VEGF-C156S transgenic mice	59
Figure 2. Phenotypical analysis of transgenic Rip1VEGF-C156S founder lines.....	61
Figure 3. Phenotypical analysis of Rip1Tag2; Rip1VEGF-C156S mice.....	64

PlGF-1 Inhibits Tumor Growth in a Transgenic Mouse Model of Insulinoma

Figure 1. Cloning of the Rip1PlGF-1 construct..... 71
 Figure 2. RT-PCR analysis of transgenic PlGF-1 expression 72
 Figure 3. Morphology of Rip1PlGF-1 transgenic islets 73
 Figure 4. Analysis of islet angiogenesis and arteriogenesis in Rip1PlGF-1 mice..... 75
 Figure 5. Expression of PlGF in control tumors and phenotype of Rip1Tag2 and Rip1Tag2;
 Rip1PlGF-1 tumors..... 76

VEGF-B₁₆₇ Promotes Tumor Angiogenesis in a Mouse Model of Pancreatic β -cell Carcinogenesis

Figure 1. The Rip1VEGF-B₁₆₇ transgene construct..... 84
 Figure 2. Histological analysis of Rip1 VEGF-B₁₆₇ islets..... 85
 Figure 3. Ultra-structural analysis of Rip1VEGF-B₁₆₇ transgenic islets..... 86
 Figure 4. Tumoral expression of VEGF-B and tumor blood vasculature in control and
 Rip1Tag2; Rip1 VEGF-B₁₆₇ mice 87

Generation of a Transgenic Mouse Model for the Study of VEGFR-2-specific Functions

Figure 1. Map of the Rip1VEGF-E_{D1701} construct..... 97
 Figure 2. RT-PCR analysis of transgenic VEGF-E expression..... 98

List of Tables*General Introduction*

Table I. Structure, interactions and binding properties of VEGF family members.....	16
---	----

Distinct Roles of Vascular Endothelial Growth Factor-D in Lymphangiogenesis and Metastasis

Table I. Islet size and microvessel density (MVD) in control versus Rip1VEGF-D mice	39
Table II. Phenotypical analysis of Rip1Tag2 and Rip1Tag2;Rip1VEGF-D tumors	44
Table III. Tumor progression and metastatic phenotype of Rip1Tag2;Rip1VEGF-D mice	46
Table IV. Immune cells infiltrating Rip1Tag2 and Rip1Tag2;Rip1VEGF-D tumors.....	48
Table V. Quantification of the blood vessel density of ectopic subcutaneous VEGF-D-negative and -positive tumors.....	51

Activation of VEGFR-3 is sufficient to promote lymphogenous metastasis

Table I. Tumor incidence, volume, and microvessel density in Rip1Tag2;Rip1VEGF-C156S mice	62
Table II. Analysis of tumor grades and metastasis in Rip1Tag2;Rip1VEGF-C156S and control mice.....	64

PlGF-1 Inhibits Tumor Growth in a Transgenic Mouse Model of Insulinoma

Table I. Tumor incidence, volume and tumoral blood vessel density in Rip1Tag2;Rip1PlGF-1 mice	77
---	----

VEGF-B₁₆₇ Promotes Tumor Angiogenesis in a Mouse Model of Pancreatic β -cell Carcinogenesis

Table I. Tumor burden and tumor microvessel density in Rip1Tag2;Rip1VEGF-B ₁₆₇ transgenic mice	88
Table II. Tumor grading of Rip1Tag2;Rip1VEGF-B ₁₆₇ versus control mice.....	89

Zusammenfassung

Mitglieder der Familie der vaskulären endothelialen Wachstumsfaktoren (VEGF) und ihre Rezeptoren (VEGFR) spielen eine wesentliche Rolle in der Entstehung und Aufrechterhaltung des physiologischen Blut- und Lymphgefäßsystems. Desweiteren werden die fünf bis anhin in Säugetieren entdeckten VEGFs, VEGF-A, -B, -C, -D und der plazentare Wachstumsfaktor (PlGF), während der Tumorigenese hochreguliert und sind an der Tumorangiogenese und -lymphangiogenese beteiligt. VEGF-A als zentraler angiogener Wachstumsfaktor fördert die Tumorangiogenese und damit das Tumorwachstum und die -progression durch Aktivierung von VEGFR-1 und -2, die auf Blutgefäßendothelzellen exprimiert werden. Im Gegensatz dazu führt die Hochregulierung des lymphangiogenen Wachstumsfaktors VEGF-C, einem Liganden für den lymphatischen VEGFR-3 sowie für VEGFR-2, zur Neubildung von tumorassoziierten Lymphgefäßen und fördert damit die passive Metastasierung von Tumorzellen zu regionalen Lymphknoten. Über die Auswirkungen von tumoralem VEGF-B und PlGF, zwei selektiven Liganden für VEGFR-1, sowie VEGF-D, dem zweiten lymphangiogenen Wachstumsfaktor und Liganden von VEGFR-3 und -2, ist hingegen wenig bekannt. Desweiteren macht die kürzliche Entdeckung von selektiven Liganden für VEGFR-2 und -3, namentlich VEGF-E und VEGF-C156S, eine Untersuchung der spezifischen Rolle dieser Rezeptoren möglich.

Um die Funktionen von VEGF-D unter physiologischen Bedingungen zu studieren habe ich transgene Mäuse analysiert, die VEGF-D spezifisch in β -Zellen der pankreatischen Langerhans'schen Inseln exprimieren (Rip1VEGF-D). Die transgene Expression von VEGF-D im endokrinen Pankreasgewebe dieser transgenen Mäuse induziert die Neubildung von grossen lymphatischen Lakunen um einen Grossteil der Inseln. Häufig enthalten diese Gefäße Anhäufungen von Immunzellen, die wahrscheinlich infolge der Dysfunktion einiger peri-insulären Lymphgefäße entstehen. Als Folge von Blut-Lymphgefäß-Verbindungen enthalten lymphatische Lakunen auch häufig Erythrozyten und Blutungen, die bis in die regionalen Lymphknoten drainiert werden und damit indirekt die Funktionalität der meisten neugebildeten Lymphgefäße beweisen. Um den Einfluss von tumorexprimiertem VEGF-D auf die Tumorigenese zu erforschen, habe ich diese Mäuse mit Rip1Tag2 Mäusen gekreuzt, einem etablierten transgenen Mausmodell für β -Zell Karzinogenese. Wie in der zuvor beschriebenen einzel-transgenen Maus fördert das durch Rip1Tag2 Tumorzellen produzierte VEGF-D das Wachstum von peri-tumoralen Lymphgefäßen, die häufig Immunzellanhäufungen und Blutungen enthalten. Gleichzeitig weisen diese doppel-transgenen Mäuse eine hohe Inzidenz von Metastasen in regionalen Lymphknoten als auch in der Lunge auf. Da die Expression von VEGF-D das invasive Verhalten der Tumoren nicht direkt beeinflusst und da alle Metastasen gut differenziert sind, fördert VEGF-D die lymphogene Metastasierung sehr wahrscheinlich durch die Neubildung von Lymphgefäßen. Interessanterweise bewirkt die Expression von VEGF-D eine signifikante Hemmung der Tumorangiogenese und des Tumorwachstums durch einen bislang unbekanntem Mechanismus. Eine kürzlich publizierte Studie über die Auswirkungen von VEGF-C auf die Rip1Tag2 Tumorigenese berichtet, dass die Expression dieses Wachstumsfaktors die Metastasierung zu regionalen Lymphknoten, jedoch nicht in die Lunge, durch die Stimulierung von tumor-assoziiertes Lymphangiogenese fördert. Überdies weisen diese Mäuse keine intra-tumoralen Immunzellanhäufungen oder Blutungen auf, und die Tumorangiogenese und das Tumorwachstum werden durch die Expression von VEGF-C

nicht beeinflusst. Die Anwendung des Rip1Tag2 Tumormodells hat es mir ermöglicht, nicht nur Ähnlichkeiten sondern auch signifikante funktionelle Unterschiede von VEGF-C und VEGF-D zu ermitteln. Interessanterweise führte die syngene und allogene Transplantation von VEGF-D produzierenden Rip1Tag2 Tumorzelllinien in die Haut von transgenen Mäusen zur Bildung von Tumoren, die dichte intra- jedoch keine peri-tumorale Lymphgefäßnetzwerke aufweisen. Überdies beeinflusst die Expression von VEGF-D auch die Angiogenese dieser Tumoren nicht. Diese Beobachtungen zeigen, dass das tumorumgebende Milieu die von VEGF-D induzierten Effekte grundlegend beeinflusst.

Da VEGF-C und -D sowohl VEGFR-3 als auch -2 binden können, ist bislang nicht erforscht, ob die selektive Aktivierung von VEGFR-3 ausreicht um Tumor Lymphangiogenese und dadurch die lymphogene Metastasierung zu fördern. Daher habe ich transgene Mäuse generiert, die VEGF-C156S im endokrinen Pankreas exprimieren und habe diese Mäuse mit Rip1Tag2 Mäusen gekreuzt. Die Analyse der einzel- und doppel-transgenen Mäuse hat ergeben, dass VEGF-C156S VEGF-C in allen untersuchten Parametern imitiert und beweist damit, dass die Aktivierung von VEGFR-3 genügt, um tumor-assoziierte Lymphangiogenese und lymphogene Metastasierung zu fördern. Die Hemmung von VEGFR-3 könnte daher durchaus zur Hemmung der Metastasenbildung beitragen.

Um die spezifischen Rollen von VEGFR-1 und -2 unter physiologischen als auch malignen Bedingungen besser zu verstehen, habe ich transgene Mäuse hergestellt, in denen die VEGFR-1-spezifischen Liganden VEGF-B₁₆₇ und PlGF-1 sowie der VEGFR-2-spezifische Ligand VEGF-E_{D1701} im endokrinen Pankreas exprimiert werden (Rip1VEGF-B₁₆₇, Rip1PlGF-1, und Rip1VEGF-E_{D1701} Mäuse). Diese einzeltransgenen Mäuse wurden vor allem auf Veränderungen der Blutgefäßmorphologie und -dichte untersucht. In einem zweiten Schritt habe ich einzeltransgene Mäuse mit Rip1Tag2 Tumormäusen gekreuzt. Diese doppeltransgenen Mäuse, die VEGF-B₁₆₇, PlGF-1 oder VEGF-E_{D1701} in Tumorzellen exprimieren, wurden auf Veränderungen der Tumorangiogenese, des Tumorwachstums und der Tumorprogression untersucht. Die vorläufigen Daten zeigen, dass die β -zell-spezifische Hochregulierung von VEGF-B₁₆₇ das physiologische Blutgefäßsystem nicht beeinflusst, jedoch die Blutgefäßdichte in Tumoren von doppeltransgenen Mäusen signifikant erhöht. Das Tumorwachstum wird hierdurch jedoch nicht begünstigt. Im Gegensatz dazu führt die Expression von PlGF-1 in einzeltransgenen Mäusen zu einer deutlichen Dilatation der Inselblutkapillaren, was sehr wahrscheinlich die Folge einer signifikanten Erniedrigung von gefäßstabilisierenden Perizyten ist. Desweiteren hemmt die tumorale Produktion von PlGF-1 die Tumorangiogenese und das Tumorwachstum, was bedeuten könnte, dass dieser Wachstumsfaktor ein natürlicher Inhibitor der pathologischen Angiogenese ist. Obgleich VEGF-B₁₆₇ und PlGF-1 denselben Rezeptor binden, bewirken sie entgegengesetzte Effekte auf das tumorale Blutgefäßsystem, was bei der Entwicklung von Angiogenese-Hemmstoffen, die auf der Inhibierung von VEGFR-1 beruhen, bedacht werden sollte. Der Phänotyp der VEGF-B₁₆₇- und PlGF-1-exprimierenden Rip1Tag2 Mäuse unterscheidet sich wesentlich von den kürzlich beschriebenen VEGF-A₁₆₅ transgenen Rip1Tag2 Mäusen, die infolge beschleunigter Tumorangiogenese und rascherem Tumorwachstum frühzeitig versterben. Die Analyse der VEGF-E_{D1701}-exprimierenden Mäuse und damit der spezifischen VEGFR-2 Signalwege wird zur Zeit in die Wege geleitet.

Summary

Members of the vascular endothelial growth factor (VEGF) family and their receptors (VEGFR) play an essential role in the development and maintenance of the blood and lymphatic vasculature. To date, five VEGFs have been identified in the mammalian genome, VEGF-A, -B, -C, -D, and placental growth factor (PlGF), which display distinct binding affinities for VEGFR-1, -2, and -3. In addition to their central function in physiological angiogenesis and lymphangiogenesis, VEGFs and VEGFRs are upregulated during carcinogenesis and are involved in the remodeling of the tumoral blood and lymphatic vasculature. By activating VEGFR-1 and -2, which are both expressed on blood endothelial cells, VEGF-A promotes the formation of new tumoral blood vessels and thereby accelerates tumor growth. In contrast, upregulation of VEGF-C, a ligand for lymphatic endothelial VEGFR-3 as well as for VEGFR-2, induces the formation of tumor-associated lymphatic vessels and thus promotes the passive metastatic dissemination of tumor cells to regional lymph nodes. Much less is known about the functional consequences of tumor-expressed VEGF-B and PlGF, two selective ligands for VEGFR-1, as well as VEGF-D, the second VEGFR-3- and -2-binding lymphangiogenic VEGF family member. Also, the biological effects of selective VEGFR-1, -2 or -3 signaling on tumor angiogenesis and tumor growth as well as tumor lymphangiogenesis and metastasis are incompletely studied. Only recently, the identification of VEGF-E, a selective ligand for VEGFR-2, as well as the generation of VEGF-C156S, a specific ligand for VEGFR-3, has enabled the study of the distinct roles of these receptors.

To investigate the function of lymphangiogenic VEGF-D under physiological conditions, I analyzed transgenic mice, in which expression of VEGF-D is specifically targeted to β -cells of pancreatic islets of Langerhans (Rip1VEGF-D mice). In these mice, expression of VEGF-D induces the formation of large lymphatic lacunae surrounding most islets. A few of these lymphatic vessels may be dysfunctional, which causes intra-lymphatic accumulations of immune cells. Moreover, lymphatic lacunae often contain erythrocytes, which may result from blood-lymphatic vessel shunts found in the vicinity of some islets. However, the fact that erythrocytes are drained to regional lymph nodes demonstrates the draining capacity of the *de novo* formed lymphatic vessels. To address the impact of VEGF-D on tumorigenesis and metastasis, I crossed Rip1VEGF-D with Rip1Tag2 mice, a well-characterized transgenic model of poorly metastatic multistage β -cell carcinogenesis. Tumoral expression of VEGF-D in Rip1Tag2 mice promotes the growth of peri-tumoral lymphatic vessels that frequently contain leucocyte clusters and hemorrhages. Concomitantly, these double-transgenic mice exhibit a high incidence of regional lymph node and distant lung metastases. Since expression of VEGF-D does not significantly affect the invasiveness of tumors and all metastases are well differentiated, these data indicate that VEGF-D promotes lymphogenous metastasis by upregulating tumor-associated lymphangiogenesis. Interestingly, the presence of VEGF-D significantly represses tumor angiogenesis and tumor growth, yet the mechanisms of this inhibition are thus far uncharacterized. Notably, syngenic and allogenic subcutaneous transplantation of VEGF-D-producing Rip1Tag2 tumor cell lines results in the formation of tumors exhibiting a dense intra-tumoral lymphatic network but

lacking peri-tumoral lymphatic vessels. In these transplanted tumors, no immune cell clusters or hemorrhages are formed in tumor-associated lymphatic vessels and tumor angiogenesis is unaffected by the expression of VEGF-D. These results demonstrate that the tumor microenvironment critically modulates VEGF-D-elicited effects. It has been recently shown that transgenic expression of VEGF-C during Rip1Tag2 tumorigenesis promotes metastasis to regional lymph nodes but not to the lungs by inducing peri-tumoral lymphangiogenesis. Tumor-associated lymphatic vessels of these mice neither contain immune cell accumulations nor hemorrhages, and tumor angiogenesis and tumor growth are not affected by the production of VEGF-C. Thus, by employing the Rip1Tag2 tumor model, I was able to identify not only similarities but also significant differences between VEGF-D and -C function.

Since VEGF-C and -D can bind both VEGFR-3 and -2, it is not fully established whether selective activation of VEGFR-3 is sufficient to induce tumoral lymphangiogenesis and to promote lymphogenous metastasis. Therefore, I established transgenic mice expressing VEGF-C156S in the endocrine pancreas and crossed these mice with Rip1Tag2 animals. The analysis of single and double transgenic mice revealed that VEGF-C156S phenocopies VEGF-C in all investigated aspects. These results indicate that VEGFR-3 may be the predominant receptor mediating VEGF-C-elicited effects in Rip1Tag2 mice and that selective activation of VEGFR-3 is sufficient to promote tumor-associated lymphangiogenesis and metastasis. Hence, VEGFR-3 might represent a valuable target for future anti-metastatic strategies.

To further understand the specific roles of VEGFR-1 and -2 signaling in physiological angiogenesis as well as in tumorigenesis, I established transgenic mouselines, which express the VEGFR-1-specific ligands VEGF-B₁₆₇ and PlGF-1 as well as the selective VEGFR-2 ligand VEGF-E_{D1701} in β -cells of pancreatic islets (Rip1VEGF-B₁₆₇, Rip1PlGF-1, and Rip1VEGF-E_{D1701} mice). These single transgenic mice were analyzed with regard to islet blood vessel morphology and density. In a second set of experiments, I crossed single-transgenic animals with Rip1Tag2 mice. These double-transgenic mice expressing either VEGF-B₁₆₇, PlGF-1 or VEGF-E_{D1701} in tumor cells, were analyzed for changes in tumor angiogenesis, tumor growth, and tumor progression. The preliminary data provide evidence that β -cell-specific upregulation of VEGF-B₁₆₇ does not critically affect physiological angiogenesis of single-transgenic mice but results in a significant increase in the tumor microvessel density of double-transgenic animals. However, tumor growth and tumor progression are not promoted by the stimulation of tumor angiogenesis. In contrast, overexpression of PlGF-1 in single-transgenic mice leads to a prominent dilation of blood capillaries, which may at least in part be caused by a significant reduction of stabilizing blood vessel-associated pericytes. Furthermore, tumoral expression of PlGF-1 significantly inhibits tumor angiogenesis and tumor growth, suggesting that this growth factor might be a natural inhibitor of pathological angiogenesis. Hence, although binding to the same receptor, VEGF-B₁₆₇ and PlGF-1 elicit opposing effects on the tumor blood vasculature. These results suggest that the two growth factors induce distinct signaling pathways via VEGFR-1, which might be considered when designing inhibitors of angiogenesis involving VEGFR-1. Importantly, the phenotype of VEGF-B₁₆₇- and PlGF-1- expressing Rip1Tag2 mice is different from the

recently described VEGF-A₁₆₅ transgenic Rip1Tag2 mice, which exhibited accelerated tumor growth and early death. The analysis of VEGF-E_{D1701}-expressing mice and effects induced by selective activation of VEGFR-2 signaling is currently underway.

1. General Introduction

1.1. The two vascular systems

1.1.1. The cardiovascular system

Large multicellular organisms use carrier molecules to deliver oxygen and nutrients to distant organs and to remove and manage metabolic waste products, thereby ensuring homeostasis of the body. In vertebrates, a closed cardiovascular system consisting of the heart, arteries, blood capillaries, and veins guides the transport of these molecules via the bloodstream to and from tissues. By repeated rhythmic contractions, the heart ventricles exert a pressure to pump the blood through arteries into organ capillaries and to return it via veins to the heart (Figure 1A). In addition to supplying tissues with oxygen and nutrients, the vascular system and blood are critically involved in the regulation of the body temperature and the systemic pH (reviewed in [1]).

According to their distinct functions, blood vessels display characteristic structural properties. Arteries and veins typically consist of three layers: an intima composed of endothelial cells, a media of smooth muscle cells, and an adventitia of fibroblasts, matrix, and elastic laminae. The adventitial layer has its own blood supply (vasa vasorum). Smooth muscle cells and elastic laminae contribute to the vessel tone and mediate the control of vessel diameter and blood flow. Arteries participate in establishing a high arterial pressure, why their media consists of multiple sheets of smooth muscle cells. In contrast, veins constitute the low-pressure section of the vascular system and therefore display only few layers of smooth muscle cells, which accounts for their much thinner vessel wall and commonly larger lumina. Extravasation of macromolecules and cells from the blood stream typically occurs from postcapillary venules. Since blood capillaries are specialized for the exchange of nutrients and oxygen with the surrounding tissue, their vessel wall is only composed of one layer of tightly coherent endothelial cells and a continuous basement membrane. Four types of capillary endothelium are discerned, which are typically found in distinct organs: (i) endothelia that include tight junctions are impermeable to various molecules and are found in the blood-brain and blood-retina barrier, (ii) continuous endothelium occurs for instance in the muscle, (iii) fenestrated endothelium is composed of endothelial cells exhibiting pores, thereby facilitating molecular exchange for instance in endocrine glands, (iv) sinusoidal or discontinuous capillaries display inter-cellular gaps, enabling the trans-capillary transport of macromolecules for example in the liver [2]. Most though not all capillaries are further stabilized by scaffolding cells such as pericytes, which are embedded in the basal membrane [3].

1.1.2. The lymphatic system

As a result of the high arterial pressure, plasma leaks from the capillaries into the extracellular space and becomes interstitial fluid. About 90% of this extravasated fluid is reabsorbed by post-capillary venules driven by osmotic forces [4]. The remaining 10% are drained by a second vascular system, the lymphatic system, and returned to the blood

circulation. Unlike the cardiovascular system, the lymphatic system is not closed, has no central pump in mammals, and exhibits a unidirectional proximal lymph flow due to valves (Figure 1A). Through its draining function, the lymphatic system counteracts the accumulation of interstitial fluid in tissues and thus the formation of edema. Lymphatic flow starts by diffusion of interstitial fluid into blind-ended lymphatic capillary networks that are present in most body tissues. Once in the lymphatics, the fluid is called lymph but has almost the same composition as the original interstitial fluid. The lymph is propelled under low pressure mostly due to the milking action of skeletal muscles and rhythmic contractions of nearby blood vessel walls. Moreover, large lymphatic ducts containing valves can contract themselves. The lymph is transported to progressively larger lymphatic vessels and passes through one or several interposed lymph nodes into large ducts, which drain the fluid back into the blood circulatory system at the right and left subclavian veins. Besides its crucial role in maintaining tissue fluid homeostasis, the lymphatic system constitutes an important component of the immune system. About 50% of the plasma proteins and cells pass through lymphatics and lymph nodes every day. Lymph nodes harbour antigen-presenting cells, B and T lymphocytes, which elicit an immune response in case pathogens are passing the lymph nodes. Another important function of the lymphatic system is the intestinal absorption and transport of long chain dietary triglycerides and lipophilic compounds such as fat-soluble vitamins (reviewed in [5]).

Structurally, the lymphatic capillaries are rather distinct from blood capillaries. They consist of a layer of extremely attenuated endothelial cells that also form microvalves and lack a continuous basal lamina and pericytes. Adjacent endothelial cells are extensively overlapping and lack inter-cellular adhesion devices in many areas. In these regions, lymphatic endothelial cells maintain a close relationship with the adjoining interstitium by anchoring filaments, which interact with components of the extra-cellular matrix (ECM). As shown in Figure 1B, an increase in interstitial fluid exerts tension on fibers of the ECM, which is transmitted via the anchoring filaments to endothelial cells and forces them to distend from each other, thereby facilitating the entry of fluid, macromolecules, and cells [6].

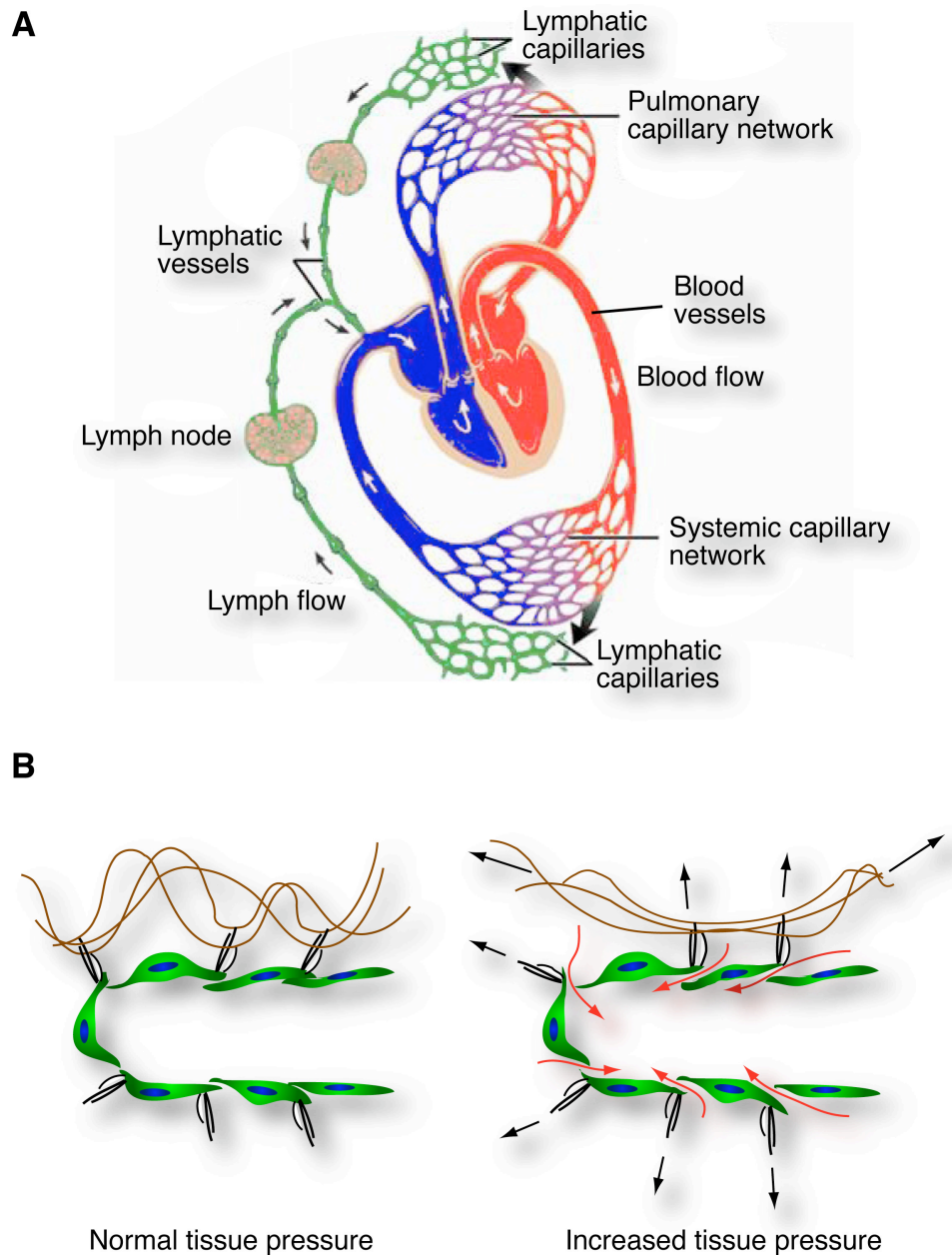


Figure 1. The blood and the lymphatic vascular systems

(A) The two vascular systems (modified from D. Sheer, J. Butler and R. Lewis, *Hole's Human Anatomy and Physiology*, 2003) (B) Regulation of interstitial fluid absorption into lymphatic capillaries upon increase in tissue pressure. Extra-cellular fibers are drawn in brown, anchoring filaments in black, black arrows indicate pulling forces, red arrows symbolize interstitial fluid flow into capillaries.

1.2. Molecular players of vascular development

1.2.1. Early blood vascular development

The cardiovascular system is the first organ that develops during embryogenesis. In an initial phase, angioblast precursors and primitive hematopoietic cells develop from a common mesodermal precursor, the so-called hemangioblast (Figure 2). In the process of vasculogenesis, the *de novo*-forming angioblasts aggregate in the embryo and yolk sac into a primitive network of simple endothelial tubes called primary vascular plexus. In parallel, the primitive hematopoietic cells form the first blood islands in the visceral yolk sac [7, 8]. The primary capillary plexus is remodeled into organized vessels by proliferation, intussusceptive growth (division of large vessels into smaller ones), and sprouting of new vessels from existing ones - the process of angiogenesis [2, 9].

In this early phase of vasculogenesis and angiogenesis, the first identified member of the vascular endothelial growth factor (VEGF) family of glycoproteins, VEGF-A, and its receptors vascular endothelial growth factor receptor (VEGFR)-1 and VEGFR-2 play a crucial role, since knock-out mice for either of these molecules result in embryonic lethality. Embryos deficient for the receptor tyrosine kinase VEGFR-2 or one or both alleles of VEGF-A fail to develop blood islands, endothelial cells, and major vessel tubes [10-12]. In contrast, in mice lacking VEGFR-1, vessels do form but exhibit excess levels of endothelial cells, which obstruct the lumina of abnormal vascular channels [13]. Thus, although both VEGFR-1 and VEGFR-2 are expressed on hematopoietic stem and blood endothelial cells, only VEGFR-2 is absolutely critical for the earliest stages of vasculogenesis, while VEGFR-1 becomes involved only later, acting as a negative regulator of VEGF-A activity during early angiogenesis. Remarkably, mutant mice containing a form of VEGFR-1 that lacks only its tyrosine kinase domain exhibit normal vascular development, indicating that only the binding portion of this receptor may be necessary to support its major actions during vascular development [14]. Detailed studies confirmed that VEGF-A is a critical growth factor during vasculogenesis as well as early and adult angiogenesis by promoting endothelial cell proliferation, migration, tubule-formation, sprouting, and the maintenance of the mature vasculature (reviewed in [15]). A third VEGFR, VEGFR-3, which is not a receptor for VEGF-A but for the lymphangiogenic growth factors VEGF-C and VEGF-D, is also expressed on blood vessels during embryogenesis, but becomes largely restricted to lymphatic vessels in the adult. Notably, mice deficient for VEGFR-3 display early embryonic lethality due to defects in the organization of large vessels prior to the emergence of lymphatics, suggesting an early role of this receptor for blood vessel development [16].

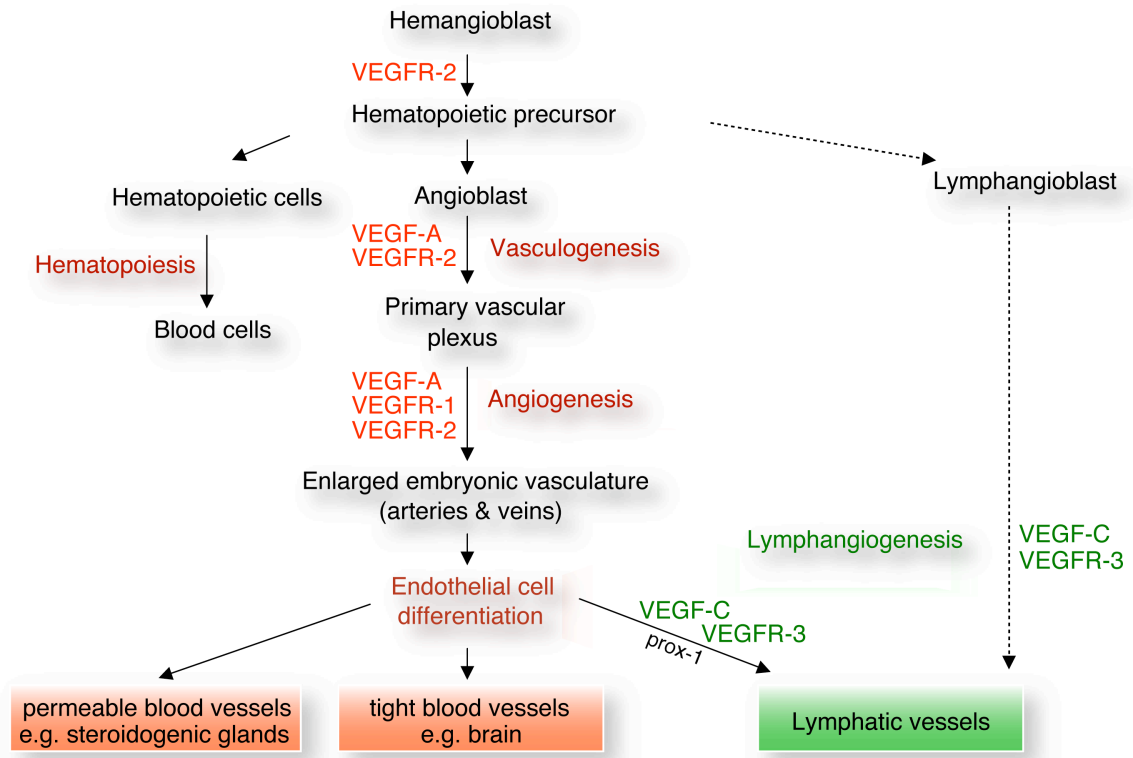


Figure 2. Involvement of VEGF family members in blood and lymphatic vessel development
(modified from Achen, *J Exp Path*, 1998)

1.2.2. Specification of blood vessels into arteries and veins

Artery and vein-specific markers are expressed on arterial and venous endothelial cells before establishment of the circulation, indicating that arterial and venous fate may be intrinsically specified early during development [15]. Although the process of arterial and venous specification is not well understood at the molecular level, there is increasing evidence that sonic hedgehog (Shh), VEGF-A, Notch4, ephrinB2, and neuropilin (NP) signaling may be important triggers of arterial/venous specialization. Shh is a transcription regulating protein, which is expressed in the notochord of developing embryos and acts as a morphogen involved in patterning many organ systems. Recent studies suggest that Shh induces the expression of VEGF-A in nearby somites of embryos, which in turn acts on adjacent angioblasts that activate the Notch pathway [17, 18]. Expression of the receptor Notch4 and the ligand Delta4 is restricted to developing endothelium and is artery-specific [19]. Mice exhibiting a mutation of Notch1/4 exhibit vascular defects in mid-gestation, and studies in zebrafish have revealed that Notch plays a critical role in specification of the dorsal aorta and the cardinal veins. Conversely, activation of the Notch pathway represses venous markers and activates expression of arterial markers, like ephrinB2, in the posterior cardinal vein [20, 21]. The Eph receptors and their membrane-bound ligands, the ephrins, can induce forward signaling through the Eph receptors as well as reverse signaling through the ephrinB-

type ligands [22]. EphrinB2 and EphB4 are specifically expressed in arterial and venous endothelial cells, respectively. Bidirectional signaling involving arterial ephrinB2-positive and venous EphB4-positive endothelial cells is not required for vasculogenesis but critical for angiogenesis of arteries and veins as well as the maintenance of artery-vein separation [23-25]. Thus, the sequential activation of Shh, VEGF-A, and Notch may activate downstream artery-specific genes such as ephrinB2 in distinct angioblasts, whereas remaining angioblasts take up a vein identity.

Another mechanism was proposed by studies of the NP receptors. These are involved in the development of the neural and cardiovascular systems and are co-receptors for VEGFs. In chick embryos, expression of endothelial NP-1 is mostly restricted to arteries, whereas NP-2 primarily marks veins [26]. Although the precise mechanisms are not elucidated yet, a recent study suggests that NP-1 and NP-2 act as major determinants for arterial/venous fate, since the sinus vein of the extra-embryonic blood vascular plexus formed from blood islands that expressed NP-2 but not NP-1. Moreover, these observations suggest that the identity of vessels may not depend on blood flow and may be determined already before vessel formation [27].

1.2.3. Maturation of blood vessels

The maturation of newly formed sprouts into differentiated blood vessels involves the recruitment of mural cells, the development of the surrounding matrix and elastic laminae, and organ-specific specialization of endothelial cells. Pericytes stabilize nascent blood vessels by providing a scaffolding support and furthermore communicate with endothelial cells by direct physical contact and paracrine signaling [3]. The platelet-derived growth factor (PDGF)-B/PDGF receptor (PDGFR)- β and angiotensin (Ang)/Tie2 signaling systems are important regulators of blood vessel maturation. Presumably in response to VEGF-A, PDGF-B is secreted by endothelial cells and pericytes and activates PDGFR- β -positive pericytes to proliferate and migrate during vascular maturation [28]. In contrast, Ang proteins may not be “instructive” but permissive molecules. Pericyte-secreted Ang-1 acts in a paracrine fashion on its receptor Tie2, which is specifically expressed in endothelial cells. Thereby, Ang-1 mediates an appropriate interaction between endothelial cells and pericytes, which enables responsiveness of endothelial cells and pericytes for further cues [29]. Ang-1 signaling is required also for the maintenance of mature blood vessels and is therefore constitutively and widely expressed also in the adult. In contrast, Ang-2 is expressed only at sites of vascular remodeling in the adult tissue and predominantly acts as an antagonist of Ang-1/Tie2 signaling [30]. It exerts a dual role on blood vessels depending on the presence or absence of VEGF-A. When VEGF-A is co-expressed with Ang-2, the latter facilitates VEGF-A-mediated vascular remodeling and angiogenesis by partly destabilizing mature vessels. In the absence of VEGF-A, Ang-2 promotes plain regression of blood vessels. Thereby, both PDGF-B/PDGFR- β and Ang/Tie2 signaling systems act in a coordinated and complementary fashion together with VEGF-A (reviewed in [22]). In addition, sphingosine-1-phosphate (S1P), its receptor, S1P1/endothelial differentiation gene (EDG1), and transforming growth factor (TGF)- β have been shown to be involved in the recruitment and differentiation of pericytes (reviewed in [2]).

1.2.4. Lymphatic vessel development

To date, experimental data from mice support the hypothesis proposed in 1909 by Florence Sabin that lymphatic endothelial cells arise by sprouting from embryonic veins (Sabin, F. R. (1909). The lymphatic system in human embryos, with a consideration of the morphology of the system as a whole. *Am J Anat* 9, 43–91). Around embryonic day 10, the homeobox transcription factor Prox1, a ‘master gene’ in the program specifying lymphatic endothelial cell fate, is expressed in a subpopulation of vein endothelial cells and promotes their transdifferentiation into lymphatic endothelial cells [31] (Figure 2). Subsequently, VEGFR-3 gets expressed and activated by VEGF-C, which acts as an essential chemotactic and survival factor for nascent lymphatic endothelial cells and stimulates the migration of such to form primary lymph sacs and the primary lymphatic plexus [32]. Recent findings have also implicated exogenous signals from hematopoietic cells in promoting the separation of the vascular and lymphatic system. Mice lacking the hematopoietic signaling molecule Syk or its substrate SLP-76 fail to show proper separation of vascular and lymphatic systems [33]. Thus, exogenous and endogenous signals interact to maintain vascular and lymphatic integrity and to prevent aberrant flow between the two systems. Postnatal remodelling of the lymphatic vasculature includes sprouting of lymphatic capillaries from the primary lymphatic plexus, whereas deeper lymphatic vessels recruit smooth muscle cells and develop lymphatic valves, thereby acquiring a collecting vessel phenotype. These processes have been recently shown to depend on NP-2, Ang-1/Ang-2/Tie2 as well as ephrinB2 signaling [6, 34]).

A second theory proposes that lymphatic vessels can also form by fusion of mesenchymal lymphatic endothelial precursor cells or lymphangioblasts (Figure 2). Although in birds, such mechanism of lymphatic vessel development has been demonstrated, convincing evidence is still missing for mammals [35]. Recently, two unique populations of stem and progenitor cells have been identified in human blood that either coexpress VEGFR-3, CD133, and CD34 or VEGFR-3, CD31, and CD14. Both cell types were shown to differentiate into lymphatic endothelial cells *in vitro*, indicating that lymphatic endothelial precursors might also contribute to lymphangiogenesis in humans [36, 37].

1.3. VEGF family members and their receptors

1.3.1. VEGFs

The VEGF family constitutes part of a cystine knot motif-containing superfamily of growth factors, which also includes PDGF-BB and TGF β [38]. To date, five VEGF members are identified in mammals, VEGF-A, -B, -C, -D, and PlGF, which are active as dimeric glycosylated proteins [39-43]. VEGFs act relatively specifically on blood and lymphatic endothelial cells due to the distinct expression pattern of their receptors VEGFR-1, -2, and -3 as well as NP co-receptors. While VEGFR-1 and VEGFR-2 are mainly found on blood endothelial cells, VEGFR-3 is largely restricted to lymphatic endothelium (see also next section). VEGF-A, the to date best-studied VEGF family member, binds to both VEGFR-1 and VEGFR-2, whereas VEGF-B and PlGF are selective ligands for VEGFR-1. Notably, although binding to the same receptor, VEGF-A and PlGF were recently shown to induce distinct intra-cellular signaling pathways [44]. VEGF-C and -D are the only known ligands for VEGFR-3 but can also bind VEGFR-2. Thus, according to their affinities for VEGFR-1 and -2, VEGF-A, -B, and PlGF exert angiogenic activities, while VEGF-C and -D predominantly act as lymphangiogenic growth factors by activating VEGFR-3 (Figure 3) [45].

VEGF-A homologs have been identified also in the genome of parapoxviruses and in the venom of different pit vipers, being generally termed VEGF-E and snake venom VEGF (svVEGF), respectively (reviewed in [46, 47]). In particular VEGF-E represents an important complementary tool in elucidating our understanding of distinct VEGFR-2-induced biological activities since this factor is the only known ligand that exclusively activates VEGFR-2 but not VEGFR-1 or -3.

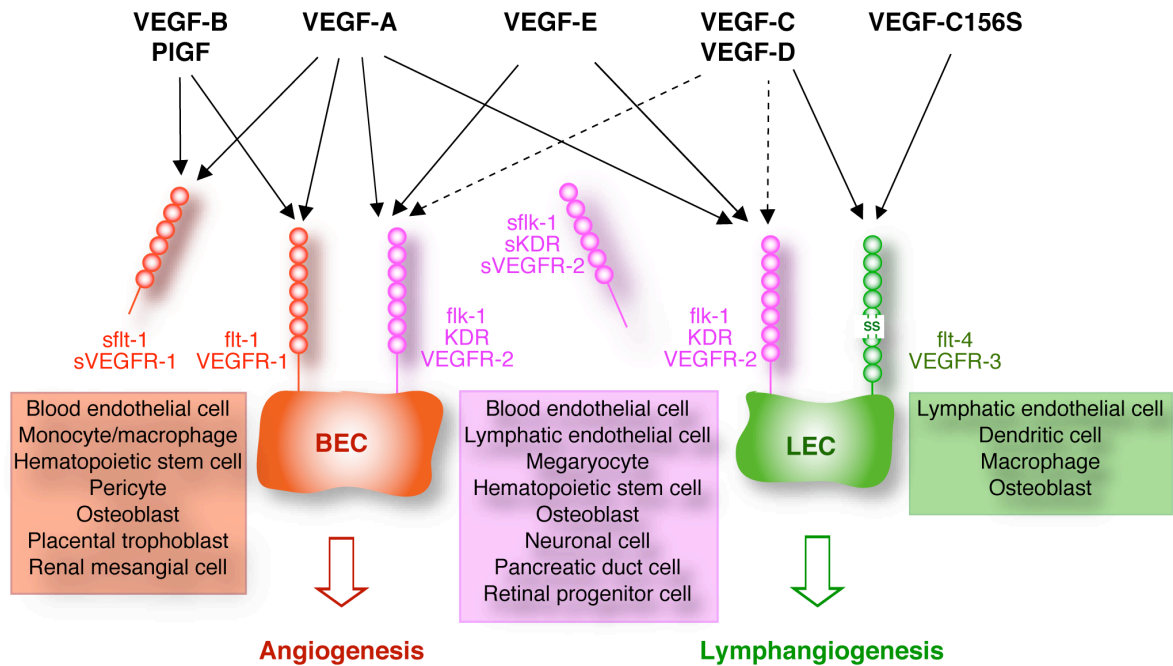


Figure 3. VEGFs and VEGF receptors

Cells expressing the distinct VEGFRs are shown in boxes of the respective receptor color. Arrows indicate affinities of VEGF family members to VEGFRs, dashed arrows indicate weak affinity depending on proteolytical processing of VEGF-C and VEGF-D. BEC, blood endothelial cell; flk, fetal liver kinase;flt, fms-like tyrosine kinase; KDR, kinase insert domain receptor; LEC, lymphatic endothelial cell; PIGF, placental growth factor; sVEGFR-1 and -2 indicate the respective soluble receptor forms.

As indicated in the summary Table I at the end of this section, all VEGF members share the highly conserved VEGF homology domain (VHD), which contains VEGFR binding sites, the cysteine knot motif composed of eight characteristically spaced cysteine residues, as well as heparin and NP binding sites [48]. Yet, angiogenic and lymphangiogenic VEGFs are structurally distinct and display different molecular properties. Alternative splicing of human angiogenic VEGFs gives rise to different isoforms, which display characteristic receptor affinities as well as interactions with the ECM through the heparin binding sites. Notably, VEGF-A_{165b} is a natural VEGF-A antagonist, which binds VEGFR-2 with the same affinity as VEGF₁₆₅, but does not stimulate downstream signalling pathways [49]. The affinity for heparin affects the bioavailability of these growth factors, since heparin-binding isoforms are mostly sequestered to heparansulfate-proteoglycans of the ECM and at the cell surface and are only active once released by the activity of heparinases, matrix metalloproteases, plasmin or urokinase [50]. By contrast, the non-heparin binding isoforms are freely diffusible [48]. Angiogenic VEGFs form covalently linked anti-parallel homodimers via intra- and inter-chain disulfide bonds among residues of the cysteine knot motif. Notably, both isoforms of VEGF-B as well as PIGF-1 are capable of forming heterodimers with VEGF-A₁₆₅, which may have important biological implications in VEGF-A-mediated angiogenesis by modulating the affinity of VEGF-A for its receptors [51, 52].

Based on their distinct structural features and biological function, the lymphangiogenic growth factors VEGF-C and -D constitute a subfamily of VEGFs. Both growth factors are produced as homodimeric pre-propeptides, in which the VHD is flanked by long N- and C-terminal peptide extensions (Figure 4 and Table I). In the C-terminus, numerous cystein residues constitute a Balbiani ring 3 protein-like motif (BR3P), which may be involved in intermolecular interactions [41, 53]. VEGF-C and -D are proteolytically processed by the intra-cellular secretory proprotein convertases (PC)5, PC7, furin, as well as extra-cellular plasmin and other thus far unknown proteases. As depicted in Figure 4, the sequential cleavage of C- and N-termini gives rise to the partially processed ΔC propeptides and the fully processed $\Delta N\Delta C$ peptides consisting of the homodimeric VHD only [45]. This maturation process critically modulates the receptor affinities of VEGF-C and -D and thereby their biological function. While the unprocessed forms bind to VEGFR-3 only, mature VEGF-C and -D display increased affinity for lymphangiogenic VEGFR-3 and are moreover capable of binding and activating blood vessel VEGFR-2, thereby mediating also angiogenic signals (Figure 3, Table I) [45]. Therefore, site-specific expression levels of VEGF-C, -D, VEGFR-3, VEGFR-2 as well as the status of VEGF-C and D processing in a given tissue determine the lymphangiogenic and angiogenic activities of these growth factors.

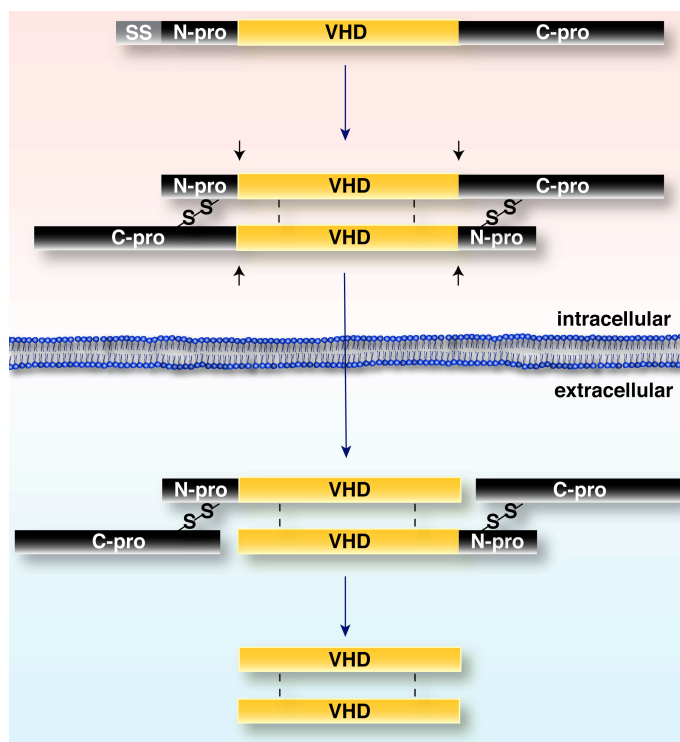


Figure 4. Processing of VEGF-C and VEGF-D

Arrows indicate cleavage sites of pre-protein convertases. SS, signal sequence; -S-S-, disulfide bonds; VHD, VEGF homology domain. The VHD is drawn in yellow, the N- and C-terminal peptide extensions in black, the plasma membrane in blue (modified from A. Stacker, *J Biol Chem*, 1999).

In contrast to angiogenic VEGFs, the fully processed VEGF-C and -D homodimers are linked exclusively via non-covalent interactions [54]. Also, only one human isoform of both VEGF-C and -D has been reported. Another dissimilarity in comparison to angiogenic VEGFs is that no affinity for heparin has been demonstrated for both lymphangiogenic growth factors.

Recently, a mutant form of VEGF-C termed VEGF-C156S has been generated by replacing the second of the eight conserved cysteine residues (Cys156) of the VHD with a serine. In contrast to VEGF-C, fully processed VEGF-C156S is a selective agonist of VEGFR-3 but not VEGFR-2 and has therefore enabled the study of VEGFR-3-specific biological functions (Figure 3, Table I) [55].

Table I. Structure, interactions and binding properties of VEGF family members

	VEGF Homology Domain (incl. cystein knot motif)	Length of isoforms* (aa)	% identity with VEGF-A165	Heparin interaction	Heterodimerization with	Receptors
VEGF-A	NH2 ccccccccc COOH	121, 145, 148, 162, 165, 165b, 183, 189, 206	100	145, 148, 162, 165, 183, 189, 206	PIGF-1 VEGF-B (VEGF-A ₁₆₅)	VEGFR-1 VEGFR-2 NP-1 (VEGF-A ₁₆₅) NP-2 (VEGF-A ₁₄₅ , VEGF-A ₁₆₅)
PIGF-1, -2, -3, -4	ccccccccc	131, 152, 203, 224	42-53	152, 224	VEGF-A ₁₆₅ VEGF-A ₁₂₁ (PIGF-1, PIGF-2)	VEGFR-1 NP-1 (PIGF-2) NP-2 (PIGF-2)
VEGF-B	ccccccccc	167, 186	41	167	VEGF-A ₁₆₅	VEGFR-1 NP-1
VEGF-C, -C156S	VEGF-C156S Cys → Ser c ccccccccc BR3P	388	32	no	-	VEGFR-2 (VEGF-C) VEGFR-3 NP-2
VEGF-D	ccccccccc BR3P	333	31	no	-	VEGFR-2 VEGFR-3 NP-2
VEGF-E (viral strains NZ-2, NZ-7, NZ-10, D1701, VR634)	ccccccccc	133	16-29	NZ-2	-	VEGFR-2 NP-1 (NZ-2, -10, D1701)
TfsvVEGF	ccccccccc	110-122	50	yes	-	VEGFR-1 VEGFR-2

BR3P: Balbiani ring 3 protein

C, Cys: Cysteine

NP: Neuropilin

Ser: Serine

TfsvVEGF: Trimeresurus flavoviridis snake venom VEGF

VEGFR: VEGF receptor

*Length of isoforms refers to the human forms except for VEGF-E and TfsvVEGF

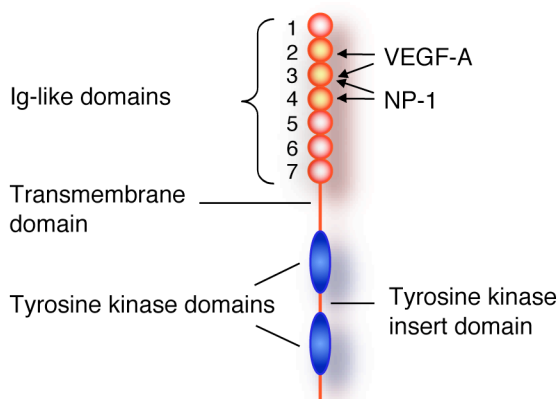
The VEGF homology domain is drawn in yellow, the peptide extensions of the VEGF-C and -D pre-propeptides in black
VEGF family members in brackets are the respective isoforms forming heterodimers or binding to indicated receptors

1.3.2. VEGFRs

The receptor tyrosine kinases VEGFR-1 (also known as fms-like tyrosine kinase (flt)-1), VEGFR-2 (also fetal liver kinase flk-1 or kinase insert domain receptor (KDR)), and VEGFR-3 (also fms-like tyrosine kinase (flt)-4) are the main signaling receptors for VEGF family members [56-58]. VEGFR-3 is present in two isoforms that differ in their C-termini through alternative splicing of the human VEGFR-3 gene [59]. In addition to the transmembrane receptors, VEGFR-1 and VEGFR-2 are also produced as alternatively spliced

soluble forms consisting of only the extra-cellular domains [60, 61]. sVEGFR-1 can act as a competitive inhibitor by sequestering VEGF-A, VEGF-B, and PlGF. Moreover, it may bind and inactivate membrane-bound VEGFR-1 and -2 through heterodimerization [60]. As such, the role of sVEGFR-1 has been studied both as a surrogate marker for disease progression and/or as a potential inhibitor of tumor angiogenesis in variety of cancers as well as for its possible contribution to diseases such as preeclampsia [62, 63]. The functional significance of sVEGFR-2 is unknown thus far.

The extra-cellular portion of transmembrane VEGFR-1 and -2 consists of seven immunoglobulin (Ig)-like domains, whereas the soluble forms contain only six (Figure 5). Also VEGFR-3 contains only six Ig-like domains since the fifth domain is proteolytically cleaved soon after biosynthesis and the resulting polypeptide chains remain linked via a disulfide bond (Figure 3)[45]. The second and third Ig-like domain of VEGFR-1 is involved in binding to VEGF-A and PlGF, whereas the third and fourth domain mediate interactions with NP-1 [64, 65]. The intra-cellular part of VEGFRs consists of a consensus tyrosine kinase sequence that is interrupted by a kinase-insert domain (Figure 5) [56].



Flk-1/ KDR/ VEGFR-2

Figure 5. Schematic representation of the VEGFR-2 structure

VEGFR-1 is similar in most structural aspects, while the fifth Ig-like domain of VEGFR-3 is cleaved and held together by disulfide bonds. Flk, fetal liver kinase; Ig, immunoglobulin; KDR, kinase insert domain receptor

Activation of receptors by their cognate ligands results in VEGFR homodimerization, cross-phosphorylation of distinct tyrosine residues in the tyrosine kinase domains and the subsequent triggering of intra-cellular signaling pathways. Furthermore, VEGFR-1 can trans-phosphorylate VEGFR-2, which leads to an enhancement of VEGF-A-mediated biological functions [44]. Recent studies also demonstrated the formation of VEGFR-1/-2 as well as VEGFR-2/-3 heterodimers. Whereas there is evidence that VEGFR-1/-2 heterodimers may be more active than the respective homodimers, the biological implications of VEGFR-2/-3 heterodimerization remains to be elucidated [44, 66].

As mentioned above, all VEGFRs are essential for the development of blood and lymphatic vessels, since mice deficient for either receptor are embryonically lethal before or during the development of the primary blood vascular plexus (see above and [47]). As shown in Figure 3, VEGFR-1 is predominantly expressed on blood endothelial cells but can be found also on many non-endothelial cells. During embryonic development, this receptor acts primarily as negative regulator of vasculogenesis and angiogenesis since mice lacking

VEGFR-1 exhibit uncontrolled endothelial cell proliferation, which results in the obstruction of vessel lumina [13]. Interestingly, expression of only the extra-cellular portion of VEGFR-1 is sufficient to rescue the phenotype [14]. The negative regulatory role of VEGFR-1 may be explained by the 10-fold higher affinity for VEGF-A but only weak tyrosine kinase activity when compared to VEGFR-2 [47]. In the adult, VEGFR-1 can provide growth and survival signals for blood endothelial cells and pericytes via the phospholipase C (PLC)- γ and mitogen activated protein kinase (MAPK) signaling pathway as well as migratory signals for macrophages [48, 67]. Importantly, VEGFR-1 is upregulated on pathological blood endothelium and is substantial for angiogenesis under ischemic, inflammatory, and malignant conditions [48, 68]. Furthermore, VEGFR-1 is involved in the preparation of the metastatic niche. VEGFR-1-positive haematopoietic progenitor cells were shown to colonize tumor-specific pre-metastatic sites prior to the arrival of tumor cells [69].

In contrast, VEGFR-2 is an essential mediator of the earliest steps of vasculogenesis. Similarly to VEGFR-1, VEGFR-2 is found on blood endothelium but also on hematopoietic precursor and other cells, and as mentioned above, embryos lacking VEGFR-2 fail to develop blood islands, endothelial cells, and major vessel tubes [10-12]. These and other experiments have demonstrated that VEGFR-2 is essential for growth, survival, and differentiation of endothelial cell progenitors and is the major mediator of mitogenic, angiogenic and permeability-enhancing effects of VEGF-A also in the adult [48]. While proliferative signals of VEGFR-2 are mainly transmitted via the PLC- γ and MAPK pathway, survival is provided via the phosphoinositide-3 kinase (PI3K)/Akt signaling cascade. PI3K-Rac, Cdc42-p38MAPK, and focal adhesion kinase FAK are involved in mediating migration, however, the mechanisms of PI3K and FAK activation are unknown so far [67]. Importantly, also lymphatic endothelial cells express VEGFR-2 to some extent, which may be one explanation for the recently reported lymphangiogenic activity of VEGF-A [70].

Also VEGFR-3 plays an essential role in early embryonic blood vessel development prior to the formation of lymphatic vessels [16]. Although being first expressed on blood endothelial cells early during development, this receptor becomes largely confined to embryonic and adult lymphatic endothelium and is the main mediator of lymphangiogenic signals induced by VEGF-C and -D. VEGFR-3-mediated proliferation is dependent on the proteine kinase C (PKC) and MAPK pathways, whereas survival signaling is mediated via PKB/Akt activation [67]. Nevertheless, VEGFR-3 is still expressed on fenestrated blood endothelium and can become re-expressed on blood vessels of tumors, thereby possibly also mediating VEGF-C and -D-induced angiogenic signals [45]. Interestingly, two subpopulations of macrophages and dendritic cells were recently described, which co-expressed immune cell markers and VEGFR-3 [37, 71]. Such cells could thus represent immune cells that were trans-differentiating into lymphatic endothelial cells, yet, such alternative mechanism of lymphangiogenesis remains to be further confirmed.

1.3.3. Neuropilins

NP-1 and -2 are transmembrane glycoproteins and have been first identified as co-receptors for axon guidance factors of the class-3 semaphorin subfamily, mediating repulsive

signals during neuronal axon guidance. The essential role of NPs in vascular development and maintenance as co-receptors for VEGF family members was discovered only later. NPs are expressed on neuronal, endothelial, and smooth muscle cells as well as monocytes [72]. In addition to semaphorins, NP-1 binds VEGF-A, VEGF-B, and PlGF-2, while NP-2 binds VEGF-A, VEGF-C, and PlGF-2 (Table I) [73]. Since semaphorins and VEGFs use the same binding site in the extra-cellular NP domain, they may compete for the receptor. Indeed such activity was shown for semaphorin-3A, which inhibited VEGF-A-induced sprout formation in an *in vitro* model of angiogenesis [74]. Yet, whether semaphorins modulate angiogenesis *in vivo* remains to be demonstrated.

The extracellular part of NPs contains two complement-binding domains that mediate interactions with semaphorins and VEGFs, two coagulation factor V/VIII homology domains involved in heparin binding and adhesion, and a MAM (meprin, A5, mu) domain, which is important for homo- and hetero-dimerization of NPs (Figure 6) [75, 76]. Although the cytoplasmic tail is short and contains no known signaling motif or homology domain, it probably plays an important, yet uncharacterized role. NPs may primarily modulate binding of VEGFs to VEGFRs and thereby VEGFR signaling rather than induce intrinsic signaling pathways [77]. Both NPs are expressed in several splice forms including soluble forms, which consist of only the extra-cellular domains and may act as natural inhibitors [78].

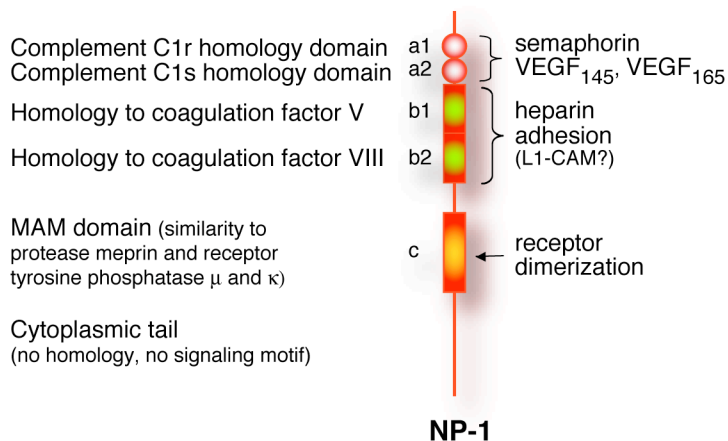


Figure 6. Schematic representation of the NP-1 structure

Ligands and functions are as indicated. MAM, meprin a5 mu; NP, neuropilin.

As mentioned above, NP-1 and -2 are involved in determining arterial/venous segregation and NP-2 is essential for lymphatic vessel development. Moreover, by associating with VEGFR-2, NP-1 enhances VEGF₁₆₅-induced migration of endothelial cells [79, 80]. A balance in these NP activities is essential, since transgenic mice in which NP-1 is expressed under the control of the ubiquitous actin promoter exhibit cardiac malformations, excessive blood vessels, and hemorrhages [81]. Conversely, inactivation of the NP-1 gene causes disorganized and insufficient vasculogenesis, transposition of large vessels as well as defects in cardiac development and neural vascularization [82]. In contrast, while exhibiting a severe reduction of small lymphatic vessels and capillaries, NP-2-deficient mice develop a normal blood vasculature [34]. Interestingly, combined NP-1/-2 knock-out mice resemble the phenotype of VEGF-A and VEGFR-2 gene-targeted mice [83]. In conclusion, NPs are

essential for VEGFR-1 and -2 to efficiently transduce VEGF-A-mediated signals in early development. Furthermore, NP-1 may also act as a heterologous cell adhesion molecule by interacting with L1-CAM via the b1 and b2 domains [84, 85]. Although the functional consequences of a possible NP-1-mediated adhesion remain to be investigated, it can be speculated that this activity may be also important for angiogenesis.

1.4. The role of VEGF family members in tumor angiogenesis and lymphangiogenesis

1.4.1. VEGFs and VEGFRs in tumor angiogenesis

In industrialized countries, cancer is presently responsible for about 25% of all deaths, therewith representing the second-most cause of death after cardiovascular diseases [86]. Like normal tissues, tumors require supply of oxygen and metabolites in order to grow beyond a size of 1-2 mm³ [87]. Therefore, they are dependent on a concomitantly growing blood vessel network, which forms like during vascular development by vasculogenesis and angiogenesis. Angiogenesis is orchestrated by a fine-tuned balance between secreted pro- and anti-angiogenic factors. Under physiologic conditions of the adult, blood endothelial cells are quiescent since anti-angiogenic factors such as thrombospondin and endostatin outweigh pro-angiogenic forces, including VEGF-A, PlGF, fibroblast growth factor 2, interleukin-8, TGF- β , PDGF and others. During carcinogenesis but also tissue regeneration and chronic inflammatory conditions, angiogenic factors are upregulated, which is commonly referred to as angiogenic switch, and become dominant over anti-angiogenic activities [88]. Importantly, not only tumor cells themselves but also cells of the tumor stroma such as endothelial cells, tumor-associated macrophages (TAMs), and carcinoma-associated fibroblasts (CAFs) secrete angiogenic growth factors. Furthermore, TAMs and CAFs produce matrix metalloproteases that activate latent or sequestered forms of these growth factors and modulate the ECM [89]. Notably, tumor blood vessels differ from the physiological vascular bed by their large size, tortuous shape, an only fragmented basement membrane, the presence of only few pericytes, and leakiness, which may result from an imbalance of angiogenic factors and inhibitors within a tumor. Particularly VEGF-A is known to induce the formation of disorganized and leaky vessels [90]. Moreover, many tumor vessels are not lined with endothelial but with tumor cells, which is termed vascular mimicry [91].

Numerous studies have established VEGF-A as a key angiogenic player in cancer (reviewed in [92]). VEGF-A is expressed in most tumors and its expression correlates with tumor microvessel density and growth. Tumoral expression of VEGF-A can be induced by a variety of stimuli, including genomic alterations such as mutant p53 and ras, erbB-2/Her2, activated epidermal growth factor receptor, bcr-abl fusion gene products, but also nitric oxide (NO) and other growth factors [47]. Due to hypoxia inducible factor (HIF)-regulated elements of its gene, VEGF-A is also strongly induced in hypoxic tumor areas [93]. In addition to mediating directly angiogenesis, VEGF-A also stimulates the recruitment of TAMs and CAFs (reviewed in [89]). Increasing data from clinical studies demonstrate that also expression of the VEGFR-1-selective ligands VEGF-B and PlGF is upregulated during tumorigenesis.

Moreover, a correlation between expression levels and tumor angiogenesis has been found in several of these reports, suggesting that both VEGF-B and PlGF might be involved in tumor angiogenesis and tumor growth [94-98]. In contrast to VEGF-A, the regulation of VEGF-B and PlGF gene expression as well as the impact of these growth factors on tumor angiogenesis is still incompletely understood. Furthermore, analysis of xenograft tumor models has revealed that VEGF-C and -D can also drive tumor angiogenesis and accelerate tumor growth, potentially as a result of VEGFR-2 activation [99, 100]. Yet, their significant contribution to angiogenesis in human tumors remains to be demonstrated.

VEGFR-2 is the main angiogenic signaling transducer of VEGF-A during tumor angiogenesis. Yet, unlike in physiological angiogenesis, VEGFR-1 signaling plays an important role in angiogenesis under pathological conditions including cancer, which is in line with the involvement of its ligands VEGF-B and PlGF in pathological angiogenesis [68, 101]. Similarly to VEGF-A, expression of VEGFR-1 but not VEGFR-2 or -3 is upregulated by hypoxia [102, 103]. In addition to mediate tumor angiogenesis, VEGFR-1 is involved in the induction of MMPs and in the paracrine release of growth factors from endothelial cells. Furthermore, in some cases VEGFR-1 is expressed by tumor cells and may mediate a chemotactic signal, thus potentially promote tumor cell migration and invasion [104].

Due to the essential role of angiogenesis for tumor growth, VEGF-A - and possibly also VEGF-B and PlGF - as well as its receptors have emerged as important targets for anti-cancer strategies. An advantage of anti-angiogenic treatment is that in contrast to the heterogenic and genetically unstable tumor cells that frequently develop resistance to chemotherapy, tumor endothelial cells are proliferating but remain genetically stable. Moreover, animal models have demonstrated that long-term inhibition of VEGF-A activity does not affect the physiological vasculature but significantly reduces tumor angiogenesis and induces even regression of tumor blood vessels, resulting in growth arrest of primary and secondary tumors [105, 106]. Detailed overviews of angiogenesis inhibitors and anti-angiogenic therapy can be found in [104, 107, 108].

1.4.2. VEGFs and VEGFRs in tumor-associated lymphangiogenesis

The fatality of cancer predominantly results from the dissemination of primary tumor cells to distant sites and the subsequent formation of metastases. Cancer cells spread via lymphatic or blood vessels or seed directly to body cavities. In the case of lymphogenous metastasis, cancer cells are passed through lymph nodes and may there form the first metastases. In patients with solid tumors, lymph node metastases are recognized for over 200 years [109]. Some of the most frequent tumor types, including melanoma, breast, lung, and gastrointestinal tract cancer, preferably spread via lymphatics, and sentinel lymph node biopsy of patients with these tumors is routinely used for refinement of prognostic and therapeutic measures. Since the lymphatic vasculature is specialized for entry and transport of immune cells, lymphogenous spread is more efficient than that via blood vessels. As mentioned above, lymphatic capillaries are larger than blood capillaries, display an only fragmented basal lamina, and display a special endothelial cell arrangement facilitating intravasation of cells. Moreover, the composition of lymph is similar to that of interstitial

fluid and flow velocities are low, thus allowing better cell viability as compared to the serum toxicity and shear stress encountered in the bloodstream [110]. In the past few years, tumor-associated lymphangiogenesis has gained increasing attention due to the discovery of lymphangiogenic growth factors, such as VEGF-C and -D, and specific markers for lymphatic endothelium, including VEGFR-3, LYVE-1, Podoplanin, and Prox-1. Recent clinical correlation studies have confirmed the proposed notion that the presence of lymphatic vessels in the vicinity of tumors favors lymphogenous metastatic dissemination of cancer cells [111, 112]. In contrast, contradictory results about the functionality and presence of intra-tumoral lymphatic vessels do not yet allow a clear conclusion with regard to their role in lymphogenous metastasis. Although there has been some debate whether preexisting lymphatic vessels are sufficient for lymphogenic metastasis, data from animal models and clinical studies combined clearly demonstrate a significant promotion of lymphogenic metastasis by tumor-induced lymphangiogenesis (reviewed in [89]).

Tumoral expression of VEGF-C emerges as a reliable marker for ongoing tumor lymphangiogenesis and increased risk of regional lymph node metastasis in many carcinomas [61, 113]. Data for VEGF-D are less consistent, suggesting that its ability to promote metastatic spread via lymphatics depends on the investigated tumor type and/or grade [114-116]. It is still unknown whether VEGF-C and D alter adhesive properties of tumor and endothelial cells and modify functional features of lymphatic vessels, which would actively enhance tumor cell adhesion to and intravasation into lymphatics. In addition, VEGF-C and D may activate lymphatic endothelial cells to secrete chemotactic factors for tumor cells [110].

Since expression of VEGF-C is stimulated by inflammatory mediators such as interleukin-1, tumor necrosis factor- α , COX-2, and COX-2-induced prostaglandins, lymphangiogenesis might be stimulated at sites of chronic inflammation to counteract inflammation-associated edema [117, 118]. This mechanism may also contribute to upregulation of VEGF-C in cancer, since tumors are known to be infiltrated by immune cells. Moreover, VEGF-A may also trigger expression of VEGF-C, thus, at sites of vessel remodeling or growth, lymphangiogenesis is stimulated in parallel to angiogenesis to maintain tissue fluid homeostasis [118]. VEGF-D, originally identified as c-fos-induced growth factor, is inducible by the AP-1 transcriptional activation pathway [42]. Moreover, it can be enhanced by cadherin-11-mediated cell-cell contacts, interleukin-7, and nitric oxide, whereas VEGF-D mRNA stability is downregulated by cytosolic β -catenin [119, 120]. β -catenin exists in different cellular pools, either associated with cadherins at the cell membrane contributing to cell adhesion, or in the cytoplasm, where it may participate in the canonical Wnt signaling pathway [121]. Repression by cytosolic β -catenin and upregulation in response to cadherin-11 suggests that expression of VEGF-D seems to depend on stable cellular interactions with the surrounding environment, which may have implications for the secretion of lymphangiogenic growth factors by migrating cells [118].

Recent data have demonstrated that the inhibition of tumor lymphangiogenesis with use of inhibitory anti-VEGFR-3 antibodies can suppress regional and distant metastasis in a mouse model of breast cancer [122]. The combined administration of anti-VEGFR-2 and -3 antibodies was even more potent and may represent a particularly promising approach for controlling metastasis. One might think that targeting tumor-associated lymphangiogenesis

might not be a promising anti-metastatic tool, since a large proportion of human tumors have already metastasized by the time of diagnosis. However, in addition to possibly prevent the occurrence of tumor cell dissemination in patients who display no detectable metastases at the timepoint of diagnosis, such therapy could also be of benefit for cancer patients already exhibiting local lymph node metastases. The “bridgehead concept of metastases” postulates that lymph node metastases form a reservoir of successfully metastasized tumor cells. These may already possess many of the properties required for further metastatic spread and may therefore disseminate more frequently to peripheral sites than cells from the primary tumor [123]. According to this hypothesis, inhibition of *de novo* lymphangiogenesis may therefore be of benefit even for cancer patients already suffering from local but not systemic lymph node metastases.

1.5. The Rip1Tag2 transgenic mouse tumor model

Mouse models of cancer enable the study of complex interactions between tumor cells and the tumor stroma as well as processes involved in tumor angiogenesis, lymphangiogenesis and metastatic disease *in vivo*. One approach of generating tumor-bearing mice is the introduction of highly oncogenic viral genes into the mouse genome. By use of tissue-specific promoters, expression of these oncogenes can be targeted to distinct organs, which are subsequently subject to malignant transformation. Using this technique, the Rip1Tag2 transgenic mouse model of β -cell carcinogenesis was established twenty years ago. In these mice, the early region of large T antigen (Tag) of simian virus 40 is expressed under the control of the rat insulin gene promoter (Rip) and thereby targeted to the insulin-producing β -cells of the endocrine pancreas [124]. Tag displays direct transforming functions and disrupts cell cycle control by sequestering and inactivating the tumor suppressor genes p53 and pRb [125]. Together, these activities induce malignant transformation and uncontrolled proliferation of β -cells resulting in the sequential formation of insulinomas over a period of 12-14 weeks.

The murine pancreas contains approximately 400 islets of Langerhans, which together constitute the endocrine part of the organ. Islets consist of several types of hormone-producing cells, including α -, β -, δ -, and PP cells, the most abundant being β -cells (80%). In Rip1Tag2 mice, β -cells start to express the transgene at embryonic day 8.5 (Figure 7). Hyperplastic islets begin to appear at around 4 weeks of age, and although all islets express Tag, only about 50% of the islets become hyperplastic at 10 weeks [126]. The onset of an angiogenic switch in a subset of hyperplastic islets triggers the formation of new blood vessels, resulting in the sequential emergence of angiogenic islets at 6 weeks and solid tumors at 9 to 10 weeks of age [127]. At 12 to 14 weeks, 2-4% of all initial islets have progressed into well-encapsulated, non-invasive benign tumors or adenomas and about 0.5% of islets into malignant, invasive carcinomas, the latter having the potential to metastasize [128]. Importantly however, metastases are very rarely encountered in Rip1Tag2 mice because the animals succumb already at 12-14 weeks of age to hypoglycemia caused by the massive tumoral production of insulin. The predictability and reproducibility of Rip1Tag2 tumorigenesis allows the study of distinct molecular events that may influence tumor growth and progression as well as tumor angiogenesis, lymphangiogenesis and metastasis.

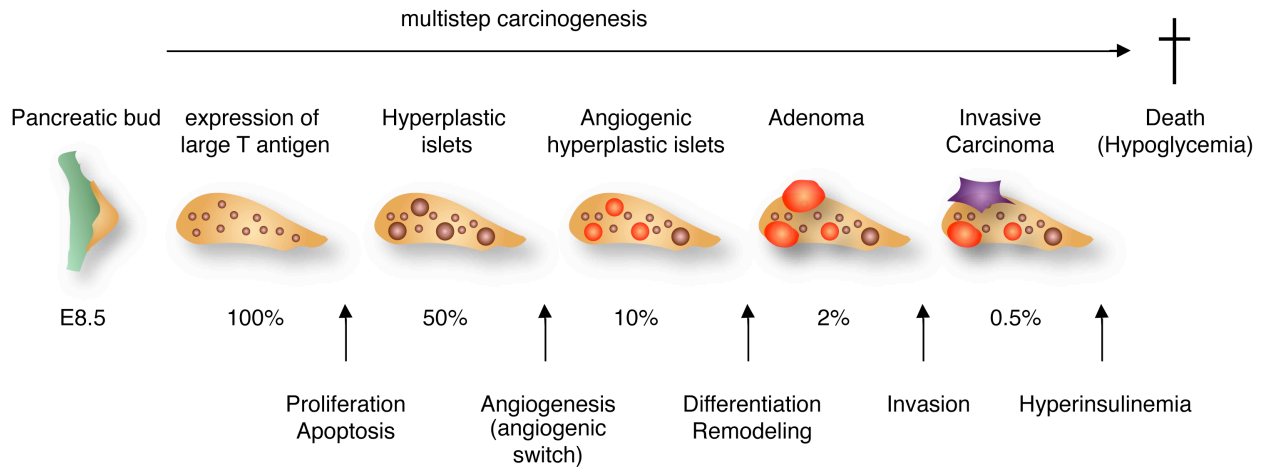


Figure 7. Multistep β -cell carcinogenesis in Rip1Tag2 transgenic mice

As indicated, islets (small brown circles) sequentially progress into hyperplastic islets (large brown circles), angiogenic islets (red circles), benign adenoma (large red shapes), and malignant carcinoma (magenta shape). Percentages indicate the subset of initial islets that have developed into a specific tumor grade at 12-14 weeks of age. The exocrine pancreatic tissue is drawn in light brown, the foregut in green. E8.5, embryonic day 8.5 (modified from G. Christofori, *Mol Endocrinol*, 1995).

1.6. Aim of the study

The objective of this study was to investigate and to compare side-by-side the biological effects elicited by different VEGF family members *in vivo* under physiological conditions as well as during carcinogenesis. Therefore, transgenic mice were generated expressing the VEGFR-1-specific ligands VEGF-B₁₆₇ and PlGF-1, the VEGFR-2-specific ligand VEGF-E_{D1701}, the VEGFR-2 and -3 ligand VEGF-D, as well as the VEGFR-3-specific ligand VEGF-C156S in β -cells of pancreatic islets of Langerhans. These single transgenic mice were analyzed with regard to different parameters including angiogenesis and lymphangiogenesis. In a second step, single transgenic mice were crossed with Rip1Tag2 mice, which resulted in the generation of double transgenic tumor mice expressing the respective ligand in tumor cells. The analysis of tumor angiogenesis and lymphangiogenesis, tumor progression, as well as metastasis allowed the identification of significant modulatory functions of the distinct VEGFs during tumorigenesis. Furthermore, the presented data demonstrate that activation of the same receptor by different VEGFs can elicit diverse or even opposing biological effects and that the same ligand can exert distinct functions depending on the encountered tumor microenvironment.

2. General Materials and Methods

Mouse tissue processing

Animal care was in accordance with Swiss Animal Protection Ordinance issued by the Swiss Federal Veterinary Office. Single transgenic Rip1VEGF-B₁₆₇, Rip1VEGF-C156S, Rip1VEGF-D, Rip1VEGF-E_{D1701}, and Rip1PIGF-1 mice were sacrificed between 12 and 13 weeks if not indicated otherwise. Generation and phenotypic characterization of Rip1Tag2 mice was as described previously [124]. Tumor-bearing Rip1Tag2;Rip1VEGF-B₁₆₇, Rip1Tag2;Rip1VEGF-C156S, Rip1Tag2;Rip1VEGF-D, Rip1Tag2;Rip1VEGF-E_{D1701}, and Rip1Tag2;Rip1PIGF-1 double transgenic and Rip1Tag2 littermate control mice were sacrificed between 12 and 13 weeks of age. Tumor incidence per mouse was determined by counting all macroscopically apparent pancreatic tumors with a minimal diameter of 1mm. The tumor volume was defined as total tumor volume per mouse in mm³. The volume of each macroscopically visible tumor was calculated by measuring the tumor diameter assuming a spherical shape of the tumors.

Tumors and pancreata were either embedded in OCT (Tissue Tek, Torrance, CA) and freshly snap frozen in liquid nitrogen or fixed overnight in 4% paraformaldehyde in PBS, dehydrated in a Microm Spin Tissue Processor STP-120 (Microm, Volketswil, Switzerland) and paraffin-embedded. 5 µm fresh frozen sections were methanol-fixed for 10 min at -20°C or fixed in 70% ethanol for 2 min at room temperature prior to storage at -80°C. 5 µm paraffin-embedded tissue sections were deparaffinized and rehydrated prior to usage according to standard procedures.

Histopathological analysis

Histologic sections were analyzed by hematoxylin and eosin staining, immunohistochemistry and immunofluorescence. The following antibodies were used for immunohistochemistry or immunofluorescence on paraffin sections: goat anti-human VEGF-B_{167/189} (R&D Systems, Minneapolis, MN), rabbit anti-rat VEGF-C (Reliatech, Braunschweig, Germany), rabbit anti-rat VEGF-D (Reliatech, Braunschweig, Germany), guinea pig anti-insulin (DakoCytomation, Glostrup, Denmark), rabbit anti-mouse LYVE-1 (Reliatech, Braunschweig, Germany), hamster anti-mouse podoplanin (8.1.1; Developmental Studies Hybridoma Bank, Iowa University, Iowa City, Iowa), rat anti-mouse CD31 (PharMingen, Franklin Lakes, NJ), mouse anti-mouse smooth muscle actin (Boehringer Mannheim, Germany), rabbit anti-mouse NG-2 (Chemicon, Hampshire, UK), biotinylated mouse anti-BrdU (Zymed, South San Francisco, CA) for detection of proliferating cells, In Situ Cell Death Detection Kit, POD (terminal deoxynucleotidyl transferase-mediated nick end labeling (TUNEL); Roche, Basel, Switzerland) for visualization of apoptotic cells. All biotinylated secondary antibodies for immunohistochemistry (Vector, Burlingame, CA) were used at a 1:200 dilution, and positive staining was visualized with the ABC horseradish peroxidase kit (Vector) and DAB Peroxidase Substrate (Sigma Chemical Co., St. Louis, MO) according to the manufacturer's recommendations. For analysis of tissue morphology, slides were slightly

counterstained with hematoxylin or eosin. Alexa Fluor 568- and 488-labeled secondary antibodies (Molecular Probes, Eugene, OR) diluted 1:400 were used for immunofluorescence analysis. 6-Diamidino-2-phenylindole (DAPI) was used for nuclear staining in immunofluorescence stainings. All paraffin-embedded sections were subject to antigen retrieval with 10 mM citrate buffer (microwave) except for VEGF-D and insulin (10 min in 0.2% Triton X-100 in PBS), CD31 (10 min 0.1% Proteinase K (Fluka) in PBS at 37°C), BrdU (1h in 2N HCl and subsequently 1 h 1x trypsin at room temperature), and TUNEL (10 min 2 μ g/ml Proteinase K (Fluka) at room temperature). Rabbit anti-VEGF-E (#1384 and #1385, kindly provided by Prof. C. Dehio, Division of Molecular Microbiology, Biozentrum, Basel, Switzerland), rat anti-mouse CD45, CD4, CD8, CD45R/B220 (all from BD Biosciences, San Jose, CA), rat anti-mouse F4/80 (Serotec, Oxford, UK), rabbit anti-mouse Prox1 (a gift from K. Alitalo, Molecular/Cancer Biology Laboratory, Biomedicum, University of Helsinki, Helsinki, Finland), rat anti-mouse flt-4 (eBioscience, San Diego, CA) and double stainings for CD-31 and LYVE-1 were exclusively performed on frozen sections and by immunofluorescence. For each staining, sections of control mice or respective serial sections of transgenic mice without primary antibody incubation were used as negative control. Stained sections were viewed on a Axioskop 2 plus light microscope (Zeiss, Feldbach, Switzerland) using the axiovision 3.1. software (Zeiss, Feldbach, Switzerland) or a Nikon Diaphot 300 immunofluorescence microscope (Nikon, Egg, Switzerland) using the Openlab 3.1.7. software (Improvision, Coventry, England).

For BrdU labeling, 100 μ g BrdU (Sigma Chemical Co., St. Louis, MO) per gram body weight were injected 90 min before sacrificing the mice. To determine tumor cell proliferation/apoptotic indices, BrdU-/TUNEL-positive nuclei were counted per randomly chosen 40x magnification field of tumor tissue, respectively. Approximately 10 fields/mouse were counted.

Accordingly, tumoral blood vessel density was assessed by counting the CD31-positive vessels per 40x magnification field of tumor tissue if not otherwise indicated.

Lymphangiogenesis was quantified by assessing the extent by which LYVE-1-positive lymphatic vessels surrounded the tumor perimeter. Tumors from all mice of a genotype were grouped into three classes: tumors that were not in contact with any lymphatic vessel (0%), tumors that were surrounded less than 50% (<50%), and tumors that were surrounded more than 50% of the tumor perimeter by lymphatics (>50%).

The blood vessel density of islets as well as Rip1Tag2;Rip1PIGF-1 and ectopic subcutaneous Rip1Tag2 and Rip1Tag2;Rip1VEGF-D tumors was determined upon immunofluorescence staining with anti-CD31 antibody and subsequent analysis with the ImageJ software of the National Institutes of Health (<http://rsb.info.nih.gov/ij/>). The islet diameter was measured on pictures of HE-stained slides using the Axiovision software 3.1. Intra-insular NG-2-positive pericytes as well as intra-tumoral CD45-positive immune cells, F4/80-positive macrophages, B220-positive B lymphocytes, and CD4- and CD8-positive T lymphocytes were visualized by immunofluorescence on serial sections and quantified with the ImageJ software.

Lectin Perfusion

For analysis of functional blood vessels, mice were inhalation-anesthetized with isoflurane (Minrad Inc., Buffalo, NY) and tail vein-injected with 100 μ l of 1 mg/ml fluorescein-labeled *lycopersicon esculentum* lectin (Vector, Burlingame, CA). After 5 min, mice were heart-perfused with 10 ml of 4% paraformaldehyde followed by 10 ml PBS. Isolated pancreata were immersed in ascending concentrations of sucrose (12%, 15% and 18%, for 1 h each), embedded in OCT and snap frozen in liquid nitrogen.

Tumor grading

All tumors found on a representative pancreatic section of a given mouse genotype were categorized into following sub-classes: normal/hyperplastic islet (including normal as well as enlarged islets), adenoma (larger than 1 mm in diameter, well differentiated tumor cells, encapsulated tumor, no invasive tumor edges), carcinoma grade I (well differentiated and homogenous appearance of tumor cells, tumor capsule partially absent, one invasive tumor edge), carcinoma grade II (partially dedifferentiated and heterogenous appearance of tumor cells, tumor capsule largely absent, more than one invasive tumor edge), carcinoma grade III or anaplastic tumor (complete loss of tumor cell differentiation, very heterogenous tumor appearance). In statistical tables, normal/hyperplastic islets and adenomas were summarized as benign, all carcinomas as malignant tumors.

Collagen Gel Assay

For collagen gel assays, islets from single transgenic Rip1VEGF-D and Rip1PIGF-1 mice as well as tumors from 8-10 week-old Rip1Tag2 and Rip1Tag2;Rip1VEGF-D mice were isolated by retrograde perfusion of the common bile duct with a collagenase/DNase solution as described (Collagenase Type IV and DNase I from Worthington, Lakewood, NJ) [129]. Human umbilical vein endothelial cells (HUVECs) were cultured in Medium199 supplemented with 20% FBS, 4 mM glutamine, 40 μ g/ml bovine brain extract, 80 units/ml heparin, and 100 U/ml penicillin (all cell culture articles were purchased from Sigma Chemical Co., St. Louis, MO). HUVECs were trypsinized, resuspended in 10% FBS RPMI, and co-cultured with islets/tumors in a three-dimensional collagen matrix (Vitrogen from Nutacon, Leimuïden, Netherlands) as described [127]. After 2–3 days, the response of endothelial cells to islets and tumors was scored. Approximately 30 islets/tumors were analyzed per genotype.

Electron microscopy

For light and transmission electron microscopy, mice were perfused with PBS followed by Karnovski solution. In collaboration with Prof. V. Djonov, isolated pancreata were postfixated in osmium tetroxide, block-stained using uranyl acetate, dehydrated through ascending concentrations of ethanol, and embedded in epoxy resin. Semithin sections were obtained at a nominal thickness of 1 μ m, stained with toluidine blue, and viewed under a

Leica light microscope. Ultrathin sections were obtained at 80-90 nm, counterstained with lead citrate, and viewed on a Philips EM-300 microscope.

Corrosion cast analysis

In collaboration with Prof. V. Djonov, Mercor (Japan Vilene Co) vessel casts were prepared of pancreata from Rip1VEGF-D J97 and C57BL/6 mice. The vasculature was perfused with a solution of 0.9% sodium chloride containing 1% heparin (Liquemine; Roche Pharma AG, Reinach, Switzerland) and 1% procaine followed by a freshly prepared solution of Mercor containing 0.1 mL accelerator per 5 mL resin according to [130]. After 2 to 4 weeks of tissue dissolution in 15% KOH, casts were dehydrated in ethanol and dried in a vacuum desiccator. Samples were glued onto stubs with carbon, sputtered with gold, and examined with a Philips XL 30 FEG scanning electron microscope.

3. Generation and analysis of transgenic mice expressing lymphangiogenic VEGF family members during Rip1Tag2 tumorigenesis

3.1. Distinct Roles of Vascular Endothelial Growth Factor-D in Lymphangiogenesis and Metastasis

Lucie Kopfstein¹, Tanja Veikkola^{2,3}, Michael Jeltsch², Valentin G. Djonov⁴, Karin Strittmatter¹, Kari Alitalo², Gerhard Christofori¹

¹Department of Clinical-Biological Sciences, Institute of Biochemistry and Genetics, University of Basel, 4058 Basel, Switzerland

²Molecular/Cancer Biology Laboratory, Biomedicum, University of Helsinki, Helsinki 00014, Finland

³Present address: Amgen, 02101 Espoo, Finland

⁴Institute of Anatomy, University of Berne, 3012 Berne, Switzerland

Running title: VEGF-D promotes lymphogenous metastasis

This work was supported by grants from the Swiss National Science Foundation, the Swiss Cancer League, the Swiss Bridge Award, the Krebsliga Beider Basel, the EU-FP6 framework programmes LYMPHANGIOGENOMICS LSHG-CT-2004-503573 and BRECOSM LSHC-CT-2004-503224, and Novartis Pharma Inc.

3.1.1. Abstract

Metastasis is the foremost cause for cancer death. In many human carcinomas, expression of the lymphangiogenic factor vascular endothelial growth factor-D (VEGF-D) correlates with regional lymph node metastasis. This study addressed the effect of VEGF-D on tumor lymphangiogenesis and metastasis. Therefore, Rip1VEGF-D transgenic mice were generated, expressing the transgene in β -cells of pancreatic islets of Langerhans. Whereas wildtype islets were not associated with lymphatics, Rip1VEGF-D islets were surrounded by lymphatic vessels, often containing leucocyte accumulations and hemorrhage. These mice were crossed with Rip1Tag2 mice, a well-characterized transgenic model of poorly metastatic pancreatic β -cell carcinogenesis. Rip1Tag2;Rip1VEGF-D mice formed tumors surrounded by lymphatics and frequently developed lymph node and lung metastases. Tumor hemangiogenesis was significantly reduced *in vivo* and *in vitro*. In contrast, tumors resulting from subcutaneous injection of Rip1Tag2;Rip1VEGF-D cells exhibited intra-tumoral lymphangiogenesis, while hemangiogenesis was unaffected. Our results demonstrate that VEGF-D-induced lymphangiogenesis promotes metastasis to lymph nodes and lungs and that VEGF-D-elicited effects are dependent on the tumor microenvironment. Furthermore, the comparison of Rip1Tag2;Rip1VEGF-D with the previously described Rip1Tag2;Rip1VEGF-C mice revealed unexpected functional differences between VEGF-D and VEGF-C.

3.1.2. Introduction

VEGF-D and -C, the only known ligands for VEGFR-3, belong to the VEGF family of ligands (reviewed in [45]). Proteolytic processing of human VEGF-D and -C by proprotein convertases, plasmin and other (thus far unknown) proteases generates the mature ~40 kDa homodimers, which display increased affinity for VEGFR-3 but also for VEGFR-2 that is predominantly expressed on blood endothelium [131, 132]. While VEGF-C exhibits the same binding properties in mice, processed mouse VEGF-D (VEGF-DANAC) exclusively activates mouse VEGFR-3 [133]. Mature human VEGF-D however activates both mouse VEGFR-2 and 3 (K. Alitalo, unpublished observations). VEGF-C binds also to the co-receptor NP-2, which is expressed on lymphatic endothelium and is essential for normal lymphatic vessel development [34]. The binding capacity of VEGF-D to NP-2 remains to be investigated.

Recent mouse knock-out studies have shown that VEGF-D is dispensable for the development of a lymphatic system during embryogenesis and cannot compensate for absent VEGF-C in VEGF-C^{-/-} mice, which fail to develop functional lymphatic vessels [32, 134]. Nevertheless, the lymphangiogenic and angiogenic potency of VEGF-D has been clearly demonstrated. Ectopic expression of mouse VEGF-D in the skin of K14-VEGF-D transgenic mice induced dermal lymphangiogenesis, and adenoviral delivery of human VEGF-D into rabbit skeletal muscle, adventitia of rabbit carotid arteries, and porcine hearts induced both lymphangiogenesis and angiogenesis [135-138].

The role of VEGF-D in tumor metastasis has been recently addressed in several clinical and animal studies. In a number of human cancers, including papillary thyroid, gastric, pancreatic, colorectal, breast, ovary and endometrial carcinoma, an elevated tumoral VEGF-D

expression correlates with an increased incidence of regional lymph node metastases [113, 114, 139-142]. In three of these studies, a concomitant increase in peri-tumoral lymphangiogenesis as the underlying mechanism of enhanced lymphogenous metastasis has been reported [139, 140, 143]. Moreover, xenotransplantation of human carcinoma-derived cell lines expressing VEGF-D into immunocompromised mice resulted in enhanced lymphogenous metastasis via induction of tumor-associated lymphangiogenesis [100, 144, 145]. Together, these studies indicate that tumoral overexpression of VEGF-D may promote tumor-associated lymphangiogenesis and thereby lymphogenous metastasis.

To investigate the effect of VEGF-D on tumor development and metastasis, we have generated Rip1VEGF-D transgenic mice, in which the expression of human VEGF-D is driven by the rat insulin promoter (Rip1) and thereby is specifically targeted to β -cells of pancreatic islets of Langerhans. Rip1VEGF-D mice were subsequently crossed to Rip1Tag2 tumor mice, a transgenic mouse model of poorly metastatic β -cell carcinogenesis [124], and tumor lymphangiogenesis, angiogenesis, and metastasis were analyzed in double-transgenic Rip1Tag2;Rip1VEGF-D mice. We furthermore aimed to compare this newly established mouse model with the previously described Rip1VEGF-C and Rip1Tag2;Rip1VEGF-C mice, where VEGF-C has been shown to promote peri-tumoral lymphangiogenesis and lymph node metastasis [146]. The side-by-side comparison of effects elicited by these two highly related lymphangiogenic growth factors revealed not only similarities but also fundamental and unexpected differences with regard to tumor growth and metastatic dissemination.

3.1.3. Materials and Methods

Transgenic Mouse Lines

Rip1VEGF-D transgenic mice were generated by M. Jeltsch and T. Veikkola (Molecular/Cancer Biology Laboratory, Biomedicum, University of Helsinki, Helsinki, Finland) according to standard procedures [147]. The cDNA encoding the 1065 bp coding region of human VEGF-D (nucleotides 411-1475, Acc. No. AJ000185) was cloned between the 704 bp BamHI/XbaI fragment of the rat insulin gene II promoter (Rip1; [124]) and a 436 bp fragment containing SV40 introns and polyadenylation signal sequences.

Genotypes were confirmed by Southern blot and PCR analysis. Routine PCR screening of Rip1VEGF-D heterozygotes was performed using a primer pair specific for the transgene (forward primer located in the Rip1 sequence: 5'-TAATGGGACAAACAGCAAAG; reverse primer located in the human VEGF-D sequence: 5'-TCCAAACTAGAAGCAGCCCTGATCT), starting from standard toe or tail genomic DNA preparations. PCR cycles were: 94°C, 5 min (x1); 94°C, 30 sec, 58°C, 30 sec, and 72°C, 30 sec (x34); and 72°C, 7 min (x1). PCR products were analyzed in 1.5% agarose gels.

Glucose measurements

Blood glucose levels of mice were measured by tail vein blood sampling using the Accu-Chek Comfort device and test stripes (Roche Diagnostics Corporation, Indianapolis, IN). Basal glucosemy was assessed on mice fasting for six hours. Intra-peritoneal glucose tolerance tests (IPGTT) were performed on 8 to 21 week-old mice with a body weight

between 25 and 35 grams. Mice were starving for 16 hours and subsequently i.p. injected with 1 gram D-(+)-Glucose anhydrous (Sigma Chemical Co., St. Louis, MO)/kg body weight. Blood glucose levels were measured 0, 20, 40, 70 and 100 min after injection. The maximum measurable blood glucose concentration was 34 mmol/l, and mice were considered hyperglycemic when fasting blood glucose levels were >6 mmol/l or peak glucose levels during the IPGTT were >13 (which was the maximum measurement for wildtype littermate controls). Data represent mean \pm standard deviation.

Immunoblotting

The processing status of VEGF-D expressed by Rip1VEGF-D islets, Rip1Tag2;Rip1VEGF-D and Rip1Tag2 tumors as well as of cell lines established from Rip1Tag2;Rip1VEGF-D and Rip1Tag2 tumors was assessed by immunoblotting. Protein lysates of tumors from twelve week-old Rip1Tag2;Rip1VEGF-D and Rip1Tag2 mice were obtained by homogenization of isolated tumors with a polytron tissue grinder in lysis buffer and subsequent centrifugation. Islets of Rip1VEGF-D mice were resuspended in standard sample buffer and sonicated for five min. 40 μ g of tumor and cell line protein and the total islet lysate were resolved by 12% SDS-PAGE, transferred to Immobilon-P membranes (Millipore) and probed with 5 μ l/ml rabbit anti-rat VEGF-D antibody (Reliatech, Braunschweig, Germany) using the Uptilight chemiluminescence system (Uptima, Montluçon, France). 10 ng of recombinant human VEGF-D (R&D Systems, Minneapolis, MN) were used as positive control.

Cell culture

Tumor cell lines were established from insulinomas of twelve week-old Rip1Tag2 and Rip1Tag2;Rip1VEGF-D mice. Therefore, tumors were excised from pancreata and single-cell suspended in cold PBS. The suspension was mixed 1:1 with DMEM supplemented with 10% fetal bovine serum, 10 % horse serum, 2 mmol/L glutamine and 100 units/mL penicillin. After 1 minute of sedimentation at room temperature, the supernatant was transferred to a new tube, re-mixed 1:1 with medium and let sediment another 10 min at room temperature. The pellet containing the tumor cells was resuspended and cells were plated on 24-well plates for further expansion. 10^6 cells were injected subcutaneously into the two flanks of mice anesthetized with isoflurane (Minrad Inc., Buffalo, NY).

ELISA

We determined tumor-derived circulating human VEGF-D levels in sera of 12 week-old C57BL/6, Rip1VEGF-D, Rip1Tag2, and Rip1Tag2;Rip1VEGF-D mice by using the Human VEGF-D Quantikine ELISA Kit (R&D Systems, Minneapolis, MN) according to the manufacturer's protocol. Blood was derived by heart puncture of mice inhalation-anesthetized with isoflurane. Sera were obtained by clotting of punctured blood for 1 hour at room temperature and subsequent centrifugation for 20 min at 3000 rpm.

For histopathological analysis, lectin perfusion, electron microscopy, and vascular cast analysis refer to General Materials and Methods

3.1.4. Results

Peri-insular lymphangiogenesis in Rip1VEGF-D transgenic mice

To generate transgenic mice expressing human VEGF-D specifically in β -cells of pancreatic islets of Langerhans, a cDNA comprising the full-length coding sequence of human VEGF-D (hVEGF-D) was cloned between the rat insulin II gene promoter fragment (Rip) and the human growth hormone introns and a polyadenylation signal (Figure 1). Injection of the transgene into fertilized C57BL/6 oocytes resulted in seven viable and fertile founder lines exhibiting stable germline transmission.

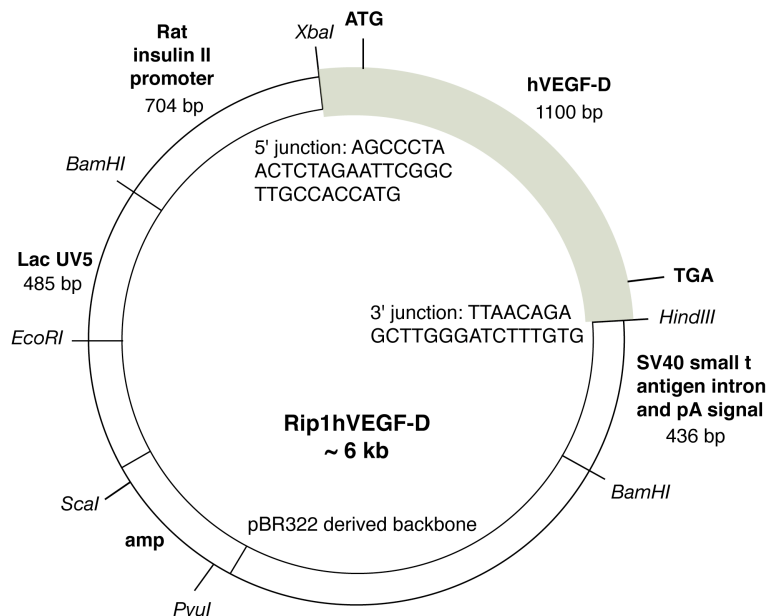


Figure 1. Cloning of the Rip1VEGF-D construct
The blunted EcoRI-hVEGF-D was ligated to the XbaI/HindIII-opened Rip1 vector.

Immunohistochemical and immunofluorescence analysis of pancreatic sections revealed that transgenic founder lines expressed VEGF-D specifically in islets of Langerhans, whereas no VEGF-D expression was detectable in islets of wildtype littermate mice (Figures 2A and B). No VEGF-C expression could be detected in Rip1VEGF-D mice by immunohistochemistry (data not shown). The founder line Rip1VEGF-D J97 exhibited the most intense β -cell-specific signal for VEGF-D and was used for phenotypical analysis. The founderlines Rip1VEGF-D B12 (only weakly expressing VEGF-D) and Rip1VEGF-D E2 (exhibiting strong VEGF-D expression) served as controls in several experiments. In the following, Rip1VEGF-D refers to the Rip1VEGF-D J97 founderline if not otherwise noted.

To investigate morphological changes elicited by transgenic VEGF-D expression, we analyzed pancreata of Rip1VEGF-D and littermate control mice by histology, immunohistochemistry, immunofluorescence, and electron microscopy. Hematoxylin and eosin stainings as well as toluidine blue-stained semi-thin sections of pancreata revealed that most islets of Rip1VEGF-D mice were separated from the surrounding exocrine tissue by large endothelium-lined clefts, whereas islets of wildtype mice were completely embedded in the exocrine pancreas (Figures 2C-F). Based on immunoreactivity for the lymphatic

endothelium marker LYVE-1, peri-insular lacunae were identified as lymphatic vessels (Figure 2H).

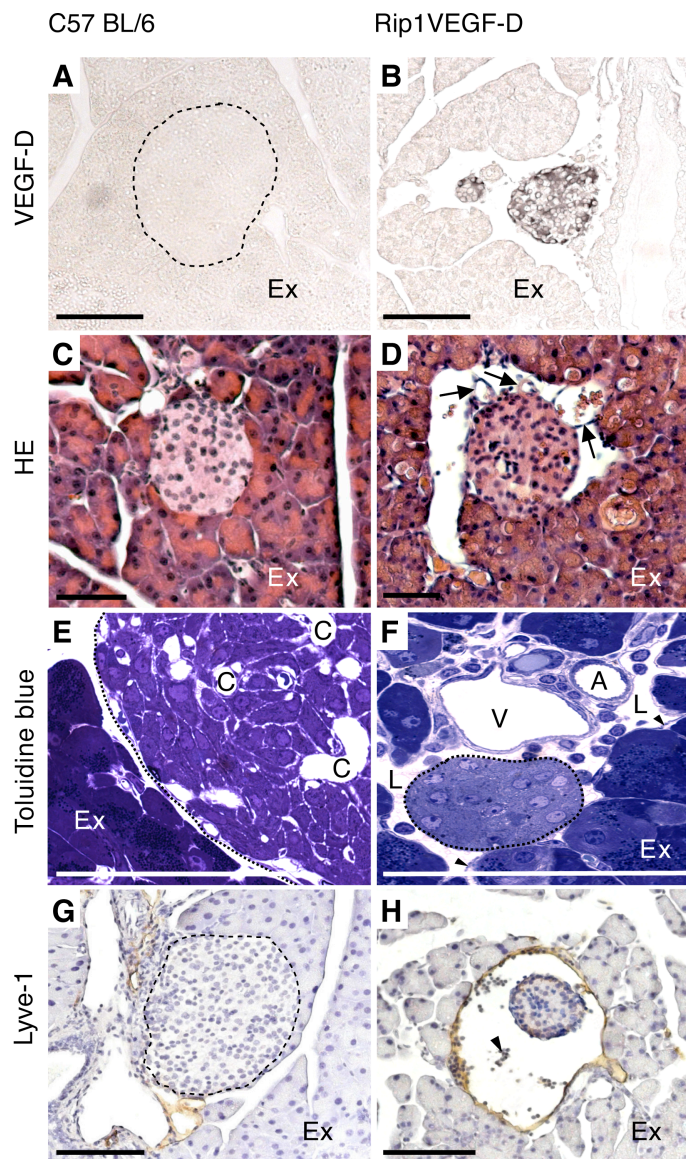


Figure 2. Histological analysis of pancreata from C57BL/6 control and transgenic Rip1VEGF-D mice

(A, B) Immunohistochemical staining for VEGF-D (grey) (C, D) Hematoxylin and eosin staining (E, F) Toluidine blue-stained semi-thin sections. Note the intra-lymphatic lymphocytes and the smaller size of the transgenic islet, which lacks blood capillaries on this section (see also quantification of islet microvessel density below) (G, H) Immunohistochemical staining for LYVE-1 (brown). Dashed lines demarcate islets, arrows in (B) indicate intra-lymphatic blood vessels, arrowheads in (F) indicate endothelial lining, arrowhead in (H) indicates immune cells; A, artery; C, blood capillary; Ex, exocrine tissue; L, lymphatic lacuna; V, vein. Scale bars (A-H): 100µm.

Analysis by transmission electron microscopy (TEM) revealed that peri-insular lacunae displayed typical features of lymphatic endothelium. As shown in Figure 3A, the endothelial cells lacked fenestrations and cells were in part overlapping (black arrowheads). Moreover, the basement membrane was discontinuous or even absent and the abluminal endothelial surface was closely associated with collagen fibrils (asterisks) produced by the adjacent fibroblasts (white arrowheads). However, no lymphatic vessels were observed in the islets themselves. Thus, similarly to VEGF-C in the previously characterized Rip1VEGF-C mice [146], VEGF-D exerts a lymphangiogenic function by promoting peri-insular lymphangiogenesis in Rip1VEGF-D mice.

In contrast to the previously described Rip1VEGF-C mice, the newly formed lymphatic vessels of Rip1VEGF-D mice contained immune cells, which accumulated with

increasing age of the mice and filled the entire lacuna (Figure 3A-G). These cells were readily detectable by hematoxylin and eosin staining, and characterization using immunofluorescence staining revealed that most of the leucocytes were CD4-positive T helper and B220-positive B lymphocytes as well as F4/80-positive macrophages. CD8-positive cytotoxic T lymphocytes were absent from the clusters. Some leucocytes were also found in islets themselves by immunofluorescence analysis (Figure 3D and 3F).

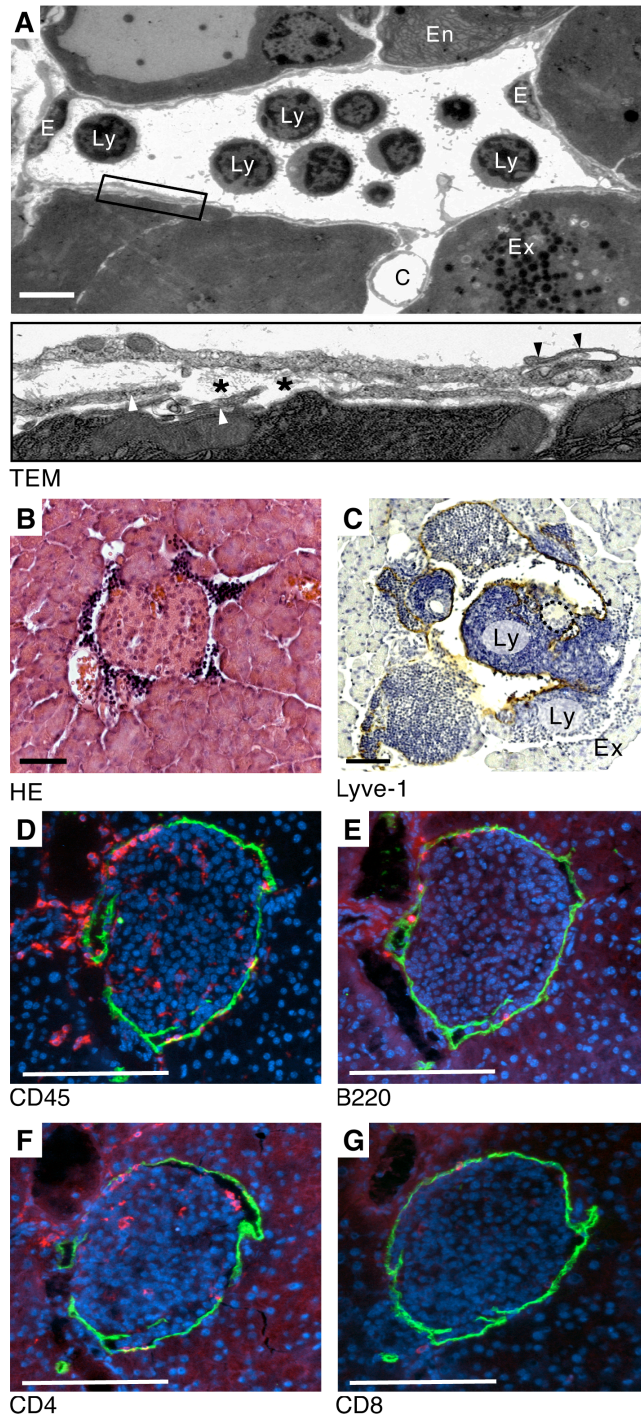


Figure 3. Intra-lymphatic immune cell accumulations in Rip1VEGF-D mice

(A) TEM showing a peri-insular lymphatic lacuna containing lymphocytes. The inset is a higher magnification of the boxed area as indicated. Asterisks indicate collagen fibrils in the abluminal space of the lacuna, black arrowheads indicate overlapping lymphatic endothelial cells, white arrowheads indicate fibroblasts

(B) Hematoxylin and eosin staining of a pancreatic section from a six month-old Rip1VEGF-D mouse (C) Immunohistochemical analysis of a 12 moth-old Rip1VEGF-D pancreas with anti-LYVE-1 antibody (brown, counter-staining with hematoxylin). The dashed line delineates the islet

(D-G) Double immuno-fluorescence analysis with anti-LYVE-1 (green) and (D) anti-CD45 (red) (E) anti-B220 (red) (F) anti-CD4 (red) and (G) anti-CD8 antibody (red) of a 12 week-old Rip1VEGF-D mouse. Nuclei are counterstained with DAPI. C, blood capillary; E, endothelial cells; En, endocrine tissue; Ex, exocrine tissue; Ly, lymphocytes. Scale bars: (A) 15µm, (B, C) 100µm, (D-G) 50µm.

Generation of transgenic mice using the Rip1 vector construct has repeatedly resulted in the induction of an immune cell-mediated diabetic phenotype (G. Christofori, personal communication). Also mice deriving of one of the Rip1VEGF-D founderlines, namely Rip1VEGF-D E2, exhibited typical symptoms of diabetes including polyuria and died within few months of age. To investigate, whether immune cell accumulations observed in Rip1VEGF-D J97 mice resulted from an immune response of the mouse immune system to the human transgene, we compared the pancreatic histology of Rip1VEGF-D J97 with that of Rip1VEGF-D E2 mice and performed several blood glucose measurements. As shown in the right panel of Figure 4A, accumulations of immune cells were found around but also actively infiltrating islets of 14 week-old Rip1VEGF-D E2 mice. Probably as a result of immune cell-mediated destruction of β -cells, only few islets were detectable on a given pancreatic section. In contrast, pancreatic sections of age-matched Rip1VEGF-D J97 mice harbored comparable numbers of islets as control mice. Also, on common hematoxylin and eosin-stained sections and upon immunohistochemical stainings counterstained with hematoxylin, immune cell accumulations were found to surround a subset of islets but were never found to infiltrate such (left panel of Figure 4A). Furthermore, repeated fasting glucose measurements revealed pathologically elevated blood glucose levels and thus diabetes in Rip1VEGF-D E2 but not Rip1VEGF-D J97 mice (data not shown). Even a more sensitive intraperitoneal glucose tolerance test demonstrated a normal glucose metabolism in Rip1VEGF-D J97 mice comparable to that of Rip1VEGF-D B12 and C57BL/6 control mice, whereas again, Rip1VEGF-D E2 mice exhibited pathologically elevated blood glucose levels (Figure 4B). Together, these data eliminate an auto-immune reaction as cause of immune cell accumulations found around islets of Rip1VEGF-D J97 mice. In comparison, in Rip1VEGF-C mice, immune cells in peri-insular lymphatic vessels were not detectable on common histologic sections and no clusters were observed [146].

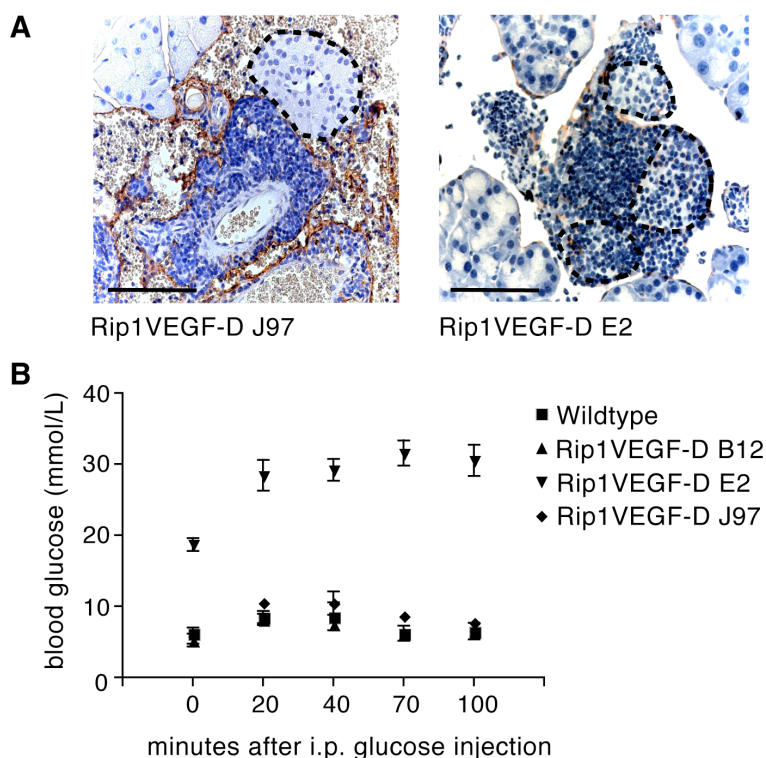


Figure 4. Islet-associated immune cells and intraperitoneal glucose tolerance tests of Rip1VEGF-D transgenic founderlines B12, E2 and J97

(A) Immunohistochemical staining with anti-Podoplanin antibody on pancreata of Rip1VEGF-D J97 and Rip1VEGF-D E2 mice (B) dynamics of serum glucose levels of two Rip1VEGF-D B12, three Rip1VEGF-D J97, three Rip1VEGF-D E2 and three C57BL/6 mice upon glucose challenge at timepoint 0. Data represent means \pm SD. Dashed lines delineate islets, Scale bars: 50 μ m.

Surprisingly, we found that many lymphatic lacunae and regional lymph nodes of Rip1VEGF-D mice contained erythrocytes, which were never found in lymphatic vessels or lymph nodes of control and Rip1VEGF-C mice (Figure 5A-D) [146]. This finding implies that in transgenic mice, red blood cells were drained from the *de novo* peri-insular lymphatic vessels via preexisting pancreatic lymphatics to the lymph nodes, which suggests a functional linkage between newly formed and inherent lymphatic vessels. Using vascular casting experiments and lectin perfusion, we assessed whether erythrocytes reached the lymphatic vasculature via blood-lymphatic vessel shunts or whether our observations resulted from artifacts. To prepare blood vascular corrosion casts, we injected a synthetic resin into the thoracic artery and the portal vein of anesthetized mice and perfused the pancreatic blood vasculature. After digestion of the organic material, we obtained pancreatic blood vascular corrosion casts. Scanning electron microscopy (SEM) of the casts visualized the dense blood capillary network of wildtype islets of Langerhans as shown in Figure 5E. However, in Rip1VEGF-D mice, also some of the islet-surrounding lymphatic lacunae were filled with the injected resin (asterisk in Figure 5F), obscuring the blood capillaries of such islets. In a second assay, we injected a fluorophore-labeled tomato lectin into the tail vein of anesthetized mice. This naturally occurring glycoprotein interacts with carbohydrates of blood endothelium. Also by this technique, the functional blood vessels are perfused and can be visualized by microscopy. As shown in Figure 5G and H, the i.v. injected lectin decorated the blood capillaries of control and transgenic pancreata. Interestingly, islets of Rip1VEGF-D mice were only poorly vascularized, often even appearing devoid of blood capillaries on several serial sections (see also quantification of islet microvessel density below). However, we could not detect any lectin on the endothelium of peri-insular lymphatic lacunae.

The vascular casting experiment confirmed the presence of blood-lymphatic vessel shunts in the vicinity of some Rip1VEGF-D islets. The lack of lectin-labeled lymphatic lacunae in transgenic mice can be explained by a smaller affinity of the lectin for carbohydrates on lymphatic endothelium. Alternatively it is possible that on the sections examined, no intra-lymphatic hemorrhage and thus no blood-lymphatic vessel shunts were present. Furthermore, these data revealed that transgenic islets appeared smaller and exhibited less blood capillaries than control islets.

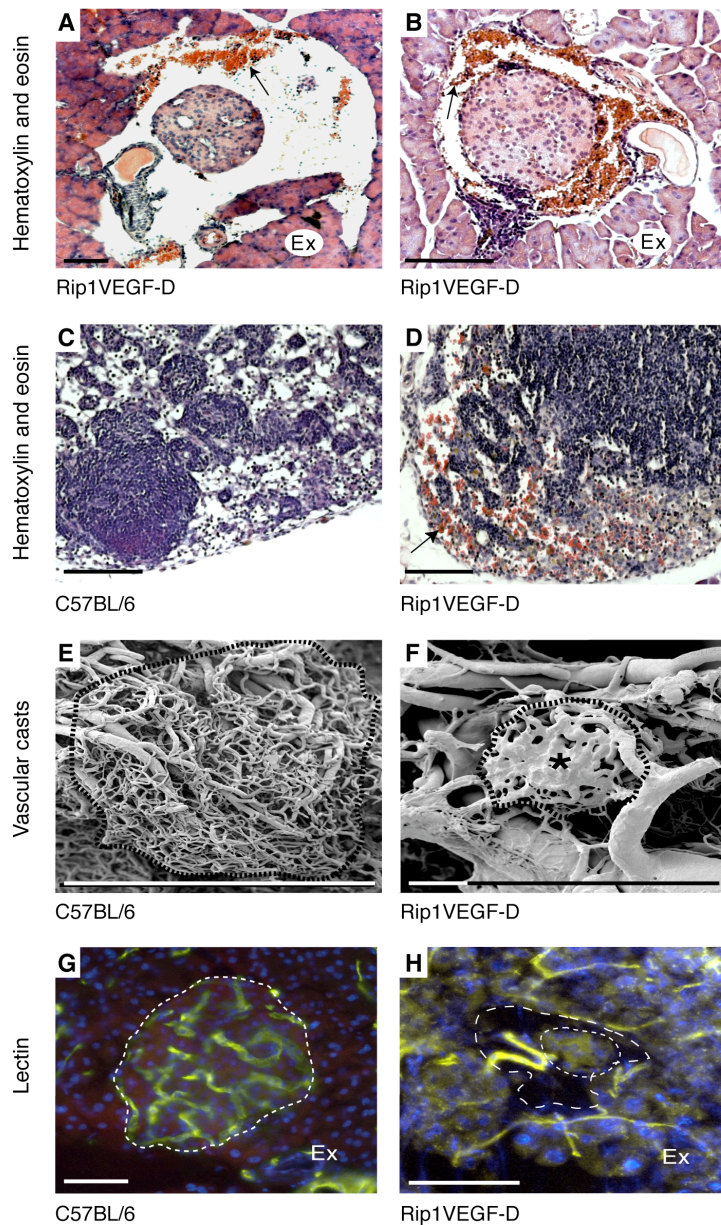


Figure 5. Peri-insular hemorrhage and blood-lymphatic vessel shunts in Rip1VEGF-D mice

(A, B) Hematoxylin and eosin staining of islets (C, D) Hematoxylin and eosin staining showing lymph nodes. (E, F) SEM of blood vascular casts from pancreata showing islets of Langerhans from a C57BL/6 and a Rip1VEGF-D mouse. (G, H) The functional pancreatic blood vasculature visualized by perfusion with lectin (yellow). Note the large blood capillary heading from the exocrine tissue through the lymphatic lacuna towards the transgenic islet. Nuclei are counterstained with DAPI (blue).

Fine dashed lines delineate islets, large dashed lines indicate the peri-insular lymphatic lacuna, arrows indicate hemorrhages; the asterisks indicates the resin-filled peri-insular lymphatic lacuna. Ex, exocrine tissue; Scale bars: (A-H) 100µm.

Together, our results indicate that transgenic expression of VEGF-D promotes the growth of peri-insular lymphatic vessels. Nevertheless, as described, we detected clear qualitative differences between VEGF-D-induced lymphatic vessels and those induced by transgenic VEGF-C in Rip1VEGF-C mice.

Repressed islet angiogenesis and reduced islet size in Rip1VEGF-D transgenic mice

The fully processed form of human VEGF-D (VEGF-D Δ N Δ C) has been repeatedly shown to activate VEGFR-2 and to thereby promote angiogenesis [133, 136-138]. Rip1VEGF-D islets expressed large amounts of VEGF-D Δ N Δ C as revealed by immunoblot analysis of isolated islets (see below, Figure 7B). Therefore, we quantified the islet microvascular density (MVD) by immunohistochemical staining with anti-CD31 antibody. However, confirming our observations from the semi-thin sections, vascular casts, and lectin

perfusion experiments mentioned above, the MVD of Rip1VEGF-D islets was significantly reduced in comparison to littermate controls (Table I).

Next, we tested islets of Rip1VEGF-D mice for their angiogenic properties using an *in vitro* collagen gel assay, in which isolated islets or tumors were co-cultured with human umbilical vein endothelial cells (HUVECs) [127, 148]. Wildtype islets do not display any angiogenic activity, whereas Rip1VEGF-A transgenic islets as well as Rip1Tag2 tumors have been reported to induce angiogenic responses in co-cultured HUVECs [148]. In keeping with previous studies, 74% of positive controls (tumors of Rip1Tag2 mice, see also below) were angiogenic and stimulated HUVECs to form tubule-like structures (see inset in Figure 6). Notably, all islets of Rip1VEGF-D transgenic mice failed to induce any angiogenic response (Figure 6).

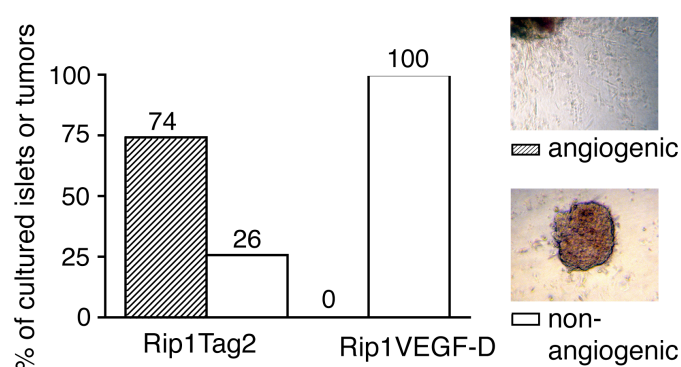


Figure 6. Collagen gel assay with Rip1VEGF-D islets

Islets and tumors derived from 9 week-old Rip1VEGF-D ($n=29$, $N=2$) and Rip1Tag2 control mice ($n=35$, $N=4$), respectively. Representative examples of non-angiogenic and angiogenic islets are shown. Results are indicated as percentages of islets or tumors in the respective angiogenesis class above the bars.

We hypothesized that impaired vascularization of transgenic islets might counteract islet growth and assessed the islet diameter on hematoxylin and eosin-stained histological sections. Indeed, measurement of islet diameters revealed that Rip1VEGF-D transgenic islets were significantly smaller than control islets (Table I).

Table I. Islet size and microvessel density (MVD) in control versus Rip1VEGF-D mice

	Controls	Rip1VEGF-D	p value
Islet diameter (mm) ^a	142.5 ± 90 ($n = 56$, $N = 4$)	105.6 ± 71 ($n = 62$, $N = 5$)	0.0146
Islet MVD (blood vessels/mm ²) ^b	1969 ± 793.3 ($n = 22$, $N = 3$)	1193 ± 1045 ($n = 30$, $N = 5$)	0.0053

^aThe size of all islets found on sections of C57 BL/6 control and Rip1VEGF-D mice was measured.

^bIslet microvessel density (MVD) was quantified by counting CD31-positive structures per measured islet area. n = number of islets, N = number of mice.

Two-tailed Student's t test. Values represent mean ± standard deviation

These results demonstrate that VEGF-D does not exert any angiogenic activity in Rip1VEGF-D mice. Rather, islet vascularization is reduced, resulting in impaired islet growth. These results contrast with the observations from Rip1VEGF-C mice, in which expression of VEGF-C does not affect islet vascularization and growth [146].

VEGF-D promotes peri- and intra-tumoral lymphangiogenesis

To assess the role of VEGF-D in tumor angiogenesis, lymphangiogenesis, and metastasis, we crossed Rip1VEGF-D with Rip1Tag2 mice, a transgenic mouse model of poorly metastatic pancreatic β -cell carcinogenesis [124]. Rip1Tag2 control and Rip1Tag2;Rip1VEGF-D double transgenic mice were sacrificed between 12 and 14 weeks of age, a time-point, when these mice succumb to hypoglycemia caused by excessive tumoral insulin production.

Immunohistochemical analysis for VEGF-D revealed that in Rip1Tag2;Rip1VEGF-D mice, most β -cells of small adenomas and carcinomas expressed VEGF-D, whereas in larger adenomas and carcinomas, the staining pattern was more heterogenous with areas devoid of VEGF-D expression (Figure 7A). Immunoblot analysis for VEGF-D showed the abundant and predominant presence of the fully processed (human) VEGF-D Δ N Δ C as well as small amounts of partially processed VEGF-D Δ C and full length VEGF-D in lysates of most Rip1Tag2;Rip1VEGF-D tumors. Small amounts of full length mouse VEGF-D and VEGF-D Δ C were occasionally detected in Rip1Tag2 control tumors (Figure 7B). To assess, whether the secreted VEGF-D protein can be found in the circulation and may potentially also act at distant organs, we performed an enzyme-linked immuno-sorbent assay (ELISA) on serum samples derived from Rip1VEGF-D and Rip1Tag2;Rip1VEGF-D as well as control mice. As depicted in Figure 7C, no elevation of circulating VEGF-D levels was observed in VEGF-D transgenic when compared to control mice, indicating that VEGF-D might be sequestered locally. However, thus far, no heparin-binding activity was reported for both VEGF-C and VEGF-D.

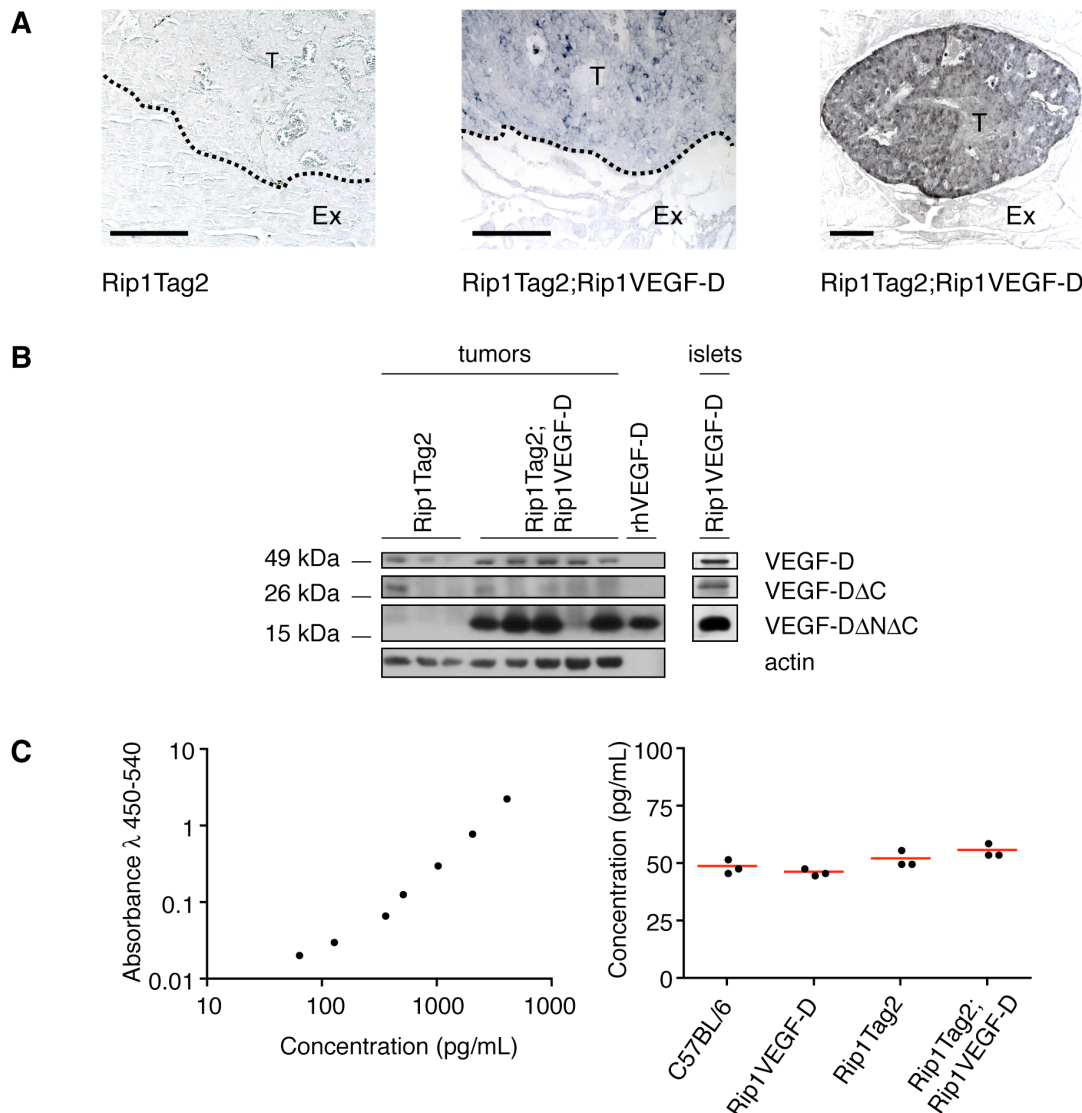


Figure 7. Expression of VEGF-D in Rip1Tag2 control and Rip1Tag2;Rip1VEGF-D tumors and Rip1VEGF-D islets

(A) Immunohistochemical staining with anti-VEGF-D antibody (grey) on pancreatic sections of twelve week-old Rip1Tag2 and Rip1Tag2;Rip1VEGF-D mice (B) Immunoblot analysis with anti-VEGF-D antibody on lysates of twelve week-old Rip1Tag2 ($n=3$, $N=2$) tumors, Rip1Tag2;Rip1VEGF-D tumors ($n=5$, $N=2$), and Rip1VEGF-D islets ($n=200$, $N=4$). Recombinant hVEGF-D Δ N Δ C (10 ng) served as positive control (C) ELISA for circulating VEGF-D on sera of control and transgenic mice as indicated (**left panel**) standard curve (**right panel**) VEGF-D serum levels. Dashed lines delineate tumors; Ex, exocrine tissue; T, tumor; VEGF-D Δ C, partially processed VEGF-D; VEGF-D Δ N Δ C, fully processed VEGF-D. Scale bars (A): 100 μ m.

To assess the lymphangiogenic activity of VEGF-D in tumor mice, we analyzed pancreatic sections of twelve week-old Rip1Tag2 control and Rip1Tag2;Rip1VEGF-D mice with different antibodies specific for lymphatic endothelium, such as LYVE-1, VEGFR-3, Podoplanin, and the transcription factor Prox-1. In agreement with previous publications, analysis of Rip1Tag2 pancreata by immunofluorescence staining for LYVE-1 revealed that lymphatic vessels were only rarely found in close association with tumors. In contrast, most tumors of Rip1Tag2;Rip1VEGF-D mice were partially or completely surrounded by lymphatic vessels (Figure 8). Collapsed and non-collapsed lymphatic vessels were also found

on the edge and occasionally in the center of larger adenomas and carcinomas of Rip1Tag2;Rip1VEGF-D mice (Figure 8D). Peri-tumoral lymphatics were immunoreactive for all markers tested (Figures 8 C-F). As expected, the Prox-1 expression was more pronounced in developing peri-tumoral lymphatic vessels than in quiescent lymphatics of the exocrine pancreas (Figures 8F)[149]. Consistent with previous reports, β -cells also expressed low levels of Prox-1 (Figure 8F) [150, 151].

To quantify peri-tumoral lymphangiogenesis, we assessed the extent by which LYVE-1-positive lymphatic vessels surrounded the tumor perimeter. Thereby we found that only 14% of control tumors were closely associated with lymphatics, while more than 60% of VEGF-D-expressing tumors were completely surrounded by lymphatic vessels (Figure 8G). Together, these results indicate that VEGF-D promotes peri- and, to some extent, also intra-tumoral *de novo* lymphangiogenesis.

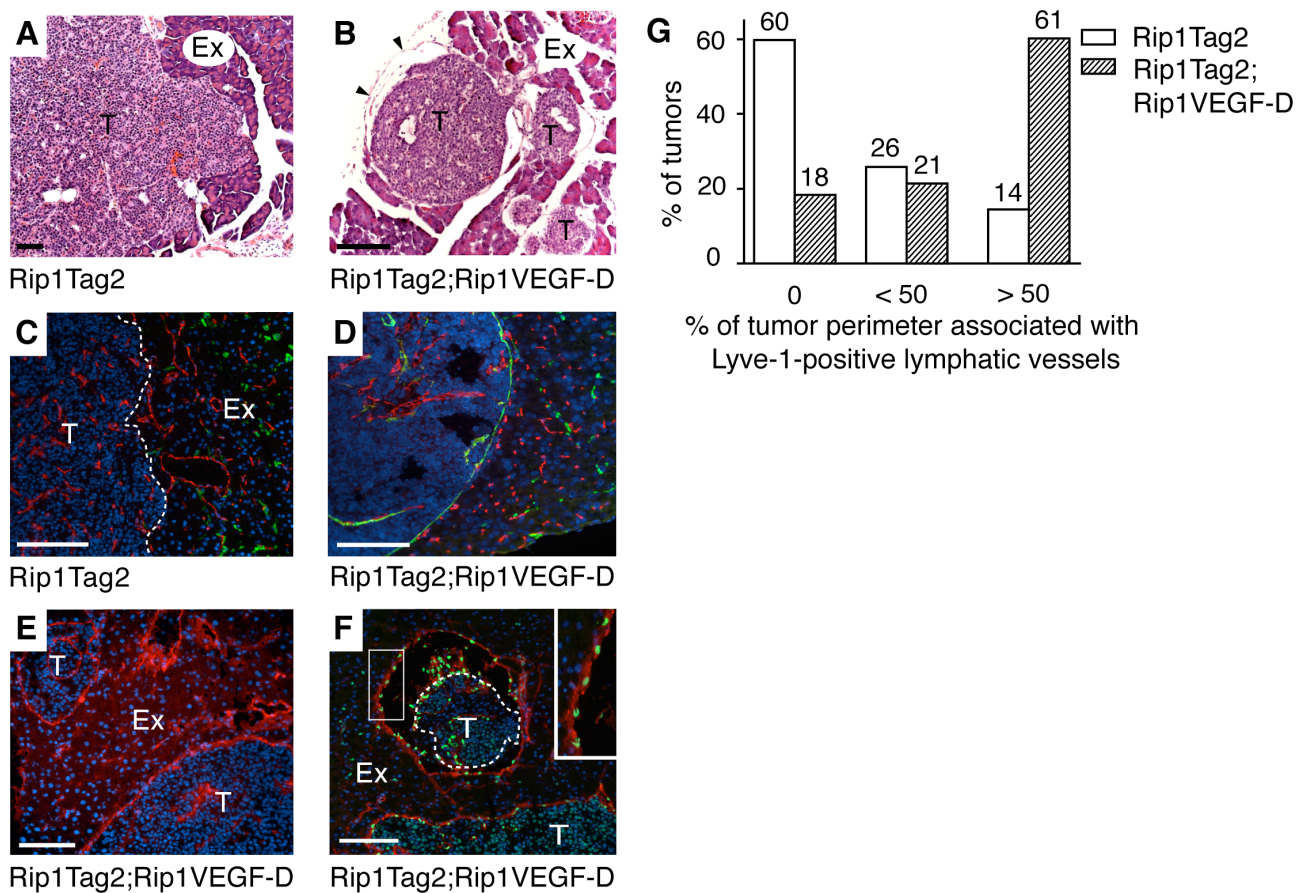


Figure 8. Peri-tumoral lymphangiogenesis in Rip1Tag2 and Rip1Tag2;Rip1VEGF-D mice (A, B) Hematoxylin and eosin staining (C, D) Double-immunofluorescence for the blood endothelium marker CD31 (red) and LYVE-1 (green) (E) Immunofluorescence analysis with anti-VEGFR-3 antibody (red) (F) Double-immunofluorescence analysis for Podoplanin (red) and Prox-1 expression (green). The inset is a magnification of the boxed area as indicated. (G) Quantification of peri-tumoral lymphangiogenesis as described in the text. Results are indicated as percentages of tumors in a given class above the bars. 490 Rip1Tag2;Rip1VEGF-D tumors (N=22) and 159 Rip1Tag2 tumors (N=9) were analyzed. (C-F) Nuclei are counterstained with DAPI (blue). Dashed lines delineate tumors; Ex, exocrine tissue, Tu, tumor. Scale bars: 100 μ m. Arrowheads in (B) indicate endothelial lining; dashed lines delineate tumors; Ex, exocrine tissue; T, tumor. Scale bars (A-F): 100 μ m.

Above we have demonstrated the presence of blood-lymphatic vessel shunts in the vicinity of VEGF-D-expressing islets. In analogy to these observations, also 32% of the tumor-associated lymphatic vessels of Rip1Tag2;Rip1VEGF-D mice (n=522, N=20) were filled with profuse hemorrhage (Figure 9). Occasionally, erythrocytes were also found next to Rip1Tag2 tumors but never inside of lymphatic vessels. We speculate that also in double-transgenic tumor mice, shunts between blood and lymphatic vessels account for the intra-lymphatic hemorrhages. Furthermore, we found erythrocytes in regional lymph nodes of Rip1Tag2;Rip1VEGF-D but not of Rip1Tag2 mice, which indirectly illustrates the draining capacity of newly formed peri-tumoral lymphatic vessels (data not shown).

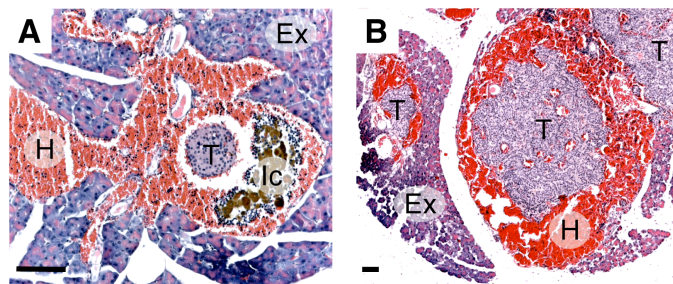


Figure 9. Hemorrhage in lymphatic vessels associated with Rip1Tag2;Rip1VEGF-D tumors

(A and B) Hematoxylin and eosin stainings of pancreatic sections. Ex, exocrine tissue; H, hemorrhage; Ic, immune cells; T, tumor. Scale bars: 100 μ m.

Impaired tumor angiogenesis and reduced tumor growth in Rip1Tag2;Rip1VEGF-D mice

As mentioned above, the fully processed form of human VEGF-D (VEGF-D Δ N Δ C) has been repeatedly shown to activate VEGFR-2 and to thereby promote angiogenesis [133, 136-138]. Since we detected high levels of VEGF-D Δ N Δ C in tumors of Rip1Tag2;Rip1VEGF-D mice, we quantified tumor angiogenesis in Rip1Tag2;Rip1VEGF-D and control mice. The measurement of tumor blood vessel density is commonly used to assess tumor-induced angiogenesis (reviewed in [152]). Therefore, we stained pancreatic sections of the two genotypes using the blood endothelial marker CD31 and counted intra-tumoral blood vessels. In analogy to the impaired angiogenesis in islets of Rip1VEGF-D mice, the tumor microvessel density was significantly lower in Rip1Tag2;Rip1VEGF-D when compared to control mice. Concomitantly with the reduced tumor angiogenesis, we observed a reduction of tumor volumes in Rip1Tag2;Rip1VEGF-D in comparison to control mice. In accordance with a limited blood supply, VEGF-D-expressing tumors contained less proliferating and significantly less apoptotic cells than control tumors, suggesting a lower turn-over of cancer cells. The tumor incidence was unaffected by the expression of VEGF-D (Table II).

Table II. Phenotypical analysis of Rip1Tag2 and Rip1Tag2;Rip1VEGF-D tumors

	Rip1Tag2	Rip1Tag2;Rip1VEGF-D	p value
Tumor incidence/ mouse ^a	6.3 ± 2.5 (n = 175, N = 28)	6.1 ± 2.7 (n = 190, N = 31)	0.8593
Total tumor volume/ mouse (mm ³) ^a	52.4 ± 39.7 (n = 175, N = 28)	29.5 ± 28.1 (n = 190, N = 31)	0.0164
Tumor blood vessel density ^b	78.9 ± 28.9 (n = 40, N = 28)	58.4 ± 24 (n = 90, N = 31)	< 0.0001
Proliferation rate of tumor cells ^c (cells per field)	130.1 ± 39.76 (n = 102, N = 11)	119.1 ± 43.9 (n = 110, N = 14)	0.0524
Apoptotic tumor cells per field ^c (cells per field)	22.47 ± 11.63 (n = 75, N = 8)	15.42 ± 10.06 (n = 102, N = 10)	< 0.0001

^an = number of tumors, N = number of mice.

^bTumor blood vessel density assessed by counting intra-tumoral CD31-positive vessels per 40x magnification field. n = number of fields, N = number of mice.

^cn = number of fields, N = number of mice.

Data were analyzed by a two-tailed Student's t test. Values represent mean ± SD.

During our analysis of tumor blood vessels, we observed that not only the quantity but also the quality of CD31-positive tumoral blood vessels was affected by the expression of VEGF-D. In many tumors of Rip1Tag2;Rip1VEGF-D mice, blood vessels were dramatically enlarged and more irregularly distributed within the tumor when compared with control tumors. Since it is known that dilated blood vessels can result from insufficient stabilization of blood vessels by pericytes, we stained Rip1Tag2 and Rip1Tag2;Rip1VEGF-D tumors with anti-smooth muscle actin and anti-NG-2 antibody, two markers for pericytes [3]. However, the blood vessels of both control and Rip1Tag2;Rip1VEGF-D tumors were comparably coated by smooth muscle cells and pericytes (Figure 10A).

To test the angiogenic capacity of tumor cell-secreted VEGF-D *in vitro*, we performed a collagen gel assay with tumors from 9 week-old Rip1Tag2 and Rip1Tag2;Rip1VEGF-D mice as described above. In line with our histological observations, we found that Rip1Tag2;Rip1VEGF-D tumors induced markedly less angiogenic response in co-cultured HUVECs than control tumors (Figure 10B). In fact, most of the tumors of 9-week old Rip1Tag2;Rip1VEGF-D mice were very small and lacked the typical reddish color of angiogenic tumors. The reduced angiogenic activity of Rip1Tag2;Rip1VEGF-D tumors demonstrates that expression of VEGF-D directly or indirectly inhibits angiogenesis in our mouse model. Again, these observations strongly contradict the results of previous studies where VEGF-DΔNΔC induced angiogenesis.

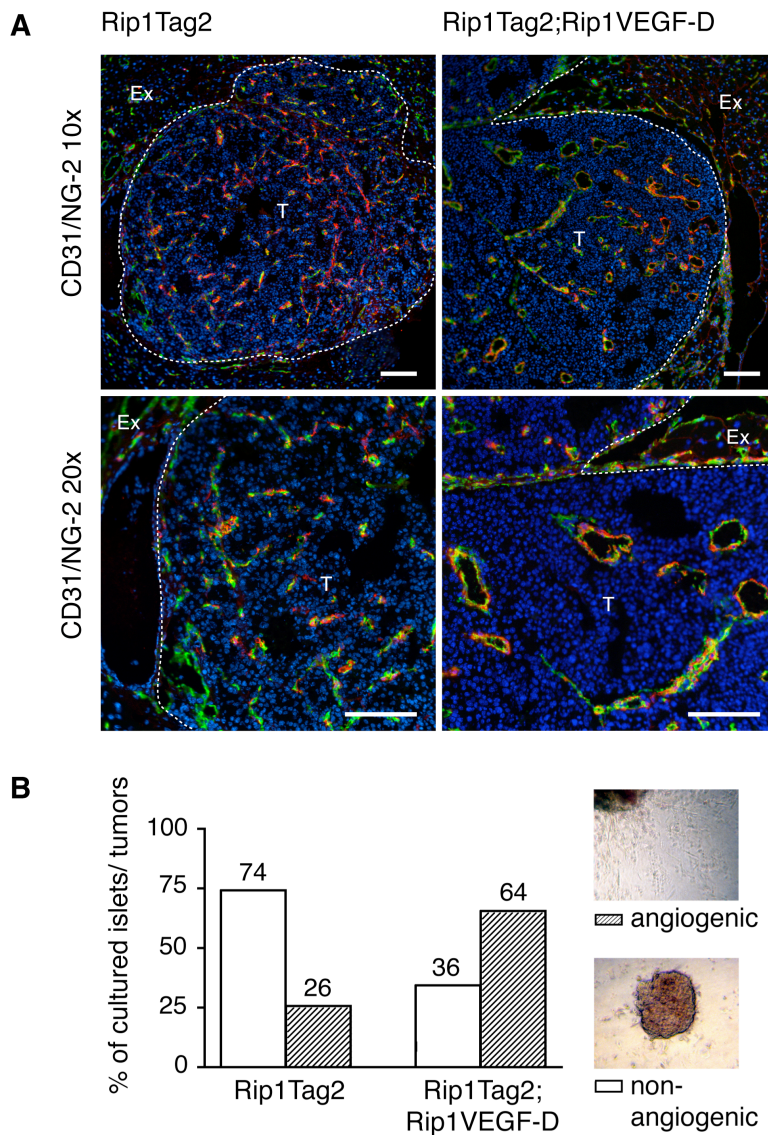


Figure 10. Pericyte-coating of intra-tumoral blood vessels and angiogenic activity of Rip1Tag2;Rip1VEGF-D tumors

(A) Double immunofluorescence staining with anti-CD31 (green) and anti-NG-2 (red) antibody. Nuclei are counterstained with DAPI. (B) Collagen gel assay. Islets and tumors were derived from 9 week-old Rip1Tag2;Rip1VEGF-D ($n=29$, $N=4$) and Rip1Tag2 control mice ($n=35$, $N=4$). Representative examples of non-angiogenic and angiogenic responses are shown. Results are indicated as percentages of islets or tumors in the respective angiogenesis class above the bars. Dashed lines delineate tumors. Ex, exocrine tissue; T, tumor. Scale bars: 50 μ m.

VEGF-D promotes metastasis to regional lymph nodes and the lungs

Evidence from clinical and experimental studies suggests that the close association of tumors with lymphatic vessels might promote lymphogenous spread of tumor cells, which may follow routes of natural drainage and subsequently form metastases in regional lymph nodes. To assess whether VEGF-D-induced peri-tumoral lymphangiogenesis promotes the lymphogenous dissemination of cancer cells, hematoxylin and eosin-stained pancreatic sections of Rip1Tag2 and Rip1Tag2;Rip1VEGF-D mice were screened for metastatic insulinoma cells. Consistent with previous reports, β -cells were only occasionally found to disseminate in lymphatic vessels of Rip1Tag2 pancreata, which may account for the fact that only 15% of the investigated control mice displayed metastases in pancreatic lymph nodes. In contrast, all investigated double-transgenic Rip1Tag2;Rip1VEGF-D mice exhibited tumor cell clusters circulating in lymphatic vessels located next to insulinomas and in the exocrine pancreas (data not shown). In 61% of these mice, β -cells were drained to the regional lymph nodes and formed secondary tumors (Figure 11A). Furthermore, 86% of

Rip1Tag2;Rip1VEGF-D mice analyzed for peripheral metastases exhibited such in the lung parenchyma and/or surface, the latter being already visible upon macroscopical inspection (Figure 11C). Tumor cells retained their well-differentiated morphology, since all metastases were immunoreactive for insulin, confirming their derivation from primary β -cell tumors (Figures 11B and D). Also, a comparative analysis of tumor grades demonstrated that expression of VEGF-D did not significantly affect the ratio of benign adenoma versus malignant carcinoma (Table III).

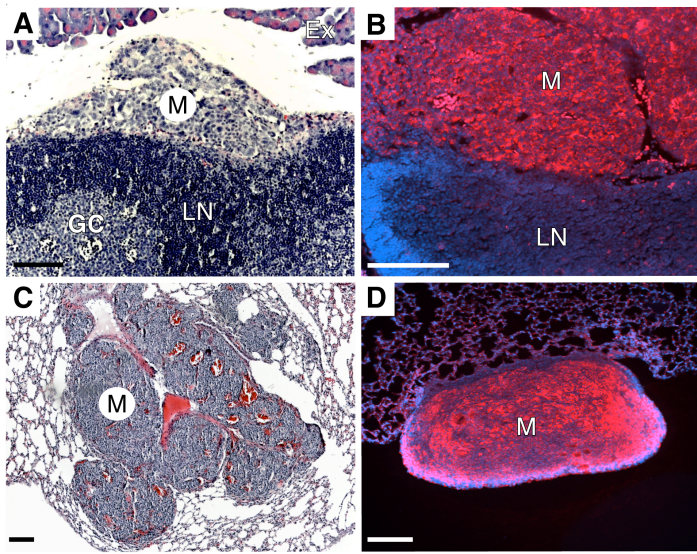


Figure 11. Regional lymph node and distant lung metastases in 12 week-old Rip1Tag2;Rip1VEGF-D double transgenic mice

(A) Hematoxylin and eosin staining of a pancreatic lymph node (B) Immunofluorescence analysis of lymph node metastasis with anti-insulin antibody (red). (C) Hematoxylin and eosin staining of a lung section (D) Immunofluorescence analysis of a lung metastasis with an anti-insulin antibody (red). (B and D) Nuclei are counterstained with DAPI (blue). Ex, exocrine tissue; GC, germinal center; LN, lymph node; M, metastasis. Scale bars: 100 μ m.

Table III. Tumor progression and metastatic phenotype of Rip1Tag2;Rip1VEGF-D mice

	Rip1Tag2	Rip1Tag2;Rip1VEGF-D
Adenoma/Carcinoma ^a	27/73 % (n = 188, N = 12)	35/65 % (n = 502, N = 20)
Lymph node metastasis ^b	15 % (2/13)	61 % (14/23)
Lung metastasis ^c	0 % (0/4)	86 % (6/7)

^an = number of tumors, N = number of mice.

^bAs detected by haematoxylin and eosin staining.

^cEntire lungs have been cut into 10 μ m sections and stained with hematoxylin and eosin. The β -cell origin of each metastasis was confirmed by immunofluorescent staining for insulin.

To assess whether lung metastases originated from hematogenous tumor cell spread, we analyzed the livers of five Rip1Tag2;Rip1VEGF-D mice displaying lung metastases by hematoxylin and eosin and immunofluorescence stainings with anti-insulin antibody. No hepatic metastases were found, suggesting a primarily lymphogenous spread of insulinoma cells (data not shown). In accordance to the vast literature on Rip1Tag2 mice, we did not detect any peripheral metastases in single-transgenic Rip1Tag2 mice. Notably, transgenic expression of VEGF-C similarly promoted regional lymph node metastasis in Rip1Tag2;Rip1VEGF-C mice [146]. However, neither the previous study nor our analysis of Rip1Tag2;Rip1VEGF-C mice unveiled any lung metastases.

Since VEGF-D expression did not significantly affect the transition from benign adenoma to invasive carcinoma and metastases were well differentiated, we hypothesize that VEGF-D did not alter tumor cell invasive properties. These data indicate that VEGF-D promotes regional and distant lymphogenous metastasis via the induction of tumor-associated lymphatic vessels.

Human VEGF-D does not elicit an immune response in non-transgenic mice

In analogy to Rip1VEGF-D mice, the analysis of hematoxylin and eosin-stained pancreatic sections of Rip1Tag2;Rip1VEGF-D mice revealed that 23% of tumor-associated lymphatic lacunae (n=412, N=20) contained leucocyte accumulations, which consisted of the same immune cell populations as mentioned above (Figure 12 and data not shown). In one mouse, several small tumors were completely engulfed in a lymph node-like cluster of leucocytes (Figure 12B). No immune cells were visible in the few tumor-associated lymphatic vessels of Rip1Tag2 control mice (n=94, N=14).

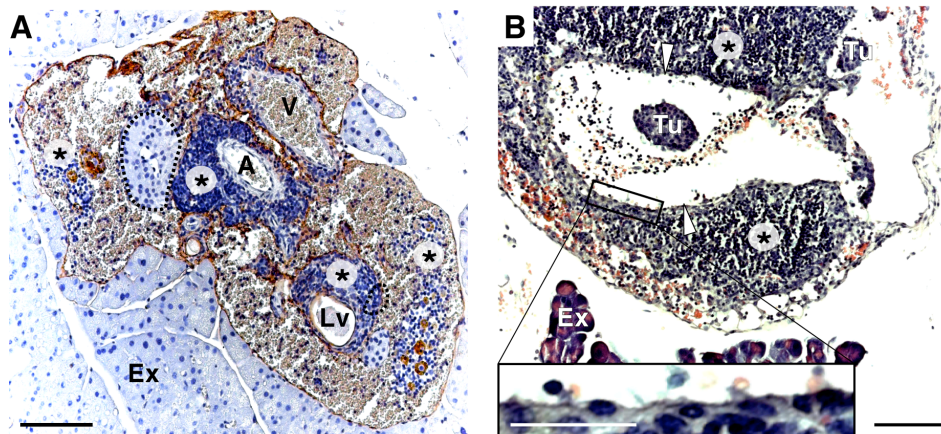


Figure 12. Immune cell accumulations in lymphatic lacunae surrounding Rip1Tag2;Rip1VEGF-D tumors

(A) Immunohistochemistry with anti-Podoplanin antibody (brown; counterstaining with hematoxylin). Note that erythrocytes fill the lymphatic lacuna (B) Hematoxylin and eosin staining. Asterisks indicate immune cell accumulations; dashed lines delineate tumors; A, artery; Ex, exocrine tissue; Lv, lymphatic vessel; T, tumor; V, vein. Scale bars: 100 μ m.

Although the data from single transgenic Rip1VEGF-D mice did not support that peri-insular immune cell accumulations resulted from an immune response of the mouse immune system against human VEGF-D transgene, we wanted to further investigate whether hVEGF-D may display immunogenic features. If so, we hypothesized that hVEGF-D-expressing tumors would be more heavily infiltrated by immune cells than control tumors. Therefore, we quantified intra-tumoral immune cells upon immunofluorescent labeling with an anti-CD45 antibody as well as immune markers for macrophages (F4/80), B lymphocytes (B220), T helper lymphocytes (CD4), and cytotoxic T lymphocytes (CD8). In line with previous studies, our analysis demonstrated that tumors of Rip1Tag2 control mice were extensively infiltrated by CD45-positive immune cells [153], most of them being F4/80-positive macrophages. However, to our surprise, tumors of double-transgenic mice contained significantly less CD45-positive leucocytes and macrophages. The numbers of intra-tumoral cytotoxic T cells was markedly reduced, yet not significantly. The amount of intra-tumoral T helper and B lymphocytes was not affected (Table IV).

Table IV. Immune cells infiltrating Rip1Tag2 and Rip1Tag2;Rip1VEGF-D tumors

	Rip1Tag2	Rip1Tag2;Rip1VEGF-D	p value
Intra-tumoral CD45 ⁺ immune cells	0.27 ± 0.15 (n = 8, N = 2)	0.11 ± 0.05 (n = 12, N = 4)	0.021
Intra-tumoral F4/80 ⁺ macrophages	0.16 ± 0.07 (n = 8, N = 2)	0.06 ± 0.03 (n = 12, N = 4)	0.006
Intra-tumoral B220 ⁺ B lymphocytes	0.007 ± 0.008 (n = 8, N = 2)	0.204 ± 0.677 (n = 12, N = 4)	0.427
Intra-tumoral CD4 ⁺ T lymphocytes	0.043 ± 0.034 (n = 8, N = 2)	0.039 ± 0.387 (n = 12, N = 4)	0.770
Intra-tumoral CD8 ⁺ T lymphocytes	0.0225 ± 0.025 (n = 8, N = 2)	0.0013 ± 0.02 (n = 12, N = 4)	0.053

Intra-tumoral immune cells were quantified by assessing the percentage of tumor area occupied by immune cells versus the percentage of DAPI-stained tumor area on one representative section per tumor.

n = number of tumors, N = number of mice.

Data were analyzed by two-tailed Student's t test with Welch correction. Values represent mean ± SD.

In a second experiment, we investigated whether hVEGF-D can elicit an immune response in non-hVEGF-D transgenic mice by transplanting hVEGF-D-expressing cell lines subcutaneously into Rip1Tag2 mice. Therefore, we established cell lines from Rip1Tag2 and Rip1Tag2;Rip1VEGF-D tumors. As depicted in Figure 13, immunoblot analysis confirmed expression of hVEGF-D in cell line C derived from a double transgenic tumor. In contrast, control tumor cell line A did not produce detectable levels of VEGF-D. We injected approximately 10⁶ Rip1Tag2;Rip1VEGF-D or Rip1Tag2 tumor cells into each flank of a given mouse according to the scheme in Figure 13 (mouse groups I-IV). We sacrificed animals four weeks after tumor cell injection, harvested the tumors, measured tumor volumes and stained tumor sections with antibodies against CD45 and F4/80 as described above. We performed statistical analyses by comparing either mouse groups I and II (Rip1Tag2 mice injected with control and VEGF-D-expressing cells, respectively) or mouse groups II and IV (Rip1Tag2 and Rip1Tag2;Rip1VEGF-D mice injected with VEGF-D-expressing cells,

respectively) As shown in Table V, Neither of the statistical results revealed any significant differences in tumor volumes or the contents of immune cells (see below, and data not shown).

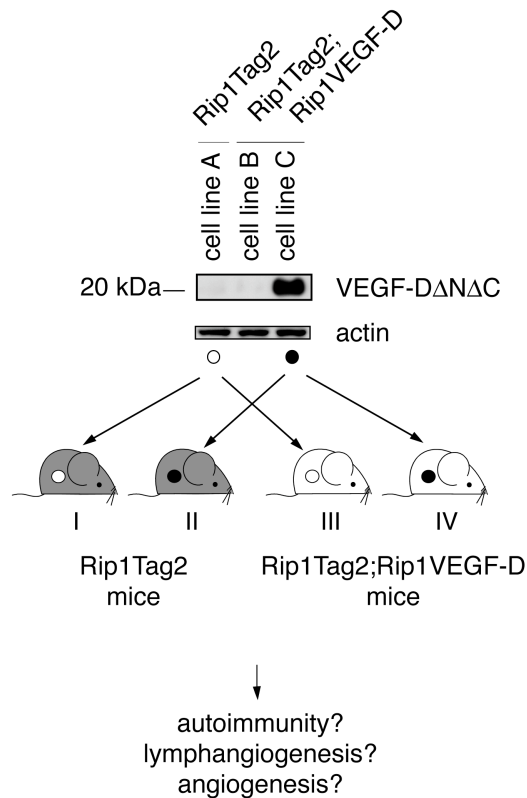


Figure 13. Syngenic and allogenic transplantation of tumor cell lines derived from Rip1Tag2 and Rip1Tag2;Rip1VEGF-D insulinomas

Immunoblotting analysis with anti-VEGF-D antibody on lysates of cell lines derived from Rip1Tag2 and Rip1Tag2;Rip1VEGF-D tumors. Staining with antibodies against actin was used as loading control. Cell lines A and C were used for subcutaneous (s.c.) injection into Rip1Tag2 and Rip1Tag2;Rip1VEGF-D mice as schematically depicted.

The lack of an increase in immune cells associated with hVEGF-D-expressing tumors as well as the absence of tumor cell destruction (reflected by comparable tumor volumes) suggest that the immune system of a non-hVEGF-D transgenic mouse does not react against hVEGF-D. Together with the fact that no destruction of β -cells occurred in Rip1VEGF-D transgenic islets and that single transgenic mice were normoglycemic at any age, these experiments exclude autoimmunity as cause for immune cell accumulations in peri-insular/-tumoral lymphatics of transgenic mice. Notably however, ectopic insulinomas were not surrounded by immune cell clusters as seen in orthotopic insulinomas (see also next section).

The tumor microenvironment modulates VEGF-D-elicited effects

Several biological effects of VEGF-D in Rip1Tag2;Rip1VEGF-D mice contrast with results from previous mouse tumor studies. Notably, xenotransplantation experiments, in which tumor cells producing hVEGF-D were engrafted into the skin of immunocompromised mice, showed increased hVEGF-D-mediated intra- but not peri-tumoral lymphangiogenesis. In addition, tumor angiogenesis and tumor growth were stimulated [100, 144]. To address whether the function of VEGF-D may depend on the tumor microenvironment, we studied the vascular phenotype of the previously described tumors grown upon subcutaneous transplantation of insulinoma cells into transgenic mice. Based on the above-described results

excluding autoimmunity to the transgene, mouse groups I and III (control cells injected into Rip1Tag2 and Rip1Tag2;Rip1VEGF-D mice, respectively) as well as II and IV (hVEGF-D-expressing cells injected into Rip1Tag2 and Rip1Tag2;Rip1VEGF-D mice, respectively) were grouped into one respective category (hVEGF-D-negative and hVEGF-D-positive cell lines, respectively). Lymphangiogenesis as well as angiogenesis associated with control and hVEGF-D-expressing tumors were then compared upon immunofluorescence staining for LYVE-1 and CD31.

The analysis of angiogenesis and lymphangiogenesis associated with ectopic tumors revealed striking differences in comparison to the previously described orthotopic insulinomas. As shown in Figure 14, expression of VEGF-D induced marked intra- but no peri-tumoral lymphangiogenesis in 29% of subcutaneous Rip1Tag2;Rip1VEGF-D tumors (n=7). No lymphatic vessels were found in or in close vicinity of Rip1Tag2 control tumors (n=6). The intra-tumoral lymphatic vessels of ectopic Rip1Tag2;Rip1VEGF-D insulinomas formed a dense lymphatic network, whereas intra-tumoral lymphatics found in orthotopic insulinomas described above were more sparse (see also Figure 8D). Furthermore, quantification of tumoral blood vessel densities demonstrated that in contrast to orthotopic insulinomas, expression of VEGF-D had no effect on tumor angiogenesis in ectopic Rip1Tag2;Rip1VEGF-D when compared to control tumors (Table V).

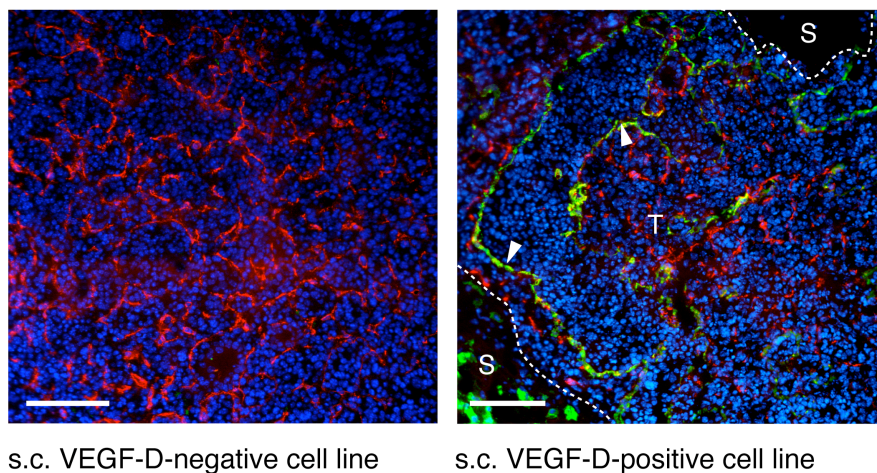


Figure 14. Angiogenesis and lymphangiogenesis in ectopic subcutaneous Rip1Tag2 and Rip1Tag2;Rip1VEGF-D insulinomas

Double immunofluorescence analysis with anti-CD31 (red) and anti-LYVE-1 antibody (green). Nuclei are counterstained with DAPI (blue). Arrowheads indicate lymphatic vessels; dashed lines delineate tumors; S, subcutis; T, tumor.

Table V. Quantification of the blood vessel density of ectopic subcutaneous VEGF-D-negative and -positive tumors

	VEGF-D-negative tumors	VEGF-D-positive tumors	p value
Tumor volume (mm ³) ^a	21.49 ± 21.99 (n = 11, N = 6)	12.85 ± 9.35 (n = 10, N = 6)	0.5964*
Intra-tumoral CD45-positive cells ^b	1.39 ± 0.65 (n = 7, N = 6)	1.47 ± 0.47 (n = 7, N = 6)	0.7398**
Intra-tumoral F4/80-positive cells ^b	1.433 ± 0.96 (n = 7, N = 6)	1.51 ± 0.61 (n = 7, N = 6)	0.8457**
Intra-tumoral lymphangiogenesis	0% (n = 7, N = 6)	29% (n = 7, N = 6)	
Tumor blood vessel density ^c	0.082 ± 0.009 (n = 5, N = 5)	0.15 ± 0.1 (n = 7, N = 6)	0.144***

^aTumor volume per mouse (in mm³) was calculated from all macroscopically apparent tumors with a minimal diameter of 1 mm, assuming a spherical shape of tumors.

^bIntra-tumoral immune cells were quantified by assessing the percentage of tumor area occupied by immune cells versus the percentage of DAPI-stained tumor area on one representative section per tumor.

^cThe tumor blood vessel density was quantified by assessing the percentage of tumor area occupied by CD31-positive structures versus the percentage of DAPI-stained tumor area.

n = number of tumors, N = number of mice.

*Data were analyzed by Mann Whitney test. Values represent mean ± SD.

**Data were analyzed by two-tailed Student's t test. Values represent mean ± SD.

***Data were analyzed by two-tailed Student's t test with Welch correction. Values represent mean ± SD.

In conclusion, these observations demonstrate that VEGF-D modulates tumor growth, lymphangiogenesis and angiogenesis differently depending on the encountered tumor microenvironment. Therefore, the phenotypic differences between our transgenic mouse model compared to previous xenotransplantation studies might – at least in part - be due to the distinct tumor microenvironment.

3.1.5. Discussion

In the recent years, tumor-associated lymphangiogenesis has gained increasing attention as a metastasis-promoting factor. Here we addressed the effect of the lymphangiogenic factor VEGF-D on tumor lymphangiogenesis, angiogenesis, and metastasis in a well-characterized transgenic mouse model of pancreatic β -cell carcinogenesis (Rip1Tag2).

We generated transgenic mice expressing human VEGF-D under the control of the Rip1 promoter, which targets expression of the transgene specifically to β -cells of pancreatic islets of Langerhans. The phenotypical characterization of Rip1VEGF-D mice revealed the presence of lymphatic lacunae growing around (but not in) most islets, while islets of wildtype littermate mice were only occasionally associated with lymphatic vessels. These observations suggest that VEGF-D expression induced *de novo* lymphangiogenesis in Rip1VEGF-D mice, which is in line with previous reports demonstrating a lymphangiogenic

function of VEGF-D in K14-VEGF-D transgenic mice, xenotransplantation, and adenoviral gene transfer experiments [135, 136, 138].

To investigate the impact of VEGF-D on tumor development and progression, we crossed Rip1VEGF-D with Rip1Tag2 mice, a transgenic mouse model of poorly metastatic β -cell carcinogenesis [124]. In line with previous studies, Rip1Tag2 control insulinomas were only rarely associated with lymphatic vessels. Also, metastases were detected only occasionally and exclusively in regional lymph nodes (15%). In contrast, transgenic expression of VEGF-D in Rip1Tag2;Rip1VEGF-D mice resulted in extensive peri- and to some extent also intra-tumoral lymphangiogenesis. The functionality of the newly formed lymphatic vessels was indirectly demonstrated by tumor cell aggregates, which circulated in lymphatics of the exocrine pancreatic tissue of double transgenic but not control mice. Moreover, the increase in tumor-associated lymphangiogenesis was associated with the frequent formation of regional lymph node (61%) and distant lung metastases (86%). Since the first organ to be afflicted by hematogenous metastasis is the liver, the lack of hepatic metastases in Rip1Tag2;Rip1VEGF-D mice suggests that also the lung metastases resulted from primarily lymphogenous spread of tumor cells [154]. The metastatic cancer cells may have reached the lungs either via lymphatic capillaries crossing the diaphragm or via the main lymph-collecting duct (ductus thoracicus), which evacuates the lymph into the venous blood stream that flows through the right ventricle of the heart into the pulmonary capillary bed. VEGF-D expression did not affect the transition from benign adenomas to malignant carcinomas. Also, metastases were well differentiated and still expressed insulin. Together with the fact that Rip1Tag2 tumors can metastasize but do so only rarely, our observations suggest that VEGF-D rather promotes passive metastasis by providing additional lymphatic escape routes for tumor cells than altering tumor cell invasive and migratory properties. Yet, since not all Rip1Tag2;Rip1VEGF-D mice exhibited metastases, such tumor cell properties may be additionally required and may represent a rate-limiting step for the dissemination of cancer cells. The data of Rip1Tag2;Rip1VEGF-D mice support the “bridgehead concept of metastases”, which postulates that lymph node metastases form a reservoir of successfully metastasized tumor cells. These may already possess many of the properties required for further spread and may therefore metastasize more frequently to peripheral sites than cells from the primary tumor [123].

Interestingly, while VEGF-D stimulated predominantly the formation of peri-insular lymphatics in orthotopic insulinomas, ectopic tumors resulting from subcutaneous (s.c.) injection of Rip1Tag2;Rip1VEGF-D cells displayed dense intra-tumoral lymphatic networks but no peri-tumoral lymphangiogenesis. Although we cannot explain the molecular mechanisms underlying the microenvironmental influence on VEGF-D-induced effects, we demonstrate that such determination occurs and significantly alters the tumor phenotype.

Recent studies using intra-muscular adenoviral gene transfer and xenotransplantation experiments have demonstrated a potent angiogenic activity of the fully processed form of VEGF-D (VEGF-D Δ N Δ C) via activation of VEGFR-2 [100, 136]. In contrast, transgenic expression of VEGF-D in the skin of K14-VEGF-D mice failed to promote angiogenesis [135]. High levels of VEGF-D Δ N Δ C were detected in islets and tumors of Rip1VEGF-D and Rip1Tag2;Rip1VEGF-D transgenic mice, respectively, while levels of circulating VEGF-D was comparable to that of control mice, suggesting that secreted VEGF-D might become sequestered to the extra-cellular matrix. However, despite pronounced insular and tumoral

expression of VEGF-D, islet and tumor angiogenesis were significantly reduced in comparison to control mice. In fact, most of the tumors of 9-week old Rip1Tag2;Rip1VEGF-D mice were very small and lacked the typical reddish color of angiogenic Rip1Tag2 tumors, suggesting that at that age, double transgenic tumors still represent hyperplastic islets in which the angiogenic switch has not yet occurred. Thus, contradicting the previously published angiogenic effects of VEGF-D Δ N Δ C, our results show that expression of VEGF-D Δ N Δ C directly or indirectly inhibits angiogenesis in our mouse model. Interestingly however, in ectopic s.c. Rip1Tag2;Rip1VEGF-D tumors, VEGF-D did not affect tumor angiogenesis when compared with subcutaneous Rip1Tag2 control tumors. One possible cause for the reduced MVD in orthotopic Rip1Tag2;Rip1VEGF-D insulinomas could be that the peri-tumoral lymphatic lacunae form a physical barrier to vascular, peri-vascular or other cells necessary for angiogenesis, which cannot be properly recruited from the exocrine pancreas to newly forming tumor blood vessel sprouts. This would explain why in subcutaneous tumors, which exhibit intra- but not peri-tumoral lymphangiogenesis, angiogenesis is not affected. If this hypothesis holds true, the contribution of circulating endothelial progenitor cells to the tumor vasculature would be insufficient for adequate tumor angiogenesis. The mechanism of VEGF-D-mediated anti-angiogenic activity is currently subject of further investigations.

32% of lymphatic lacunae surrounding Rip1VEGF-D islets and Rip1Tag2;Rip1VEGF-D tumors contained erythrocytes or profuse hemorrhage. We demonstrated that in Rip1VEGF-D mice, intra-lymphatic bleedings resulted from blood-lymphatic vessel shunts in the vicinity of islets. It remains to be shown whether these shunts formed upon deregulated VEGF-D-induced lymphangiogenesis or whether blood vessels heading from the exocrine tissue through the lymphatic lacunae into islets or tumors were mechanically instable. However, the design of future lymphangiogenic therapies for patients suffering from primary or secondary lymphedema should consider that VEGF-D might induce similar unfavorable side effects.

Furthermore, 23% of the newly formed islet- and tumor-associated lymphatic vessels of Rip1VEGF-D and Rip1Tag2;Rip1VEGF-D mice contained immune cells, which formed large clusters with increasing age of the mice. These clusters predominantly consisted of T helper and B lymphocytes as well as macrophages, whereas cytotoxic T cells were only rarely detected. Since the intra-lymphatic leucocyte accumulations are reminiscent of a lymph congestion, one possible explanation would be that immune cell clusters resulted from a malfunction of a few of the islet-/tumor-associated lymphatic vessels. In contrast, we found no significant differences in the numbers of intra-tumoral lymphocytes but less intra-tumoral macrophages in orthotopic Rip1Tag2;Rip1VEGF-D compared to control tumors. These results were not reproducible in ectopic tumors, since a comparative analysis of s.c. VEGF-D-positive and VEGF-D-negative insulinomas revealed equal numbers of tumor-associated immune cells. Although currently, we cannot conclusively explain the reduction of intra-tumoral macrophages in orthotopic tumors, we hypothesize that the reduced tumoral MVD may restrict the number of monocytes accessing Rip1Tag2;Rip1VEGF-D tumors.

hVEGF-D is 48% identical to hVEGF-C, and both molecules display similar binding properties for VEGFR-3 and VEGFR-2 (reviewed in [45]). Recently, VEGF-C has been

studied in the Rip1Tag2 mouse model [146], which enabled us to directly compare biological effects elicited by VEGF-D and VEGF-C. Similarly to VEGF-D, transgenic expression of VEGF-C induced peri- but not intra-tumoral lymphangiogenesis in Rip1Tag2;Rip1VEGF-C mice, thereby promoting the dissemination of tumor cells to regional lymph nodes. However, neither this nor our study revealed lung metastases in Rip1Tag2;Rip1VEGF-C mice. Yet, a systematic screen for such is still pending and the occurrence of lung metastases cannot be conclusively excluded. Although also VEGF-C has been shown to promote angiogenesis, no such activity could be evidenced in Rip1Tag2;Rip1VEGF-C tumors [155, 156]. Nevertheless, in contrast to transgenic VEGF-D, expression of VEGF-C had no negative impact on tumor angiogenesis and tumor growth. Also, no intra-lymphatic hemorrhages and no immune cell clusters were found in Rip1Tag2;Rip1VEGF-C mice. The qualitative dissimilarity of VEGF-D- and VEGF-C-elicited effects indicate that these factors may induce the formation of lymphatic vessels that differ on the functional and molecular level. For example, it is possible that endothelial cells of newly formed lymphatic vessels release distinct paracrine factors depending on whether endothelial cells have been stimulated by VEGF-D or VEGF-C. These paracrine factors may differently influence primary tumor and tumor endothelial cells, facilitating lung metastasis and inhibiting angiogenesis in VEGF-D- but not VEGF-C-transgenic mice, respectively. Future studies on Rip1Tag2;Rip1VEGF-D and Rip1Tag2;Rip1VEGF-C mice as well as cultured primary endothelial cells from lymphatic capillaries are required to identify distinct molecular alterations induced by VEGF-D and VEGF-C.

In conclusion, our results support the notion that VEGF-D expressed by tumor cells promotes metastasis to regional lymph nodes and the lungs by inducing peri-tumoral lymphangiogenesis. In contrast, tumor angiogenesis is reduced. Furthermore, we demonstrate that the tumor microenvironment critically modulates whether VEGF-D-induced lymphangiogenesis occurs in the tumor parenchyma or at the tumor periphery and whether expression of VEGF-D affects tumor angiogenesis.

3.2. Activation of VEGFR-3 is sufficient to promote lymphogenous metastasis

Lucie Kopfstein¹, Pascal Lorentz¹, Tanja Veikkola², Kari Alitalo², Gerhard Christofori¹

¹Department of Clinical-Biological Sciences, Institute of Biochemistry and Genetics,
University of Basel, 4058 Basel, Switzerland

²Molecular/Cancer Biology Laboratory, Biomedicum, University of Helsinki, Helsinki 00014,
Finland

Running title: VEGF-C156S promotes metastasis

This work was supported by grants from the Swiss National Science Foundation, the Swiss Cancer League, the Swiss Bridge Award, the Krebsliga Beider Basel, the EU-FP6 framework programmes LYMPHANGIOGENOMICS LSHG-CT-2004-503573 and BRECOSM LSHC-CT-2004-503224, and Novartis Pharma Inc.

3.2.1. Abstract

In many human carcinomas, expression of the lymphangiogenic vascular endothelial growth factor-C (VEGF-C) and VEGF-D correlates with increased tumor-associated lymphangiogenesis and the emergence of regional lymph node metastases. Both factors can activate VEGF receptor 3 (VEGFR-3), the expression of which is largely restricted to lymphatic endothelium in the adult, and VEGFR-2, which is found on both blood and lymphatic vessels. By employing a recently engineered selective ligand for VEGFR-3 (VEGF-C156S) we aimed to assess whether the stimulation of tumor lymphangiogenesis via VEGFR-3 is sufficient to promote lymphogenous metastasis. Therefore, we generated transgenic mice, expressing VEGF-C156S in β -cells of pancreatic islets of Langerhans. Whereas wildtype islets were not associated with lymphatics, Rip1VEGF-C156S islets were often surrounded by large lymphatic lacunae. These mice were crossed with Rip1Tag2 mice, a transgenic model of poorly metastatic pancreatic β -cell carcinogenesis. While control mice neither exhibited pronounced tumor-associated lymphangiogenesis nor metastases, tumors of Rip1Tag2;Rip1VEGF-C156S mice were in close contact with newly-formed lymphatic vessels and frequently developed regional lymph node metastases. Our results demonstrate that VEGF-C156S-induced activation of VEGFR-3 is sufficient to promote tumor-associated lymphangiogenesis and lymphogenous metastasis.

3.2.2. Introduction

The vascular endothelial growth factor (VEGF) family of glycoproteins and their receptors (VEGFRs) are important players of physiological and pathological angiogenesis and lymphangiogenesis. To date, five mammalian VEGF family members have been identified, including VEGF-A, VEGF-B, VEGF-C, VEGF-D, and PlGF. VEGF-A, VEGF-B and PlGF have been linked to angiogenic processes via activation of blood endothelial VEGFR-1 and VEGFR-2. In contrast, VEGF-C and VEGF-D are the only identified natural ligands for VEGFR-3, the expression of which is largely restricted to lymphatic endothelium. However, the fully processed forms of VEGF-C and VEGF-D are able to also activate VEGFR-2. Although predominantly expressed on blood endothelium, VEGFR-2 is also found on some lymphatic vessels [67]. Therefore, mature VEGF-C and VEGF-D exhibit lymphangiogenic activities via activation of both VEGFR-3 and VEGFR-2 and can promote angiogenesis via VEGFR-2 [41, 53, 131, 132, 135, 155, 157]. Moreover, VEGF-C was shown to induce the formation of VEGFR-2/VEGFR-3 heterodimers *in vitro*, which may modulate sensitivity to VEGFR-2 signaling in vessels co-expressing the two receptors [158-162].

The fatality of cancer predominantly results from the formation of metastases rather than from the primary tumor itself. Among many tumor cell-intrinsic alterations such as gain of migratory and invasive properties of cancer cells, also processes in the tumor stroma contribute to metastatic dissemination. These include lymphangiogenesis triggered by tumor-

secreted soluble factors, such as VEGF-C and VEGF-D, resulting in an increase in the number and size of lymphatic escape routes for metastatic tumor cells (reviewed in [89]). Accordingly, a variety of human tumors express high levels of VEGF-C and VEGF-D, which correlates with tumor-associated lymphangiogenesis and the emergence of regional lymph node metastases (reviewed in [163]). Furthermore, experiments using xenotransplantation and transgenic mouse models have demonstrated that VEGF-C and VEGF-D expressed by tumor cells enhance lymphogenous metastasis via induction of tumor-associated lymphangiogenesis [100, 144, 146]. However, several of these studies reported a simultaneous increase in tumor angiogenesis, which suggests the parallel activation of VEGFR-2 [100]. Therefore, it is not clear whether activation of VEGFR-3 is sufficient for tumor-associated lymphangiogenesis and lymphogenous metastasis and to what extent VEGF-C- and VEGF-D-mediated induction of VEGFR-2 signaling contributes to or even is required for these processes.

Recently, a mutant form of VEGF-C, VEGF-C156S, has been generated by replacing the second of the eight conserved cysteine residues of the VEGF homology domain (VHD) (Cys156) with a serine. In contrast to VEGF-C, VEGF-C156S is a selective agonist of VEGFR-3 but not VEGFR-2 and has therefore enabled the study of VEGFR-3-intrinsic biological functions [55]. A transgenic mouse model, in which VEGF-C156S is expressed in basal keratinocytes of the skin, has demonstrated that VEGFR-3 activation by VEGF-C156S promoted dermal lymphangiogenesis without influencing angiogenesis [135].

The present study addresses whether activation of VEGFR-3 is sufficient to promote tumor lymphangiogenesis and thereby the spread of cancer cells to regional lymph nodes. Therefore, we have generated transgenic mice, in which expression of VEGF-C156S is driven by the rat insulin promoter (Rip1) and thereby is specifically targeted to β -cells of pancreatic islets of Langerhans. These mice were subsequently crossed with Rip1Tag2 mice, a transgenic mouse model of poorly metastatic β -cell carcinogenesis [124], and tumor lymphangiogenesis, angiogenesis, and metastasis were analyzed. Furthermore, we aimed to compare the investigated parameters with results obtained from a previous analysis of Rip1Tag2;Rip1VEGF-C mice, which exhibited increased tumor-associated lymphangiogenesis and lymphogenous metastasis [146].

3.2.3. Materials and Methods

Cloning of the Rip1VEGF-C156Sdel36 construct

The original Rip1VEGF-C156S construct was kindly provided by T. Veikkola (Molecular/Cancer Biology Laboratory, Biomedicum, University of Helsinki, Helsinki, Finland). This construct was generated by blunt ligation of the HindIII/NotI cDNA fragment encoding the 1998 bp coding region of full length human VEGF-C156S (nucleotides 80 – 2076, Acc. No. NM_005429) between the 704 bp BamHI/XbaI fragment of the rat insulin gene II promoter and a 436 bp fragment containing SV40 introns and polyadenylation signal sequences of the HindIII/XbaI opened Rip1 vector (Rip1; [124]). To enable excision of the Rip1VEGF-C156S transgene insert with BamHI for generation of transgenic mice, a third BamHI restriction site located between the Rip1 and the hVEGF-C156S sequence was eliminated by a double digest with XbaI and SpeI followed by blunt religation of the vector.

Therefore, 10 μ l of DNA was incubated for one hour at 37°C with 10 μ l 10x Klenow buffer, 10 μ l of 10 mM ATP, 2 μ l of Klenow enzyme, and 1 μ l of T4 DNA ligase adjusted with sterile H₂O to a 100 μ l reaction volume (Klenow buffer: 0.5M Tris-HCl pH 7.5, 0.1 M MgCl₂, 10 mM DTT, 0.5 mg/ml BSA, 200 μ M dNTPs; Klenow enzyme and T4 DNA ligase from Boehringer Mannheim/Roche, Mannheim, Germany). The new construct lacking 36 bp between the Rip1 and the hVEGF-C156S sequence was named Rip1VEGF-C156Sdel36.

Generation of Rip1VEGF-C156S Transgenic Mice

50 μ g of the Rip1VEGF-C156Sdel36 plasmid was digested with 10 μ L BamHI in a total volume of 155 μ L for five hours and resolved on a 0.8% agarose gel. The ~ 3 kb band containing the BamHI-cut Rip1VEGF-C156S transgene construct was excised from the gel and purified once with the QIAEX II gel extraction kit (Qiagen, Hombrechtikon, Switzerland) kit. The purified Rip1VEGF-C156Sdel36 DNA fragment was used for injection into fertilized C57BL/6 oocytes to generate Rip1VEGF-C156S transgenic mice according to standard procedures at the Transgenic Mouse Core Facility TMCF, Biozentrum, Basel [147].

Genotypes were confirmed by PCR analysis of standard toe genomic DNA preparations using a primer pair specific for the transgene (forward primer located in the Rip1 sequence: 5'-TCC GGA CTC GAC CTC TCG GAC; reverse primer located in the VEGF-C sequence: 5'-CCC CAC ATC TAT ACA CAC CTC C). PCR cycles were: 94°C, 5 min (x1); 94°C, 30 sec, 64°C, 30 sec, and 72°C, 1 min 30 sec (x34); and 72°C, 10 min (x1). PCR products were analyzed in 1.5% agarose gels. Routine PCR screening of Rip1VEGF-C156S heterozygotes was performed according to the same protocol.

For histopathological analysis, lectin perfusion, electron microscopy, and vascular cast analysis refer to General Materials and Methods

3.2.4. Results

Generation of Rip1VEGF-C156S transgenic mice

To generate transgenic mice specifically expressing human VEGF-C156S (hVEGF-C156S) in β -cells of pancreatic islets of Langerhans, the hVEGF-C156S cDNA was cloned between the rat insulin II gene promoter fragment (Rip) and the human growth hormone introns and a polyadenylation signal (Rip1; [124]). The original Rip1VEGF-C156S construct was generated by blunt ligation of a HindIII/NotI cDNA fragment encoding the 1998 bp coding region of full length human VEGF-C156S to the XbaI/HindIII-opened Rip1 vector. To prepare the Rip1VEGF-C156S construct for injection into fertilized mouse oocytes, the Rip1VEGF-C156S transgene had to be excised from the vector by a BamHI restriction digest (BamHI being the only suitable restriction site). Therefore, a third BamHI restriction site located in the multiple cloning site between the Rip1 and the hVEGF-C156S sequence was removed, which resulted in the Rip1VEGF-C156Sdel36 plasmid lacking 36 bp of the original vector (Figure 1). Injection of the Rip1VEGF-C156S transgene construct into fertilized C57BL/6 oocytes resulted in two viable and fertile founder lines exhibiting stable germline transmission named Rip1VEGF-C156S-1 and Rip1VEGF-C156S-2.

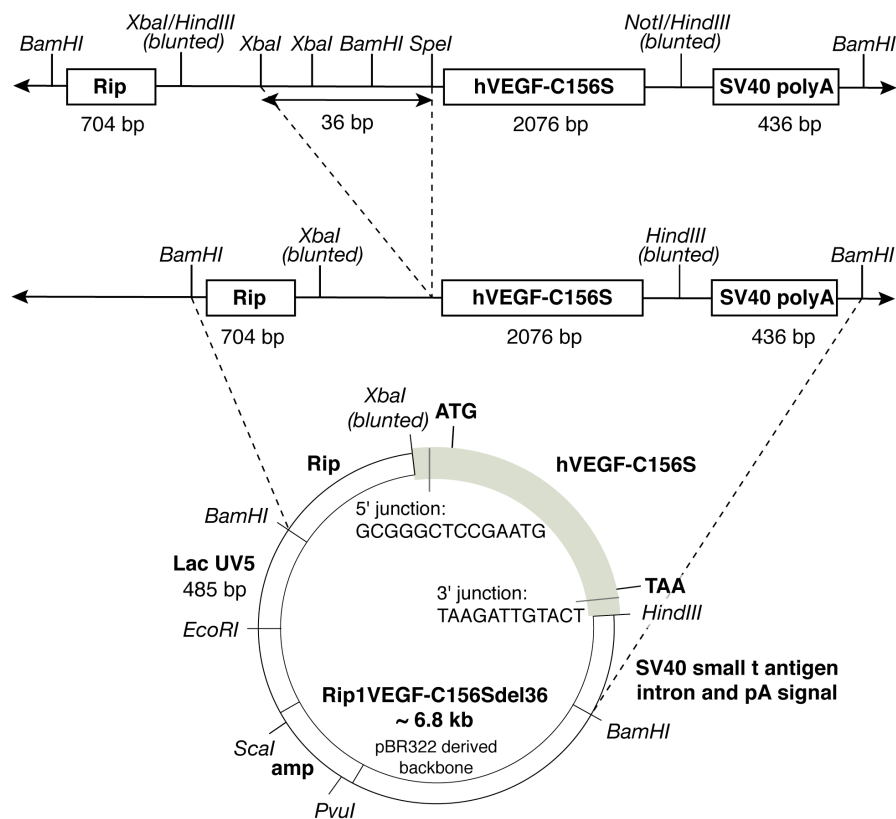


Figure 1. Modification of the Rip1 VEGF-C156S construct for generation of Rip1VEGF-C156S transgenic mice

VEGF-C156S induces peri-insular lymphangiogenesis in Rip1VEGF-C156S transgenic mice

To test whether the transgene was expressed, pancreatic sections from transgenic and control littermate mice were stained with anti-VEGF-C antibody. For both transgenic founderlines, immunofluorescence analysis revealed strong VEGF-C immunoreactivity in the majority of islet cells as would be expected from the relative abundance of insulin-expressing β -cells in islets (approximately 80%). In contrast, no VEGF-C expression was detectable in islets of wildtype littermate mice (Figure 2A). To investigate morphological changes elicited by transgenic expression of VEGF-C156S, we analyzed pancreata by histology, immunohistochemistry and immunofluorescence. Hematoxylin and eosin stainings of pancreata from Rip1VEGFC156S transgenic mice revealed that most islets were separated from the surrounding exocrine tissue by large vascular structures. Based on immunoreactivity for the lymphatic endothelium marker Podoplanin, these peri-insular structures were identified as enlarged lymphatic capillaries. Using these methods, no lymphatic vessels were detected in transgenic islets themselves or associated with islets of control littermate mice (Figure 2A). Also on the ultra-structural level visualized using toluidine blue-stained semi-thin sections, enlarged lymphatic vessels were frequently found in close proximity to islets of Rip1VEGF-C156S but not C57BL/6 littermate control mice (Figure 2B). Importantly, no impact of VEGF-C156S on blood vessels could be detected when comparing Rip1VEGF-C156S with control mice (data not shown). Notably, the phenotype of Rip1VEGF-C156S was identical to that previously described for Rip1VEGF-C mice, which displayed peri-insular lymphangiogenesis without affecting angiogenesis [146].

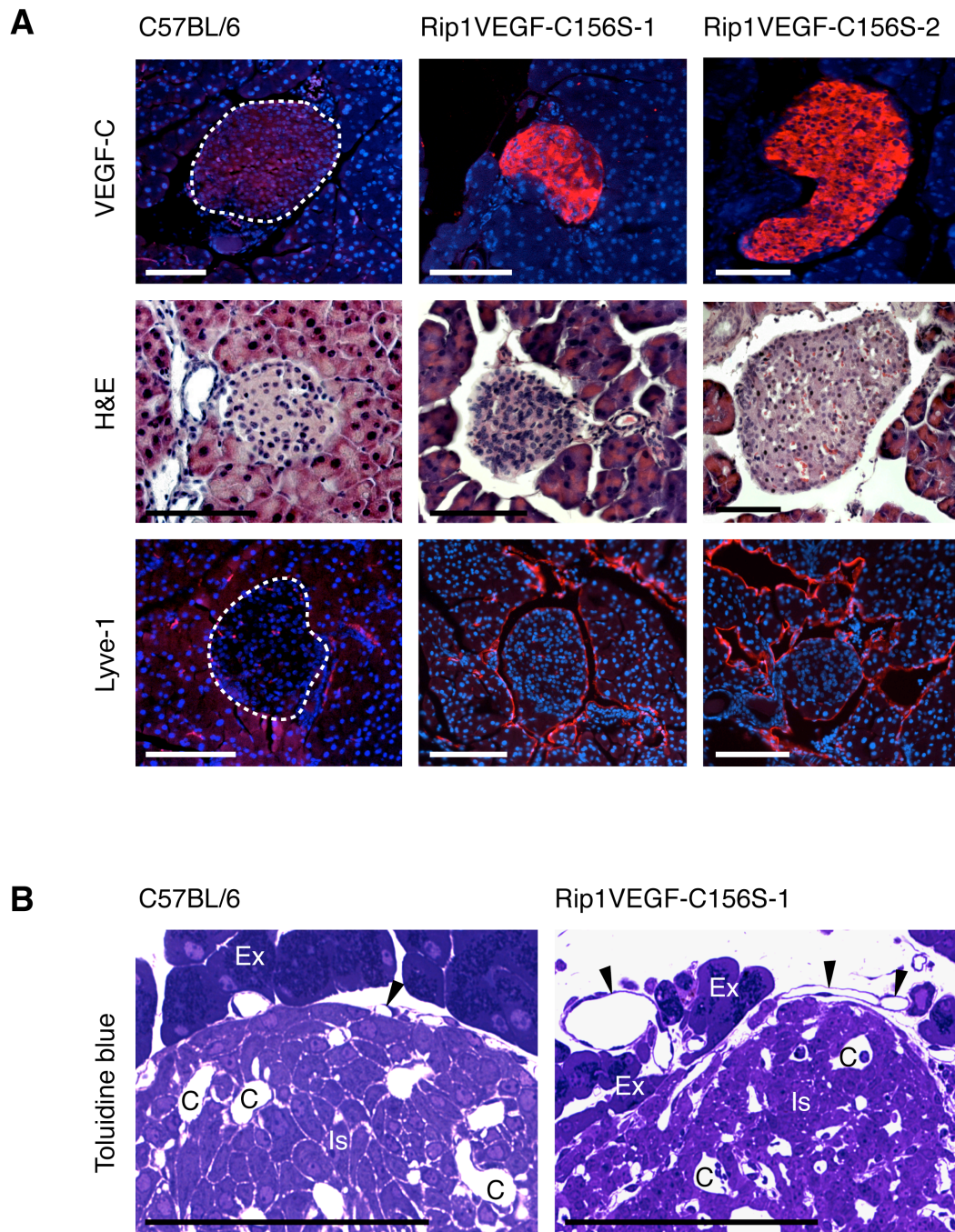


Figure 2. Phenotypic analysis of transgenic Rip1VEGF-C156S founder lines

(A, **Upper panel**) Immunofluorescent staining with anti-VEGF-C antibody (red). Nuclei are counterstained with DAPI (A, **middle panel**) Hematoxylin and eosin staining of pancreatic sections (A, **lower panel**) Immunofluorescent staining with anti-LYVE-1 antibody. Nuclei are counterstained with DAPI. (B) Toluidine-blue-stained semithin sections from transgenic and control pancreata as indicated. Dashed lines delineate islets; arrowheads indicate lymphatic capillaries; C, capillary; Ex, exocrine tissue; Is, islet. Scale bars: (A) 100 μ m, (B) 50 μ m.

VEGF-C156S promotes peri- and intra-tumoral lymphangiogenesis

To assess the role of VEGF-C156S in tumor angiogenesis, lymphangiogenesis, and metastasis, we crossed Rip1VEGF-C156S-2 with Rip1Tag2 mice, a transgenic mouse model of pancreatic β -cell carcinogenesis [124]. Of note, β -cell tumors that develop in Rip1Tag2 mice are capable of local invasion, but metastasis is only rarely encountered. Rip1Tag2 control and Rip1Tag2;Rip1VEGF-C156S double transgenic mice were sacrificed between 12 and 14 weeks of age, a time-point, when these mice succumb to hypoglycemia caused by excessive tumoral insulin production.

The analysis of Rip1Tag2;Rip1VEGF-C156S and control tumor mice revealed no significant differences with regard to tumor incidence (defined as the number of tumors per pancreas having a diameter >1 mm) and tumor volume (defined as the sum of all macroscopically detectable tumors per pancreas having a diameter >1 mm and assuming that the tumors are spherical). Since angiogenesis is predominantly mediated via VEGFR-1 and VEGFR-2, we investigated whether VEGF-C156S as a selective ligand for VEGFR-3 had any impact on tumor angiogenesis. To measure the tumor blood vessel density, we stained pancreatic sections of the two genotypes using the blood endothelial marker CD31 and counted intra-tumoral blood vessels. As expected, expression of the selective VEGFR-3 ligand had no effect on tumor angiogenesis, which was reflected by comparable tumor microvessel densities in both mouse lines (Table 1).

Table 1. Tumor incidence, volume, and microvessel density in Rip1Tag2;Rip1VEGF-C156S mice

	Rip1Tag2	Rip1Tag2;Rip1VEGF-C156S	p value
Tumor incidence/ mouse ^a	7 \pm 3.2 (n = 77, N = 11)	6.1 \pm 1.5 (n = 49, N = 8)	0.4364*
Total tumor volume/ mouse (mm ³) ^a	41.5 \pm 37.4 (n = 77, N = 11)	23.9 \pm 28.5 (n = 49, N = 8)	0.2797**
Tumor blood vessel density ^b	67.2 \pm 13.42 (n = 59, N = 6)	63.71 \pm 19.21 (n = 68, N = 7)	0.2389**

^an = number of tumors, N = number of mice.

^bTumor blood vessel density assessed by counting intra-tumoral CD31-positive vessels per 40x magnification field. n = number of fields, N = number of mice.

*Data were analyzed by a two-tailed Student's t test. Values represent mean \pm SD.

**Data were analyzed by a two-tailed Student's t test with Welch correction. Values represent mean \pm SD.

In contrast, analysis of pancreata by hematoxylin and eosin staining unveiled striking morphological differences at the tumor periphery comparable to those observed in single transgenic mice. Most double-transgenic tumors were separated from the exocrine tissue by large endothelium-lined lacunae, which partially or completely enclosed the tumors. Based on their immunoreactivity for the lymphatic endothelium markers Podoplanin and LYVE-1, these lacunae were identified as lymphatic vessels. In large tumors, lymphatic vessels were also found in the tumor center. In agreement with recent publications, Rip1Tag2 tumors were only rarely found in close association with lymphatic vessels (Figure 3A)[146, 150].

Quantification of peri-tumoral lymphangiogenesis was performed by assessing the extent by which LYVE-1-positive lymphatic vessels surrounded the tumor perimeter. Thereby we confirmed that 74 % of insulinomas in double-transgenic animals had closely apposed lymphatics encompassing most or all of the insulinoma circumference. In contrast, only 40 % of Rip1Tag2 control tumors were to some extent associated with lymphatics (Figure 3B). These results indicate that VEGF-C156S promotes tumor-associated lymphangiogenesis.

VEGF-C156S promotes regional lymph node metastasis

Evidence from clinical and experimental studies suggests that the close association of tumors with lymphatic vessels might promote lymphogenous spread of tumor cells, which may follow routes of natural drainage and subsequently form metastases in regional lymph nodes [146]. To assess whether VEGF-C156S-induced peri-tumoral lymphangiogenesis promotes the lymphogenous dissemination of cancer cells, hematoxylin and eosin-stained pancreatic sections of Rip1Tag2 and Rip1Tag2;Rip1VEGF-C156S mice were screened for metastatic insulinoma cells. Consistent with previous reports, β -cells were only occasionally found to disseminate in lymphatic vessels of Rip1Tag2 pancreata, which may also account for the fact that none of the investigated control mice displayed metastases in pancreatic lymph nodes. In contrast, double-transgenic Rip1Tag2;Rip1VEGF-C156S mice frequently exhibited tumor cell clusters circulating in lymphatic vessels located next to tumors and in the exocrine pancreas (data not shown). Concomitantly, metastases were found at the afferent rim of at least one lymph node on all pancreatic sections exhibiting lymph nodes (Figure 3C, Table II). Tumor cells still retained their well-differentiated morphology, and no signs of anaplasia such as an altered nucleus/cytoplasm ratio or nuclear atypia were observed. Furthermore, all metastases were immunoreactive for insulin, confirming their derivation from primary β -cell tumors (data not shown). A comparative analysis of tumor grades demonstrated that the expression of VEGF-C156S did not affect the ratio of benign adenoma versus malignant carcinoma (Table II). In summary, our data demonstrate that activation of VEGFR-3 alone results in the formation of a dense tumor-associated lymphatic network and promotes the formation of regional lymph node metastases.

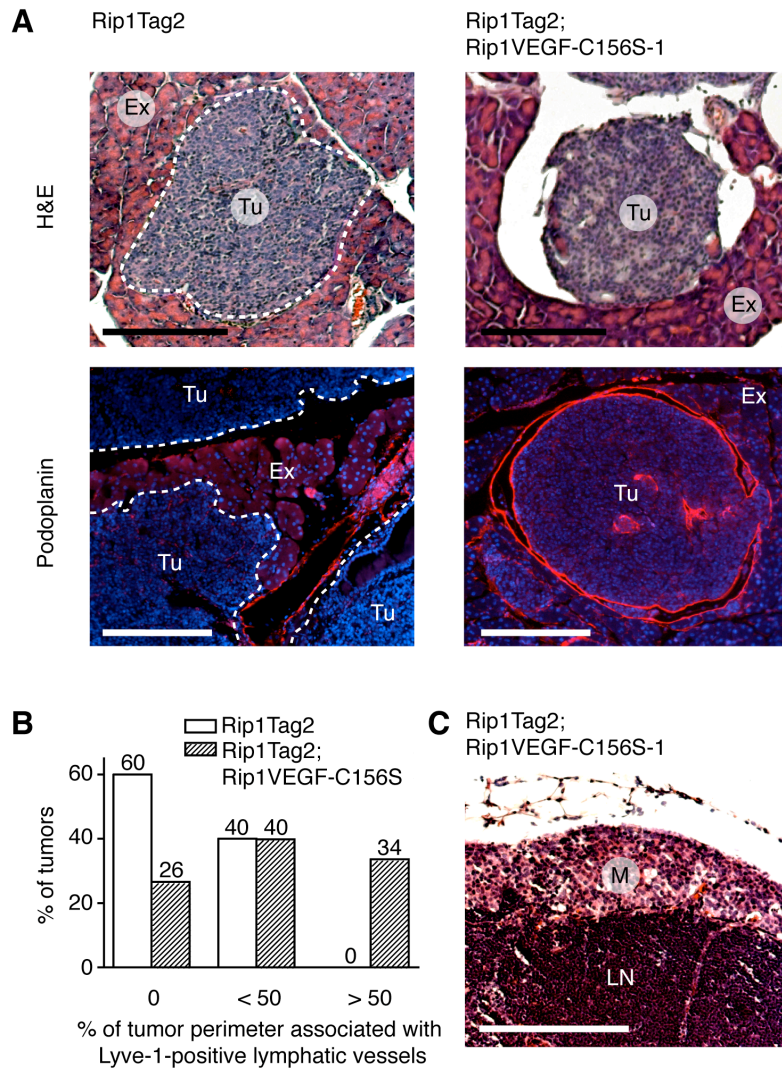


Figure 3 .
Phenotypical analysis
of Rip1Tag2;
Rip1VEGF-C156S
mice

(A) Hematoxylin and eosin and immunofluorescence staining with anti-Podoplanin antibody (B) Quantification of peri-tumoral lymphangiogenesis as described in the text. Results are indicated as percentages of tumors in a given class above the bars. 113 tumors of seven

Rip1Tag2;Rip1VEGF-C156S mice and 170 tumors of six Rip1Tag2 mice were analyzed. (C) Hematoxylin and eosin staining of a regional lymph node metastasis. Dashed lines delineate tumors; Ex, exocrine tissue; LN, lymph node; M, metastasis; Tu, tumor. Scale bars: 100 μ m.

Table II. Analysis of tumor grades and metastasis in Rip1Tag2;Rip1VEGF-C156S and control mice.

	Rip1Tag2	Rip1Tag2;Rip1VEGF-C156S
Adenoma/Carcinoma ^a	20/80 % (n = 333, N = 6)	17/83 % (n = 218, N = 5)
Lymph node metastasis ^b	0 % (0/2)	100 % (3/3)

^an = number of tumors, N = number of mice.

^bAs detected by haematoxylin and eosin staining. Only mice with histologically detected pancreatic lymph nodes were included in this analysis.

3.2.5. Discussion

Here we have addressed whether selective activation of VEGFR-3 is sufficient to promote tumor-associated lymphangiogenesis and metastasis by expressing the VEGFR-3-selective ligand VEGF-C156S in tumors of Rip1Tag2 mice, a transgenic mouse model of poorly metastatic multistep β -cell carcinogenesis [124]. For this purpose, we generated two lines of Rip1VEGF-C156S transgenic mice, in which expression of VEGF-C156S is specifically targeted to β -cells of the endocrine pancreas. While in control littermate mice, small lymphatic capillaries were detected only rarely in the vicinity of islets and exclusively upon visualization by electron microscopy, most islets of Rip1VEGF-C156S mice were partially or completely encompassed by large endothelium-lined lacunae immuno-reactive for the lymphatic vessel markers Podoplanin and LYVE-1. These observations demonstrate that the selective activation of VEGFR-3 promotes lymphangiogenesis in Rip1VEGF-C156S mice. Since our and previous studies of wildtype mice have revealed the presence of a few lymphatic capillaries close to islets of Langerhans, we hypothesize that the enlarged peri-insular lymphatic lacunae found in Rip1VEGF-C156S transgenic mice result from the dilation and growth of pre-existing lymphatic capillaries [164]. In accordance with our results, the analysis of K14-VEGF-C156S transgenic mice showed that expression of VEGF-C156S in the skin stimulated the growth of dermal lymphatic vessels [135]. Interestingly, the phenotype of Rip1VEGF-C156S mice is identical to that of the recently published Rip1VEGF-C mice, which expressed wildtype VEGF-C in islets of Langerhans [146]. This observation indicates that in the Rip1 model, all effects of transgenic VEGF-C expression are mediated predominantly via VEGFR-3 and not VEGFR-2.

To assess whether activation of VEGFR-3 is sufficient to stimulate tumor lymphangiogenesis and promote metastasis, we crossed Rip1VEGF-C156S with Rip1Tag2 mice, a transgenic mouse model of poorly metastatic multistep β -cell carcinogenesis [124]. In line with previous reports, small lymphatic capillaries were detected in the vicinity of some insulinomas of Rip1Tag2 control mice (40%), while the majority of tumors lacked any contact with lymphatic vessels. In contrast, transgenic expression of VEGF-C156S and thus activation of VEGFR-3 in double transgenic Rip1Tag2;Rip1VEGF-C156S mice resulted in the growth of large lymphatic lacunae, which partially (40%) or completely (34%) surrounded most tumors. These results demonstrate that activation of VEGFR-3 by a selective ligand is sufficient to promote tumor-associated lymphangiogenesis.

Tumors of Rip1Tag2 mice are intrinsically metastatic but realize their metastatic potential only rarely, which may be due to the early death of these mice resulting from excessive tumoral insulin production and subsequent hypoglycemia [124]. In fact, most reports studying the process of metastasis formation with use of the Rip1Tag2 model did not find any metastases in these mice [146, 148, 150]. However, VEGF-C expressed in Rip1Tag2;Rip1VEGF-C double transgenic mice promoted metastasis to regional lymph nodes by stimulating tumor-associated lymphangiogenesis. To investigate, whether VEGF-C156S-induced peri-tumoral lymphangiogenesis is sufficient to promote lymphogenous metastasis, we screened lymph nodes of three Rip1Tag2;Rip1VEGF-C156S mice for insulinoma metastases. Indeed, in every investigated double transgenic mouse, one or more metastases were found in regional pancreatic lymph nodes. All metastases were well differentiated and still express insulin. Furthermore, a comparative analysis of primary tumor gradings demonstrated that expression of VEGF-C156S did not affect the ratio of benign

adenoma versus malignant carcinoma, suggesting that VEGF-C156S does not promote invasive and migratory capabilities of tumor cells. Together with the fact that Rip1Tag2 tumors can metastasize but do so only exceptionally, our observations suggest that VEGF-C156S-induced activation of VEGFR-3 promotes lymphogenous metastasis by stimulating tumor-associated lymphangiogenesis.

Although in the adult vasculature mainly restricted to lymphatic endothelium, recent studies have evidenced that VEGFR-3 is to some extent expressed also on quiescent vascular endothelial cells, primarily in fenestrated capillaries such as in pancreatic islets [158]. Moreover, VEGFR-3 was reported to become re-expressed on the blood vasculature of tumors [146, 165]. Therefore, we investigated whether VEGF-C156S may promote tumor angiogenesis and assessed the tumoral microvessel density using the specific blood endothelial marker CD31. Statistical analyses revealed comparable tumor microvessel densities in Rip1Tag2;Rip1VEGF-C156S and control mice, demonstrating that VEGF-C156S has no effect on tumor angiogenesis and suggesting that a potential expression of VEGFR-3 on tumor blood endothelium may play only a subordinate role in these mice. Importantly, also wildtype VEGF-C, which can activate both VEGFR-2 and VEGFR-3 and thereby promoted angiogenesis in several experimental studies, exhibited no angiogenic activity in Rip1Tag2;Rip1VEGF-C tumors [146, 155, 156]. However, the processing state of wildtype VEGF-C in tumors of Rip1Tag2;Rip1VEGF-C mice remains to be elucidated, since the angiogenic ability of VEGF-C is dependent on its proteolytic processing to the mature form [131].

Taken together, our data demonstrate that activation of VEGFR-3 alone is sufficient to promote the formation of a tumor-associated lymphatic network, which increases the contact area between tumor cells and potential lymphatic escape routes, thereby promoting the passive spread of cancer cells to regional lymph nodes. The comparison of Rip1Tag2;Rip1VEGF-C156S and the previously published Rip1Tag2;Rip1VEGF-C mice suggests that at least on the macro- and microscopic level, Rip1Tag2;Rip1VEGF-C156S phenocopy Rip1Tag2;Rip1VEGF-C mice [146]. Future studies on cultured primary endothelial cells deriving from lymphatic capillaries of both transgenic mouse lines will elucidate whether VEGF-C and VEGF-C156S induce distinct biological effects on the molecular level. Furthermore, it will be interesting to investigate whether activation of VEGFR-3 by VEGF-C156S can induce the formation of VEGFR-2/VEGFR-3 heterodimers such as observed for VEGF-C. Nevertheless, our results suggest that the selective inhibition of VEGFR-3 signaling may already significantly reduce the risk of further metastatic dissemination of tumor cells.

4. Generation and analysis of transgenic mice expressing angiogenic VEGF family members during Rip1Tag2 tumorigenesis

4.1. PIGF-1 Inhibits Tumor Growth in a Transgenic Mouse Model of Insulinoma

Lucie Kopfstein¹, Tibor Schomber¹, Valentin G. Djonov², Karin Strittmatter¹, Gerhard Christofori¹

¹Department of Clinical-Biological Sciences, Institute of Biochemistry and Genetics,
University of Basel, 4058 Basel, Switzerland

²Institute of Anatomy, University of Berne, 3012 Berne, Switzerland

Running title: PIGF-1 Represses Tumor Growth

This work was supported by grants from the Swiss National Science Foundation, the Swiss Cancer League, the Swiss Bridge Award, the Krebsliga Beider Basel, the EU-FP6 framework programmes LYMPHANGIOGENOMICS LSHG-CT-2004-503573 and BRECOSM LSHC-CT-2004-503224, and Novartis Pharma Inc.

4.1.1. Abstract

Placental growth factor (PlGF) belongs to the vascular endothelial growth factor (VEGF) family of ligands, which are important players of angiogenesis and lymphangiogenesis. In contrast to VEGF-A, PlGF is not critical for vascular development but may be a critical regulator of VEGF-A-dependent pathological angiogenesis. In many human carcinomas, expression of PlGF correlates with increased tumor angiogenesis and growth. However, the formation of inactive PlGF-1/VEGF-A heterodimers has been recently described, suggesting that PlGF-1 might also act as an antagonist of VEGF-A-mediated tumor angiogenesis. To assess the dual role of PlGF-1 in tumor angiogenesis, we generated Rip1PlGF-1 transgenic mice, which express human PlGF-1 in β -cells of pancreatic islets of Langerhans. In comparison to the islet vasculature of control mice, the blood capillaries of transgenic islets are dramatically dilated thereby increasing the islet area occupied by blood vessels. In contrast, PlGF-1 does not affect the number of islet blood vessels. By crossing Rip1PlGF-1 with Rip1Tag2 mice, a transgenic model of pancreatic β -cell carcinogenesis, double-transgenic mice have been generated that express PlGF-1 in tumor cells. Transgenic expression of PlGF-1 during Rip1Tag2 tumorigenesis significantly reduces the tumor microvessel density as well as the tumor burden in comparison to control mice, which suggests that PlGF-1 acts as an antagonist of VEGF-A-mediated tumor angiogenesis.

4.1.2. Introduction

Placental growth factor (PlGF) is a member of the vascular endothelial growth factor (VEGF) family of ligands that control blood and lymphatic vessel development [45]. Originally identified in human placenta, PlGF is also expressed in heart, lung, thyroid gland, and skeletal muscle [166]. Alternative splicing of the human PlGF gene generates at least four isoforms, which differ in size and receptor binding properties. While PlGF-1 and PlGF-3 are freely diffusible, PlGF-2 and PlGF-4 are mostly sequestered by heparan sulfates of the extracellular matrix [167-171]. In the mouse, only the PlGF-2 homolog is expressed [172]. VEGF-A, the best-studied angiogenic VEGF family member to date, binds to VEGFR-1, VEGFR-2, and the co-receptors NP-1 and NP-2, which are expressed on blood vessel endothelium. Notably, the angiogenic effects of VEGF-A are mainly mediated via VEGFR-2. In contrast, all PlGFs are selective ligands for VEGFR-1, and PlGF-2 in addition binds to NP-1 and NP-2 [167].

Although VEGFR-1 has only low tyrosine kinase activity and deletion of its tyrosine kinase domain does not affect vascular development, intrinsic signaling of VEGFR-1 may mediate some of the PlGF-induced biological effects [14, 44]. PlGF-2 is more potent than PlGF-1 in inducing proliferation of endothelial cells and angiogenesis, which may be due to its ability to also activate NP receptors [79, 173, 174]. However, there is evidence that VEGFR-1 also acts as a decoy receptor for VEGF-A, and VEGFR-1-selective ligands such as PlGF might indirectly potentiate effects of VEGF-A by displacing it from VEGFR-1 and increasing its availability for activation of VEGFR-2 [60, 170, 175]. Recently, adenoviral gene transfer of PlGF-2 has been shown to upregulate expression of VEGF-A [176].

Furthermore, PIGF-1-induced activation of VEGFR-1 resulted in transphosphorylation of VEGFR-2 and thereby amplification of VEGF-A-driven angiogenesis via VEGFR-2 [44, 177]. Alternatively, when both factors are produced in the same cell, PIGF-1 can form inactive heterodimers with VEGF-A and inhibit VEGF-A-induced angiogenic responses *in vitro* and *in vivo* [52, 178]. Thus, PIGF-induced signaling pathways and biologic activities may depend on the spatial expression as well as alternative splicing of PIGF, and in particular PIGF-1 appears to play a dual role during angiogenesis.

Studies of PIGF-deficient mice have revealed that PIGF is not critical for the development and the maintenance of the physiologic vasculature. Yet, these mice show impaired angiogenesis, plasma extravasation, and collateral vessel growth in ischemic retina, limb and heart, wounded or inflamed skin, and cancer, suggesting that PIGF might be involved in pathological angiogenesis [68, 101, 179]. The analysis of transgenic mice expressing PIGF-2 in the skin has demonstrated increased blood vessel permeability responses and monocyte recruitment [180, 181]. In contrast, adenoviral delivery of PIGF-1 or PIGF-2 into skin, ischemic myocardium or limb induced the formation of impermeable blood vessels by stimulating their coverage with smooth muscle cells [179].

The precise role of PIGF in tumorigenesis is not fully understood. PIGF is expressed in a variety of human malignancies, including hemangioblastoma, meningioma, brain tumors, melanoma, as well as renal cell, breast, non-small cell lung, gastric, and colorectal carcinoma [96-98, 182-187]. Three of these reports correlated increased PIGF expression levels with pronounced tumor angiogenesis and growth [97, 183, 186]. Similarly, a study using PIGF-2-overexpressing Lewis Lung Carcinoma cell lines reported a PIGF-2-mediated increase in tumor angiogenesis and growth [101]. In contrast, transplantation experiments with PIGF-1-transfected mouse fibrosarcoma cells demonstrated impaired tumor growth resulting from the formation of inactive PIGF-1/VEGF-A heterodimers [178].

This study aimed to address the dual role of PIGF-1 on tumor angiogenesis in a well-characterized transgenic mouse tumor model of multistep β -cell carcinogenesis [124]. We have generated Rip1PIGF-1 transgenic mice, in which expression of human PIGF-1 is driven by the rat insulin promoter (Rip1) and thereby specifically targeted to β -cells of pancreatic islets of Langerhans. Rip1PIGF-1 mice are currently being crossed with Rip1Tag2 tumor mice, thereby generating Rip1Tag2;Rip1PIGF-1 mice. Rip1Tag2 and Rip1Tag2;Rip1PIGF-1 mice are being analyzed for tumor angiogenesis, the recruitment of smooth muscle and inflammatory cells to the tumor vasculature, and tumor growth. In addition, these mice will enable future studies of the *in vivo* formation of PIGF-1/VEGF-A heterodimers.

4.1.3. Methods

Cloning of the Rip1PlGF-1 construct

Total RNA was isolated from freshly snap frozen human placental tissue using TRIzol Reagent (Invitrogen, Carlsbad, CA) according to the manufacturer's protocol. Subsequently, placental RNA was reverse transcribed into cDNA using reverse transcriptase and random hexamers from Sigma Chemical Co., St. Louis, MO according to standard procedures. The 450 bp sequence of human PlGF-1 (hPlGF-1, gene accession number X54936, nucleotides 322-771) was amplified from the cDNA by PCR using the forward primer 5'- GCT CTA GAG ACG TCT GAG AAG ATG CCG GT (XbaI site underlined) and the reverse primer 5'- CCC AAG CTT GGT GGG TTA CCT CCG GGG (HindIII site underlined). PCR cycles were: 94°C, 5 min (x1); 94°C, 30 sec, 60°C, 30 sec, and 72°C, 1min 30 sec (x10); and 72°C, 7 min (x1). The band appearing at the expected size of PlGF-1 was extracted from the gel with the QIAEX II gel extraction kit (Qiagen, Hombrechtikon, Switzerland) and subcloned into the pBluescript SK+ vector (Sigma Chemical Co., St. Louis, MO) using XbaI and HindIII. After verification by sequencing, the PlGF-1 cDNA was subcloned into the Rip1 vector between the 704 bp rat insulin II promoter and a 436 bp stretch containing SV40 small T intron and polyadenylation signal sequences using XbaI and Hind III (Rip1; [124]).

Generation of Rip1PlGF-1 transgenic mice

100 µg of the Rip1PlGF-1 plasmid were digested with 10 µL BamHI in a total volume of 400 µL for five hours and resolved on a 0.8% agarose gel. The ~ 1.5 kb transgene construct comprising Rip1, full length hPlGF-1, and the SV40 small T intron and polyadenylation signal sequences was extracted from the gel and purified once with the QIAEX II gel extraction kit. The purified Rip1PlGF-1 fragment was used for injection into the pronucleus of fertilized C57BL/6 oocytes at the Transgenic Mouse Core Facility (TMCF, Biozentrum, Basel) according to standard procedures.

Genotypes were confirmed by PCR analysis using a primer pair specific for the transgene (forward primer located in the Rip1 sequence: 5'-TAA TGG GAC AAA CAG CAA AG; reverse primer located in the human PlGF-1 sequence: 5'-CCA CAC TTC CTG GAA GGG), starting from standard toe genomic DNA preparations. PCR cycles were: 94°C, 5 min (x1); 94°C, 30 sec, 57°C, 30 sec, and 72°C, 30 sec (x34); and 72°C, 7 min (x1). PCR products were analyzed in 1.5% agarose gels. Routine PCR screening of Rip1VEGF-PlGF-1 heterozygotes was performed according to the same protocol.

RT-PCR analysis of PlGF-1 expression

Mice were sacrificed at 3-4 weeks because of the higher ratio of endocrine to exocrine pancreas in young mice. Half of the pancreas was homogenized in TRIzol reagent for RNA isolation according to the manufacturer's protocol (Sigma Chemical Co., St. Louis, MO). 500 ng of total RNA was reverse transcribed using reverse transcriptase and random hexamers from Sigma Chemical Co., St. Louis, MO. The cDNA was screened for PLGF-1 by PCR using the forward primer 5'- GCT CAG AGA CGT CCT GAG AAG ATG CCG GT and the reverse primer 5'- CCC AAG CTT GGT GGG TTA CCT CCG GGG. PCR cycles were: 94°C, 5 min (x1); 94°C, 30 sec, 60°C, 30 sec, and 72°C, 1 min 30 sec (x10); and 72°C, 7 min (x1). PCR products were analyzed in 1.5% agarose gels.

For histopathological analysis, lectin perfusion, electron microscopy, and vascular cast analysis refer to General Materials and Methods

4.1.4. Results

Generation of Rip1PlGF-1 transgenic mice

To generate transgenic mice expressing human PlGF-1 specifically in β -cells of pancreatic islets of Langerhans, the 450 bp coding sequence of PlGF-1 was amplified from human placental tissue by RT-PCR. The cDNA fragment was subsequently cloned between the rat insulin II gene promoter fragment (Rip) and the human growth hormone introns and polyadenylation signals of the Rip1 vector using XbaI and HindIII (Figure 1). Injection of the transgene into fertilized C57BL/6 oocytes resulted in two viable and fertile founder lines exhibiting stable germline transmission termed Rip1PlGF-1-1 and Rip1PlGF-1-2.

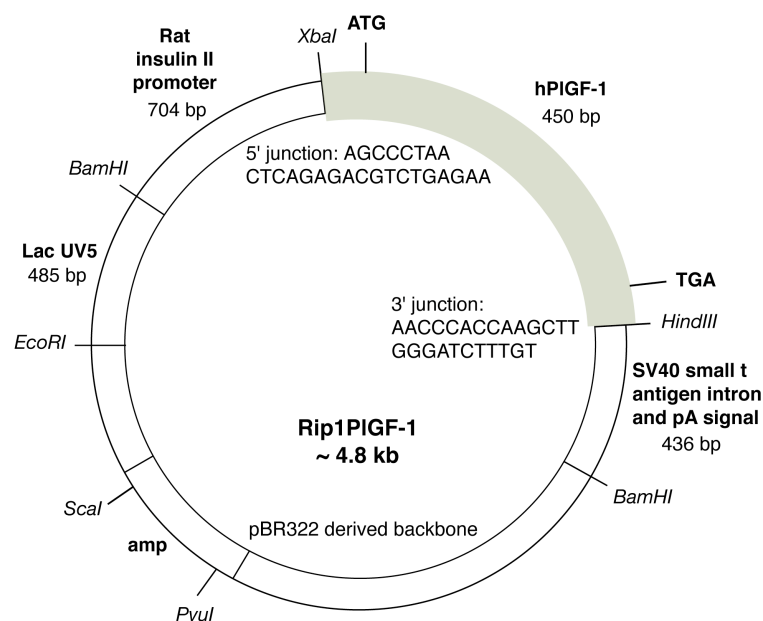


Figure 1. Cloning of the Rip1PlGF-1 construct

Dilated islet blood vessels in Rip1PlGF-1 transgenic mice

Since expression of the transgene was difficult to assess by immunohistochemical and immunofluorescence analysis due to the lack of suitable antibodies, we performed RT-PCR for PlGF-1 on RNA extracted from pancreata of the two transgenic founderlines. Using this technique, the founderline Rip1PlGF-1-2 was found to express PlGF-1, whereas no PlGF-1 expression was detected in pancreata of line Rip1PlGF-1-1 (Figure 2). Thus, all experiments were continued with the founderline Rip1PlGF-1-2. If not indicated otherwise, Rip1PlGF-1 denotes the Rip1PlGF-1-2 mouse line.

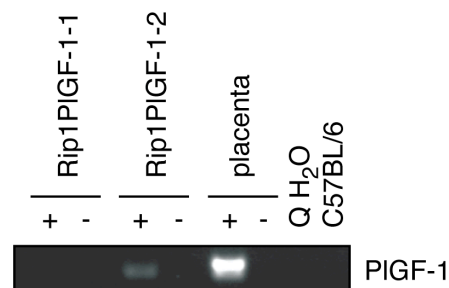


Figure 2. RT-PCR analysis of transgenic PlGF-1 expression

Pancreatic RNA from Rip1PlGF-1-1 and Rip1PlGF-1-2 mice was tested for expression of PlGF-1. Placental RNA served as positive control, RNA from C57BL/6 pancreata and H₂O as negative controls. + indicates with, - without the addition of reverse transcriptase

To investigate morphological changes induced by the expression of PlGF-1, we analyzed pancreata of Rip1PlGF-1 and littermate control mice by histology, immunohistochemistry and immunofluorescence. Hematoxylin and eosin stainings as well as toluidine blue-stained semi-thin sections of pancreata revealed dramatically dilated vascular structures containing erythrocytes in islets of Rip1PlGF-1-2 mice. Based on immunoreactivity for the blood endothelial marker CD31, these structures were identified as blood capillaries. In contrast, islets of non-expressing Rip1PlGF-1-1 and control littermate mice exhibited small blood vessels with hardly detectable lumina (Figure 3). To determine, whether the enlarged islet blood vessels of Rip1PlGF-1-2 mice allowed a physiological blood flow, a fluorophore-labeled lectin was injected into the tail vein of anaesthetized mice. The employed tomato-derived lectin is a natural glycoprotein that interacts with carbohydrates of blood endothelium. Using this technique, only the functional blood vessels are labeled and can be detected using immunofluorescence microscopy. As shown in the lower panels of Figure 3B, the injected lectin visualized the entire pancreatic blood vascular network of both control and transgenic mice, thereby revealing that the dilated insular capillaries of Rip1PlGF-1-2 mice were functional and readily perfused (Figure 3).

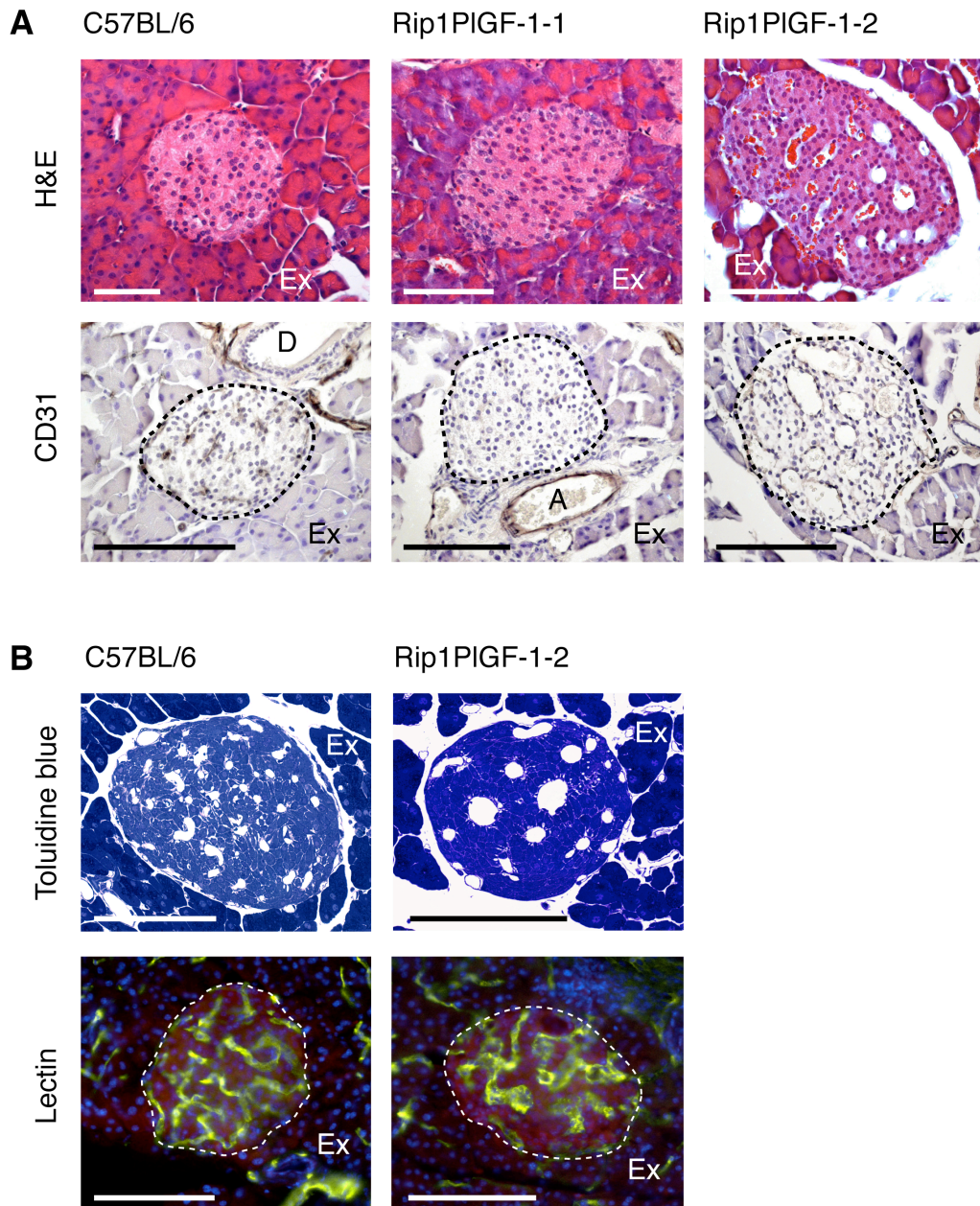


Figure 3. Morphology of Rip1PlGF-1 transgenic islets

(A) Hematoxylin and eosin stainings and immunohistochemical analysis of C57BL/6, Rip1PlGF-1-1, and Rip1PlGF-1-2 transgenic mice with anti-CD31 antibody as indicated (B, upper panel) Toluidine blue-stained semi-thin sections of control and transgenic islets (B, lower panel) Lectin (yellow)-perfused C57BL/6 and PlGF-1-2 transgenic mice. Islets have been stained with anti-insulin antibody (red). Nuclei are counterstained with DAPI. Scale bars: 100 μ m

Several studies have demonstrated angiogenic activities of PlGF-1, which appears to be limited to pathological conditions (reviewed in [72]). To assess whether PlGF-1 promoted the growth of blood vessels in islets of Rip1PlGF-1 transgenic mice, we stained pancreatic sections with anti-CD31 antibody and quantified the islet microvessel density by computer-assisted morphometric analysis. As depicted in Figure 4A, overexpression of PlGF-1 had no significant effect on the number of intra-insular blood capillaries. However, the increase in vessel diameter resulted in a significant increase of CD31-positive islet area when compared to control mice ($p = 0.0239$, two-tailed Student's *t* test). We hypothesized that PlGF-1 might stimulate blood endothelial cells to proliferate but might not induce sprouting angiogenesis, which would explain that blood vessel numbers were unchanged but the vessel diameter was increased in Rip1PlGF-1 mice. To assess a proliferative effect of PlGF-1 on endothelial cells, we performed an *in vitro* angiogenesis assay, in which isolated islets of Rip1PlGF-1 mice were co-cultured with human umbilical vein endothelial cells (HUVECs) in a three-dimensional collagen gel matrix as described previously [127, 148]. HUVECs respond by chemotactic migration, proliferation, and tube formation when co-cultured with islets or tumors that are actively undergoing angiogenesis, whereas in the case of a non-angiogenic islet, endothelial cells do not respond. It is known from the literature that wildtype islets do not induce angiogenic responses in this assay, while VEGF-A₁₆₅-expressing islets derived from Rip1VEGF-A transgenic mice as well as Rip1Tag2 tumors exhibit pronounced angiogenic activity, resulting in proliferation of HUVECs and formation of tubule-like structures [148]. In our assay, a representative rate of 74% of Rip1Tag2 tumors stimulated *in vitro* angiogenesis, whereas Rip1PlGF-1 transgenic islets did not induce proliferation and tube formation of endothelial cells and thus were completely non-angiogenic (Figure 4B). These results indicate that in our assays, PlGF-1 has no effect on endothelial cell proliferation.

A previous study has demonstrated that a significant reduction of pericytes leads to the dilation of blood vessels [188]. Since PlGF-1 did not induce proliferation of endothelial cells in our assays, we hypothesized that the hyperdilation phenotype of islet capillaries of Rip1PlGF-1 mice might result from inappropriate pericyte-coating of blood capillaries. To address this question, we stained pancreatic sections of Rip1PlGF-1 and control mice with the pericyte marker NG-2. Statistical evaluation demonstrated that the number of pericyte-coated blood capillaries per transgenic islet was comparable to that of control islets. However, the percentage of NG-2-positive islet area was significantly reduced in transgenic compared to control mice ($p = 0.0306$, two-tailed Student's *t* test). These data suggest that blood vessels in PlGF-1-expressing islets are less well stabilized by pericytes than islet that of control mice, which may account for the hyperdilation phenotype of Rip1PlGF-1 islet capillaries (Figure 4C).

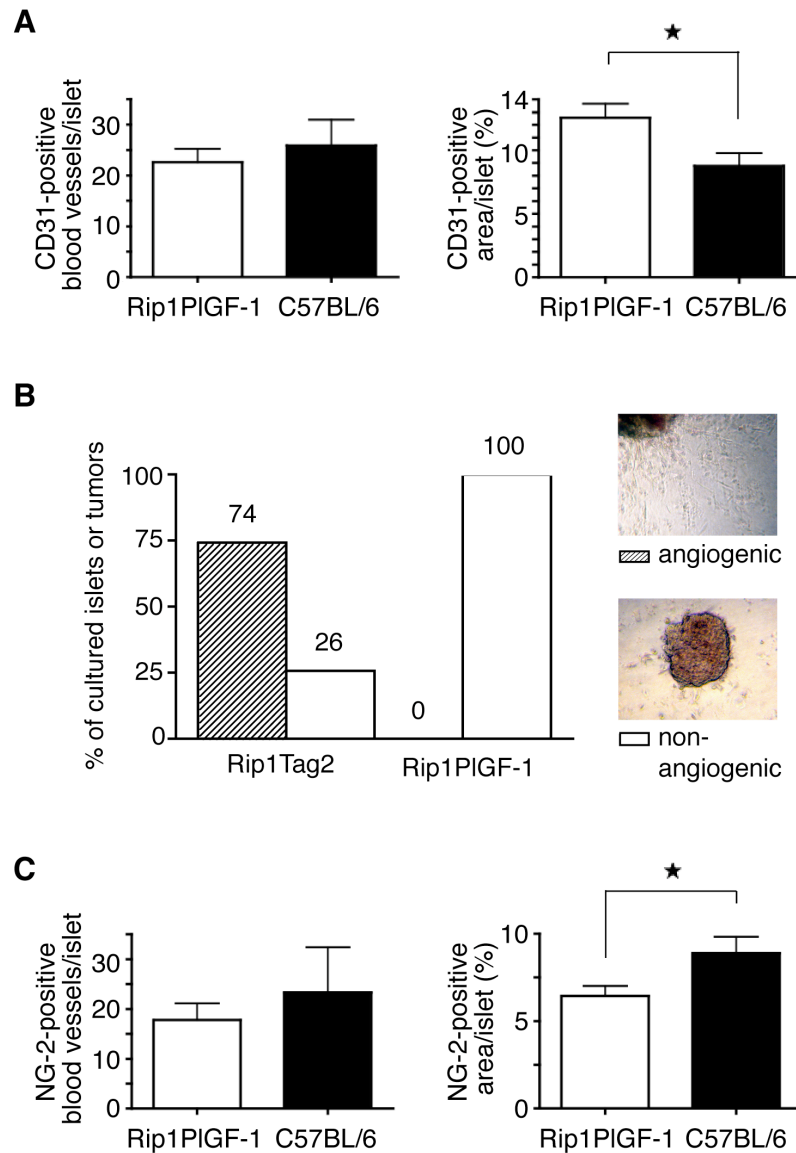


Figure 4. Analysis of islet angiogenesis and arteriogenesis in Rip1PlGF-1 mice

(A, left panel) Islet blood vessel density upon immunofluorescent staining with anti-CD31 antibody (Rip1PlGF-1, $n=13$: 22.6 ± 9.7 , C57BL/6, $n=9$: 25.9 ± 15.3 , $p=0.5454$, unpaired Student's t test) (A, right panel) Percentage of islet area occupied by CD31-positive structures (Rip1PlGF-1, $n=12$: 12.6 ± 3.8 , C57BL/6, $n=9$: 8.8 ± 3 , $p=0.0239$, unpaired Student's t test) (B) Islets and tumors derived from 9 week-old Rip1PlGF-1 ($n=16$, $N=2$) and Rip1Tag2 control mice ($n=35$, $N=4$), respectively. Examples of angiogenic and non-angiogenic islets are shown in insets. Results are indicated as % of islets or tumors in the respective angiogenesis class above bars (C, left panel) Number of islet blood vessels coated with NG-2-positive pericytes (Rip1PlGF-1, $n=12$: 17.8 ± 11.6 , C57BL/6, $n=9$: 23.3 ± 27.3 , $p=0.5825$, unpaired Student's t test with Welch correction) (C, right panel) Percentage of islet area occupied by NG-2-positive structures (Rip1PlGF-1, $n=12$: 6.5 ± 2 , C57BL/6, $n=9$: 8.9 ± 2.8 , $p=0.0306$, unpaired Student's t test).

Transgenic PlGF-1 represses tumor growth in Rip1Tag2;Rip1PlGF-1 mice

To assess the impact of PlGF-1 on tumor angiogenesis and growth, we crossed Rip1PlGF-1 mice with Rip1Tag2 mice, a well-characterized model of multistep β -cell carcinogenesis [124]. Rip1Tag2 control and Rip1Tag2;Rip1PlGF-1 double transgenic mice were sacrificed between 12 and 14 weeks of age, a time-point, when these mice succumb to hypoglycemia caused by excessive tumoral insulin production. To assess the state of endogenous PlGF expression in Rip1Tag2 control tumors, lysates of 12 week-old control tumors were analyzed by immunoblotting with anti-PlGF antibody. Interestingly, this experiment revealed that some of the control tumors upregulated endogenous mouse PlGF-2, suggesting that this factor may play a role during Rip1Tag2 tumorigenesis (Figure 5A).

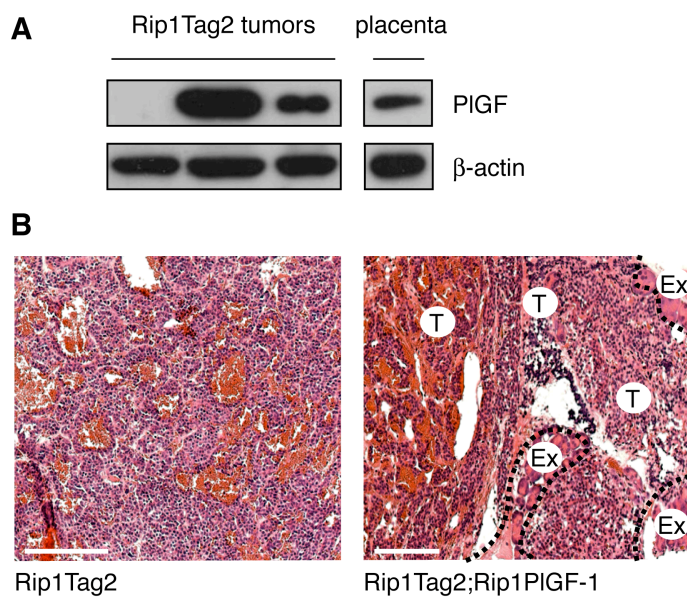


Figure 5. Expression of PlGF in control tumors and phenotype of Rip1Tag2 and Rip1Tag2; Rip1PlGF-1 tumors

(A) Immunoblot analysis of Rip1Tag2 tumors with anti-PlGF antibody. Mouse placenta served as positive control (B) Hematoxylin and eosin staining of tumors as indicated. Scale bars: 100 μ m.

The analysis of hematoxylin and eosin-stained pancreatic sections is currently ongoing. Our preliminary evaluation showed that Rip1Tag2;Rip1PlGF-1 tumors appeared more invasive and often developed important hemorrhage, yet these findings require further examination (Figure 5B). To investigate the impact of PlGF-1 on tumor angiogenesis, we assessed the microvessel density of tumors from both genotypes upon immunofluorescence staining with anti-CD31 antibody. Thereby we found that the number of blood vessels in Rip1Tag2;Rip1PlGF-1 tumors was significantly smaller than that in control tumors, suggesting that expression of PlGF-1 counteracted tumor angiogenesis (Table I). Since repressed tumor angiogenesis might negatively influence tumor growth, we also quantified the tumor burden. In line with this hypothesis, the tumor volumes of Rip1Tag2;Rip1PlGF-1 mice were significantly reduced when compared to control mice, while the tumor incidence was unaffected by transgenic expression of PlGF-1 (Table I). Together, these data imply that expression of PlGF-1 counteracts tumor angiogenesis and thereby represses tumor growth in Rip1Tag2;Rip1PlGF-1 mice.

Table 1. Tumor incidence, volume and tumoral blood vessel density in Rip1Tag2;Rip1PIGF-1 mice

	Rip1Tag2	Rip1Tag2;Rip1PIGF-1	p value
Tumor incidence/mouse ^a	6.3 ± 2.6 (n = 119, N = 19)	5.9 ± 1.9 (n = 77, N = 13)	0.6931
Total tumor volume/ mouse (mm ³) ^b	106.3 ± 62.2 (n = 119, N = 19)	44.7 ± 35.9 (n = 77, N = 13)	0.0031
Tumor blood vessel density ^c	826.8 ± 167.9 (n = 3, N = 9)	473.9 ± 218.9 (n = 3, N = 9)	0.0015

^aTumor incidence per mouse was determined macroscopically by counting all apparent pancreatic tumors with a minimal size of 1 mm in diameter.

^bTumor volume per mouse (in mm³) was calculated from all macroscopically apparent pancreatic tumors with a minimal diameter of 1 mm, assuming a spherical shape of tumors.

^cTumor blood vessel density was assessed by counting CD31-positive structures per tumor.

n = number of tumors, N = number of mice.

Data were analyzed with two-tailed Student's t test; values represent mean ± SD.

4.1.5. Discussion

Here we report the establishment of a transgenic mouse model to study the effect of PIGF-1 on angiogenesis under physiological conditions as well as during tumorigenesis. One mouse line was generated expressing human PIGF-1 under the control of the rat insulin promoter (Rip1, [124]), which targets expression of the transgene specifically to β -cells of pancreatic islets of Langerhans. Analysis of the islet blood vasculature revealed no quantitative differences with regard to the islet blood vessel density when comparing Rip1PIGF-1 and littermate control mice. Furthermore, isolated islets did not stimulate the proliferation and tube formation of co-cultured endothelial cells in an *in vitro* angiogenesis assay, whereas control tumors induced a potent angiogenic response. Two previous studies analyzing the biological effect of PIGF-1 in a mouse cornea assay reported conflicting results, demonstrating either a potent or no angiogenic activity of the PIGF-1 homodimer [174, 178]. Our data underline that PIGF-1 neither promotes angiogenesis under physiological conditions *in vivo* nor elicits angiogenic responses *in vitro*. Notably, a recent study of Rip1VEGF-A₁₆₅ mice similarly reported that transgenic expression of the prototype angiogenic VEGF family member VEGF-A₁₆₅ in the endocrine pancreas did not increase the blood vessel density of transgenic islets. However, 50% of Rip1VEGF-A₁₆₅ islets induced an angiogenic response in the collagen gel assay, demonstrating that the collagen gel assay is a sensitive tool to assess angiogenic activity of growth factors even when no such effect can be observed in transgenic islets *in vivo* [148].

While transgenic PIGF-1 had no effect on the blood vessel quantity, striking qualitative differences were found when comparing the morphology of the islet vasculature of Rip1PIGF-1 with that of wildtype littermate mice. Analysis of pancreata by common histology as well as by electron microscopy revealed that in comparison to control islets, all intra- but not extra-insular blood vessels of transgenic mice are dramatically enlarged, resulting in a significant increase of islet area occupied by CD31-positive structures. As

demonstrated by i.v. injection of lectin, these blood vessels are functional and readily perfused. Since PlGF-1 did not stimulate the proliferation of blood endothelial cells, we hypothesized that the enlargement of the blood capillary diameters may result from insufficient pericyte stabilization. Pericytes are important components of the vessel wall, conferring scaffolding stability to the endothelial tube and modulating the process of angiogenesis in a paracrine cross-talk with endothelial cells [3]. The essential function of pericytes was previously demonstrated with use of genetically modified mice, in which reduced amounts of pericytes caused microaneurysms as well as hemorrhages [188]. Therefore, we assessed the pericyte recruitment to CD31-positive blood vessels in Rip1PlGF-1 transgenic and control islets with use of the pericyte marker NG-2. Indeed, although the number of pericyte-coated blood vessels is unaffected by the expression of PlGF-1, the percentage of islet area occupied by NG-2-positive structures is significantly reduced in transgenic compared to control islets. These results indicate that the blood capillaries of Rip1PlGF-1 transgenic islets are less well coated with pericytes than that of control islets, which might – at least in part - account for the capillary hyperdilation phenotype. Interestingly, PlGF-2 expressed in basal keratinocytes of K14-PlGF-2 transgenic mice similarly induced a strong enlargement of dermal vessels. However, in addition, both an increase in total and pericyte-coated blood vessel numbers was documented, implying that PlGF-2 is involved in promoting angiogenesis and arteriogenesis [180]. Thus, PlGF-1 and PlGF-2 may have opposing functions, either destabilizing blood vessels or promoting pericyte-recruitment, angiogenesis, and arteriogenesis respectively.

To investigate the effect of PlGF-1 on tumor angiogenesis and tumor growth, Rip1PlGF-1 mice have been crossed with Rip1Tag2 mice, a transgenic mouse model of multistep β -cell carcinogenesis [124, 127]. Tumor growth in Rip1Tag2 mice is critically dependent on an angiogenic switch occurring at about six weeks of age, which involves the onset of VEGF-A expression [189]. Since PlGF-1 has been proposed to critically modulate VEGF-A-mediated pathological angiogenesis, the Rip1Tag2 tumor model is well suited to analyze such effects. Notably, RT-PCR analysis of tumor lysates revealed that many Rip1Tag2 control tumors expressed endogenous mouse PlGF-2. Although not further investigated during our analysis, this finding suggests that PlGF-2 plays a critical role during Rip1Tag2 tumorigenesis. Our preliminary analysis of Rip1Tag2;Rip1PlGF-1 and control mice revealed that transgenic expression of PlGF-1 does not affect tumor incidence but significantly reduces the tumor volume. Concomitantly, the tumor blood vessel density is significantly decreased in Rip1Tag2;Rip1PlGF-1 mice, suggesting that expression of PlGF-1 counteracts angiogenesis and thereby tumor growth. Two previous studies have reported that PlGF-1 can heterodimerize with VEGF-A, thereby antagonizing the binding of VEGF-A to VEGFR-2 and inhibiting VEGF-A-induced angiogenic responses [52, 178]. Since in Rip1Tag2;Rip1PlGF-1 tumors PlGF-1 and VEGF-A are expressed in the same cell, such heterodimerization could be one mechanism underlying repressed tumor angiogenesis in Rip1Tag2;Rip1PlGF-1 mice. Furthermore, as seen in Rip1PlGF-1 single transgenic mice, nascent blood vessels of Rip1Tag2;Rip1PlGF-1 tumors may be destabilized by inappropriate pericyte recruitment. It is known that in comparison to the normal vasculature, tumor blood vessels are disorganized and leaky. Thus, a further aggravation of an already poor tumor

blood vessel quality by repressed pericyte coverage may result in vessel regression and thus reduced numbers of CD31-positive tumor blood vessels. In line with this hypothesis, the histologic examination of tumors insinuates that Rip1Tag2;Rip1PlGF-1 exhibit more hemorrhages than control tumors, yet, this finding is still preliminary and the subject of ongoing analyses. Also the significance of our observation that Rip1Tag2;Rip1PlGF-1 tumors appear more invasive than control tumors remains to be confirmed by detailed investigation.

In summary, our preliminary observations suggest that the presence of PlGF-1 counteracts adequate pericyte coating of blood capillaries, resulting in the hyperdilation of blood capillaries. No angiogenic or arteriogenic activity was detected. Moreover, during tumorigenesis, expression of PlGF-1 significantly reduces tumor angiogenesis and therewith tumor growth. The establishment of Rip1PlGF-1 single transgenic and Rip1Tag2;Rip1PlGF-1 tumor-bearing mice will now also enable studies of other known or proposed activities of PlGF-1 *in vivo*, including the recruitment of hematopoietic stem cells and inflammatory cells. Furthermore, we have recently generated Rip1PlGF-2 transgenic mice and are in the process of generating double-transgenic Rip1Tag2;Rip1PlGF-2 mice, which will allow a direct comparison of biological effects of PlGF-1 and PlGF-2 in the same experimental setting.

4.2. VEGF-B₁₆₇ Promotes Tumor Angiogenesis in a Mouse Model of Pancreatic β -cell Carcinogenesis

Lucie Kopfstein¹, Karin Strittmatter¹, Pascal Lorentz¹, Michael Jeltsch², Valentin G. Djonov³,
Kari Alitalo², Gerhard Christofori¹

¹Department of Clinical-Biological Sciences, Institute of Biochemistry and Genetics,
University of Basel, 4058 Basel, Switzerland

²Molecular/Cancer Biology Laboratory, Biomedicum, University of Helsinki, Helsinki 00014,
Finland

³Institute of Anatomy, University of Berne, 3012 Berne, Switzerland

Running title: VEGF-B₁₆₇ promotes tumor angiogenesis

This work was supported by grants from the Swiss National Science Foundation, the Swiss Cancer League, the Swiss Bridge Award, the Krebsliga Beider Basel, the EU-FP6 framework programmes LYMPHANGIOGENOMICS LSHG-CT-2004-503573 and BRECOSM LSHC-CT-2004-503224, and Novartis Pharma Inc.

4.2.1. Abstract

Vascular endothelial growth factor (VEGF)-B is a member of the VEGF family of cytokines regulating blood and lymphatic vessel development. Accumulating evidence suggests that VEGF-B may be involved in mediating tumor angiogenesis and may promote epithelial-to-mesenchymal transition (EMT) and thus invasiveness of cancer cells. To assess the effect of tumoral VEGF-B expression on tumor angiogenesis and invasiveness, we have generated Rip1VEGF-B₁₆₇ transgenic mice, in which expression of the transgene is targeted to β -cells of pancreatic islets of Langerhans. Four healthy and fertile founderlines were obtained, which exhibited slightly more and dilated capillaries in the islet periphery. Currently, Rip1VEGF-B₁₆₇ mice are being crossed with Rip1Tag2 mice, a well-characterized transgenic model of multistep β -cell carcinogenesis. Our preliminary analysis demonstrates that tumoral expression of VEGF-B₁₆₇ significantly promotes tumor angiogenesis, while the tumor volume and tumor invasiveness remain unaffected. Unexpectedly, the tumor incidence is significantly reduced in these mice. The phenotypic characterization of Rip1VEGF-B₁₆₇ and Rip1Tag2;Rip1VEGF-B₁₆₇ mice with regard to these parameters as well as to the recruitment of pericytes and hematopoietic stem cells is the subject of ongoing investigations.

4.2.2. Introduction

VEGF-B belongs to the VEGF family of ligands, which are involved in physiological and pathological blood vessel angiogenesis and lymphangiogenesis. Alternative splicing gives rise to the two isoforms VEGF-B₁₆₇ and VEGF-B₁₈₉, VEGF-B₁₆₇ being the predominant form *in vivo* and most abundantly detected in heart, skeletal muscle, central nervous system, pancreas, and prostate, showing overlapping tissue distribution with VEGF-A [94, 190-192]. While VEGF-B₁₆₇ binds heparan-sulfate proteoglycans and is therefore mostly sequestered on the cell surface or in the extracellular matrix, VEGF-B₁₈₉ is freely diffusible. When produced in the same cell, both VEGF-B isoforms can form heterodimers with VEGF-A *in vitro* [191].

VEGF-A is a ligand for VEGFR-1, VEGFR-2, and the co-receptors NP-1 and NP-2, mediating angiogenic effects predominantly via VEGFR-2. In contrast, VEGF-B only binds to VEGFR-1 and NP-1. Similarly to VEGFR-2, VEGFR-1 is predominantly expressed on blood endothelial cells. Moreover, it is found on many non-endothelial cells including monocytes/macrophages, hematopoietic stem cells, pericytes, and tumor cells. The signaling pathways induced by VEGF-B-mediated VEGFR-1 activation are not yet conclusively elucidated. Although VEGFR-1 has only weak tyrosine kinase activity, it may display intrinsic signaling functions [101]. Other reports claim that VEGFR-1 might act as a decoy receptor for VEGF-A and that VEGFR-1-selective ligands such as VEGF-B might indirectly stimulate VEGF-A signaling by displacing VEGF-A from VEGFR-1, thereby increasing the VEGFR-2-activating fraction of VEGF-A [60, 170, 175]. Alternatively, heterodimerization of VEGF-B with VEGF-A may alter the receptor specificity of VEGF-A [191].

Studies of VEGF-B-deficient mice have unveiled that VEGF-B plays a role during cardiac and cerebral development [193-195]. Furthermore, these mice show impaired recovery following myocardial or cerebral ischaemic insults, reduced angiogenic responses in

collagen-induced arthritis and fail to develop pulmonary hypertension in response to hypoxia [193, 196-198]. Thus, although VEGF-B is not critical during systemic vascular development, it may be involved in pathological vascular remodeling. These observations are in line with the fact that endothelial cells of pathologic vasculature upregulate VEGFR-1 expression [44, 68]. Experiments using VEGF-B-releasing Matrigel plugs and electrotransfer of plasmids expressing VEGF-B have demonstrated that VEGF-B can exert angiogenic effects *in vivo* [199]. Furthermore, transgenic mice expressing VEGF-B in endothelial cells display enhanced vascular growth in an *in vivo* Matrigel assay and during cutaneous wound healing. Notably, no vascular permeability-promoting activity, such as the one known for VEGF-A, was observed [200].

The role of the VEGF-B/VEGFR-1 system in tumorigenesis has been recently addressed in several clinical and experimental studies. VEGF-B is expressed in a variety of human cancers, including melanoma, meningioma, fibrosarcoma, breast, squamous cell, renal cell and head and neck carcinoma [94, 96, 201]. In oral squamous cell carcinoma, elevated VEGF-B expression correlates with increased tumor microvessel density, suggesting that VEGF-B might be involved in the process of tumor angiogenesis [95]. One mechanism by which VEGF-B may support tumor neo-angiogenesis is the recruitment of VEGFR-1-positive hematopoietic stem cells and pericytes [202]. Furthermore, two *in vitro* studies show that VEGF-B can stimulate migration and invasion but not proliferation of different pancreatic and colorectal cancer cells via activation of VEGFR-1 [203, 204]. Consistent with these reports, VEGF-B has been shown to induce epithelial-to-mesenchymal (EMT) transition via VEGFR-1 in a pancreatic cancer cell line [205].

To investigate the effect of VEGF-B on tumor angiogenesis and tumor progression, we have generated Rip1VEGF-B₁₆₇ transgenic mice, in which the expression of human VEGF-B₁₆₇ is driven by the rat insulin promoter (Rip1) and thereby is targeted to β -cells of pancreatic islets of Langerhans. Rip1VEGF-B₁₆₇ mice were crossed with Rip1Tag2 tumor mice, a transgenic mouse model of β -cell carcinogenesis [124]. Here we report the preliminary data of analyses performed on single transgenic Rip1VEGF-B₁₆₇ and double transgenic Rip1Tag2;Rip1VEGF-B₁₆₇ mice with regard to islet and tumor angiogenesis as well as tumor growth. Since Rip1Tag2 tumor cells may express VEGFR-1, we also investigated whether expression of VEGF-B₁₆₇ promotes invasiveness *in vivo* as a correlate to its previously described ability to induce EMT *in vitro*.

4.2.3. Materials and Methods

Generation of Rip1VEGF-B₁₆₇ transgenic Mice

The Rip1VEGF-B₁₆₇ vector was kindly provided by M. Jeltsch (Molecular/Cancer Biology Laboratory, Biomedicum, University of Helsinki, Helsinki, Finland). The construct comprises a 704 bp BamHI/XbaI fragment of the rat insulin gene II promoter, the cDNA fragment encoding the 565 bp coding region of full length human VEGF-B₁₆₇ (nucleotides 1-565, Accession number EMBL:U43369), and a 436 bp stretch containing SV40 introns and polyadenylation signal sequences (Rip1; [124]). 100 µg of the Rip1VEGF-B₁₆₇ plasmid were digested with 10 µL BamHI in a total volume of 450 µL for five hours and resolved on a 0.8% agarose gel. The ~ 1.7 kb band comprising the Rip1, the human VEGF-B₁₆₇, and the SV40 small T intron and polyadenylation signal sequences was excised from the gel and purified once with the GENE CLEAN SPIN kit (QBiogene, Luzern, Switzerland). The purified Rip1VEGF-B₁₆₇ fragment was used for injection into the male pronucleus of fertilized C57BL/6 oocytes according to standard procedures at the Transgenic Mouse Core Facility TMCF, Biozentrum, Basel [147].

Genotypes were confirmed by PCR analysis of standard toe genomic DNA preparations using a primer pair specific for the transgene (forward primer located in the Rip1 sequence: 5'-TAA TGG GAC AAA CAG CAA AG; reverse primer located in the Rip1VEGF-B₁₆₇ sequence: 5'-CGC GAG TAT ACA CAT CTA TCC). PCR cycles were: 94°C, 5 min (x1); 94°C, 30 sec, 57°C, 30 sec, and 72°C, 30 sec (x34); and 72°C, 10 min (x1). Routine PCR screening of Rip1VEGF-B₁₆₇ heterozygotes was performed according to the same protocol.

For histopathological analysis, tumor grading, lectin perfusion, and electron microscopy refer to General Materials and Methods

4.2.4. Results

Generation of Rip1VEGF-B₁₆₇ transgenic mice

To generate transgenic mice expressing VEGF-B₁₆₇ specifically in β -cells of pancreatic islets of Langerhans, a cDNA containing the full-length coding sequence of human VEGF-B₁₆₇ was cloned between the rat insulin II gene promoter fragment (Rip) and the SV40 small t antigen intron and polyadenylation signal (Figure 1). Injection of the transgene into fertilized C57BL/6 oocytes resulted in four viable, healthy, and fertile founderlines exhibiting stable germline transmission (Rip1VEGF-B1 to Rip1VEGF-B4).

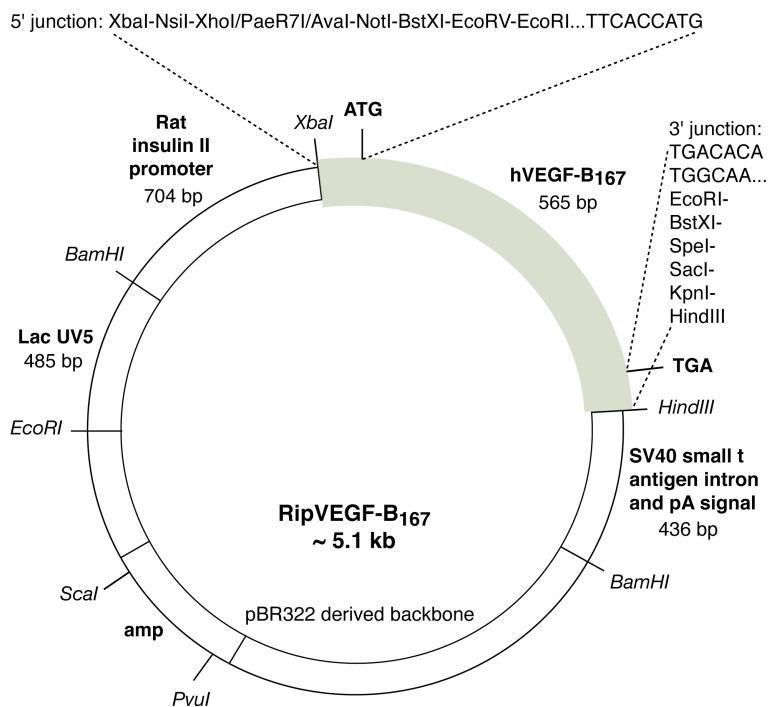


Figure 1. The Rip1VEGF-B₁₆₇ transgene construct
The XbaI/HindIII fragment containing human VEGF-B₁₆₇ was ligated into the XbaI/HindIII-opened Rip1 vector. The restriction sites located in the 5' and 3' multiple cloning sites acquired from the previous vector are indicated.

Transgenic founder lines were tested for β -cell-specific expression of VEGF-B by immunofluorescence analysis using an anti-VEGF-B antibody. Thereby, founderlines Rip1VEGF-B1, -B2, and -B3 were shown to express the transgene, whereas islets of Rip1VEGF-B4 and control littermate mice did not exhibit any detectable levels of VEGF-B in several experiments (Figure 2 and data not shown). The founderline Rip1VEGF-B1 was selected for phenotypical analysis in most experiments, thus in the following, Rip1VEGF-B₁₆₇ refers to the Rip1VEGF-B1 founderline if not noted otherwise.

The islet blood vessel architecture of Rip1VEGF-B₁₆₇ transgenic mice

In order to characterize morphological alterations induced by transgenic expression of VEGF-B₁₆₇, we analyzed pancreata of Rip1VEGF-B₁₆₇ and littermate control mice by histology and immunofluorescence. Inspection of hematoxylin and eosin-stained sections revealed that Rip1VEGF-B1 transgenic islets were frequently located next to large blood vessels, whereas control islets were mainly found in the deeper parenchyma of the exocrine tissue. A statistical evaluation of this finding is currently underway (Figure 2). In other respects, no distinct phenotype of transgenic islets was apparent. To visualize the islet blood vasculature, we performed immunofluorescence stainings using anti-CD31 antibody and injected a fluorophore-coupled tomato-derived lectin into the tail vein of anaesthetized mice. This naturally occurring glycoprotein associates with high affinity with sugar chains of blood endothelium. As shown in Figure 2, both control and VEGF-B₁₆₇-expressing islets exhibited a comparably dense and well-perfused network of blood capillaries. In contrast, in comparison to control islets, we detected more CD31-positive capillaries in the periphery of transgenic islets (arrows).

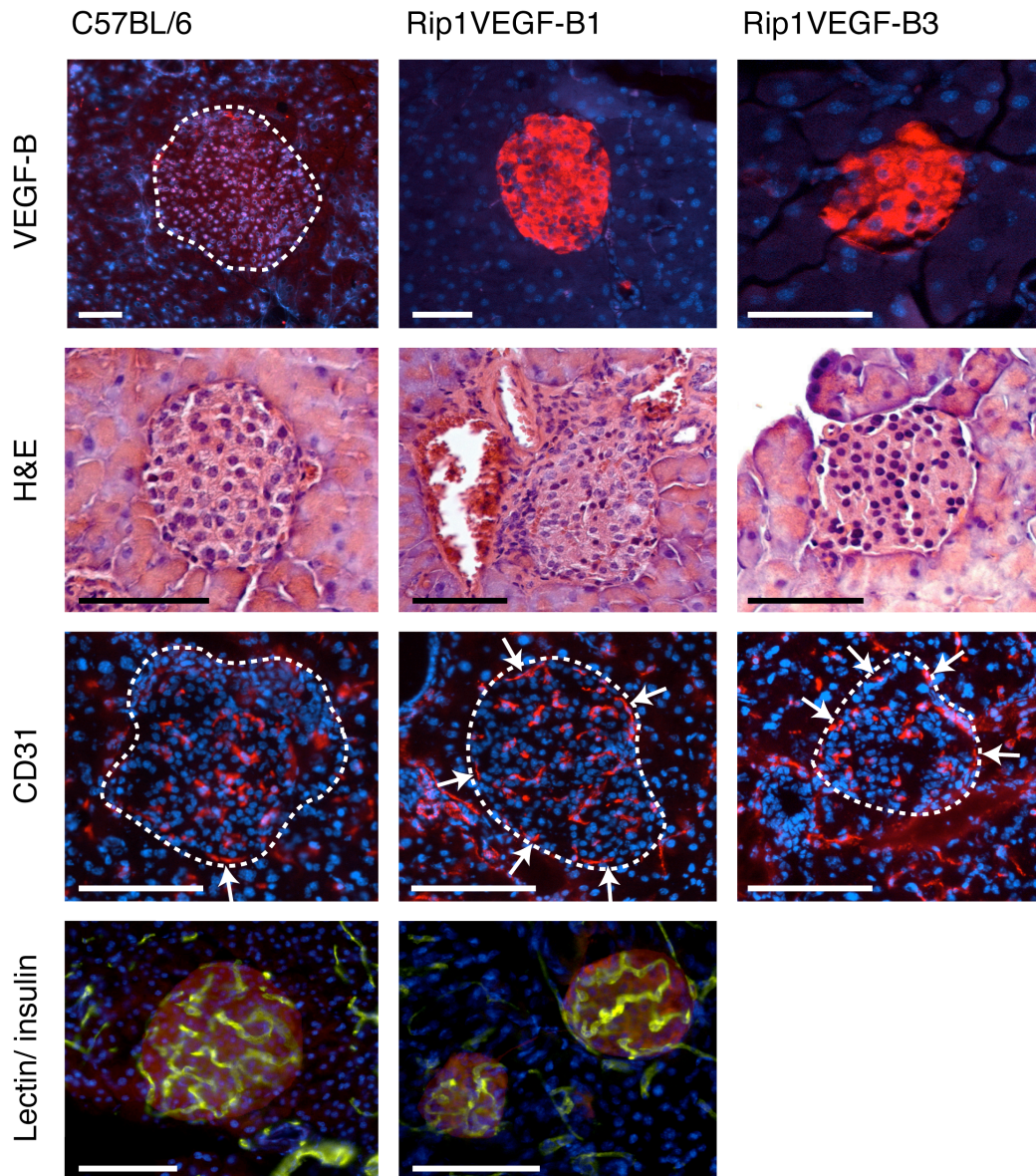


Figure 2. Histological analysis of Rip1 VEGF-B₁₆₇ islets

Pancreatic sections from Rip1VEGF-B1, -B3 and control littermate mice were analyzed by immunofluorescence staining with anti-VEGF-B antibody (red), hematoxylin and eosin staining, and immunofluorescence staining with anti-CD31 antibody (red) as indicated. I.v. injected lectin was detected by immunofluorescence (yellow), islets were visualized using anti-insulin antibody (red). Nuclei were counterstained with DAPI. Dashed lines demarcate islets, arrows indicate peripheral islet capillaries. Scale bars: 100 μ m

To unveil phenotypic alterations on the ultra-structural level, we prepared toluidine blue-stained semithin-sections of a Rip1VEGF-B3 and a C57BL/6 control mouse. As shown in Figure 3, capillaries located in the rim of transgenic islets were slightly dilated in comparison to peripheral capillaries of control islets (Figure 3, asterisks). Furthermore, the islet microvessel density appeared increased in VEGF-B₁₆₇-expressing islets. Both observations are currently being analyzed to allow statistical evaluation.

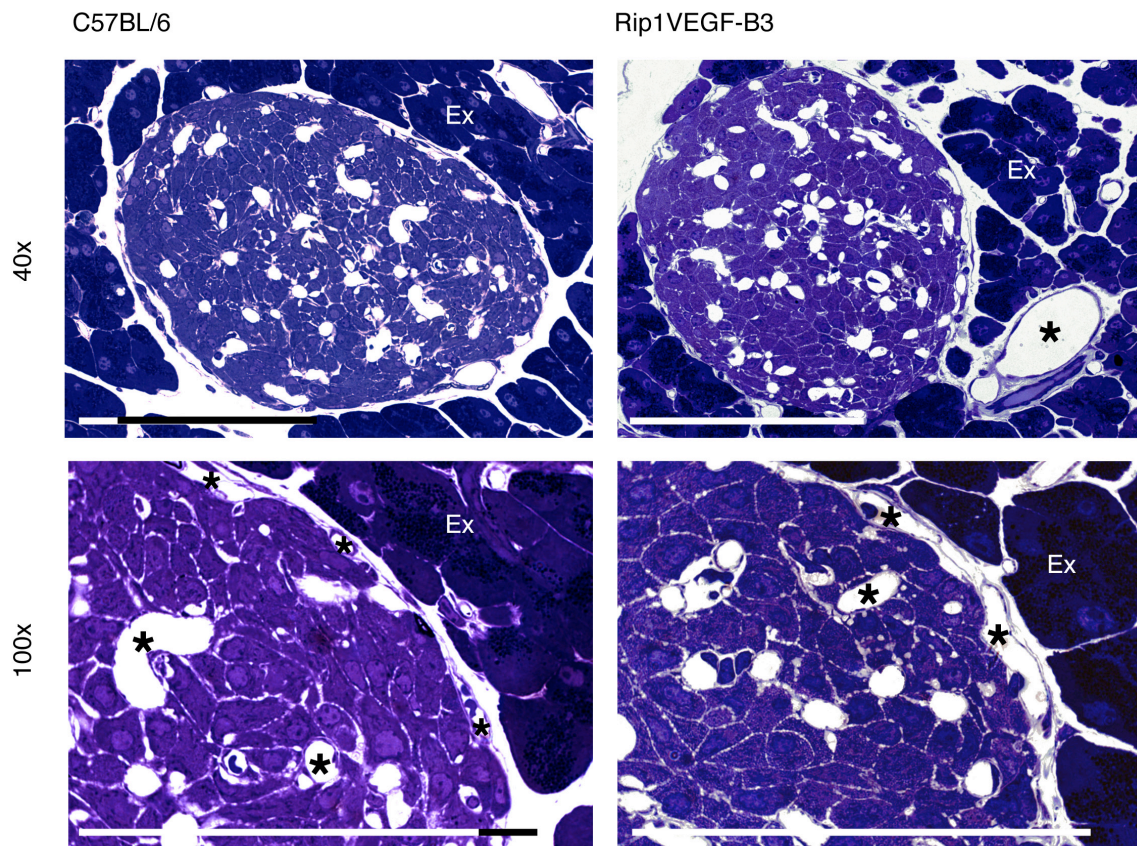


Figure 3. Ultra-structural analysis of Rip1VEGF-B₁₆₇ transgenic islets
 40x and 100x magnifications of toluidine blue-stained semi-thin sections of C57BL/6 control and Rip1VEGF-B₁₆₇ transgenic mice as indicated. Ex, exocrine tissue; asterisks indicate blood capillaries. Scale bars: 50 μ m

The lack of more striking structural or organizational alterations of islet blood vessels in Rip1VEGF-B₁₆₇ transgenic mice may indicate that at least in the absence of a pathological challenge such as hypoxia or inflammation, VEGF-B₁₆₇ does not significantly modulate angiogenesis in Rip1VEGF-B₁₆₇ transgenic mice.

Transgenic VEGF-B₁₆₇ promotes tumor angiogenesis but not tumor growth in Rip1Tag2;Rip1VEGF-B₁₆₇ mice (preliminary data)

Accumulating evidence from the literature implies a particular involvement of VEGF-B and its receptor VEGFR-1 in pathological angiogenesis [179, 193]. To assess the impact of overexpressed VEGF-B on tumor angiogenesis and tumor progression, we crossed Rip1VEGF-B₁₆₇ with Rip1Tag2 transgenic mice, a well-established model of multistep β -cell carcinogenesis [124]. As revealed by immunofluorescence staining with anti-VEGF-B antibody, the majority of Rip1Tag2 control tumors did not express VEGF-B. Interestingly however, we detected immunoreactivity for VEGF-B in sharply demarcated areas of some

control tumors (Figure 4). In contrast, all insulinomas of Rip1Tag2;Rip1VEGF-B₁₆₇ mice expressed large amounts of VEGF-B₁₆₇ (Figure 4).

To measure tumor angiogenesis, we quantified the microvessel density of tumors by immunohistochemical staining of pancreatic sections with anti-CD31 antibody and subsequent counting of intra-tumoral CD31-immunoreactive vascular structures (Figure 4). Double transgenic tumors exhibited significantly more blood vessels than tumors of control mice, suggesting that transgenic expression of VEGF-B₁₆₇ promoted tumor angiogenesis ($p = 0.0004$, two-tailed Student's *t* test, Table I). Furthermore, based on the above described finding that islets of Rip1VEGF-B₁₆₇ mice appeared to be frequently located next to large blood vessels, we investigated such correlation in Rip1Tag2;Rip1VEGF-B₁₆₇ mice. However, as shown in Table I, equal percentages of double transgenic and Rip1Tag2 control tumors were detected in the vicinity of large vessels.

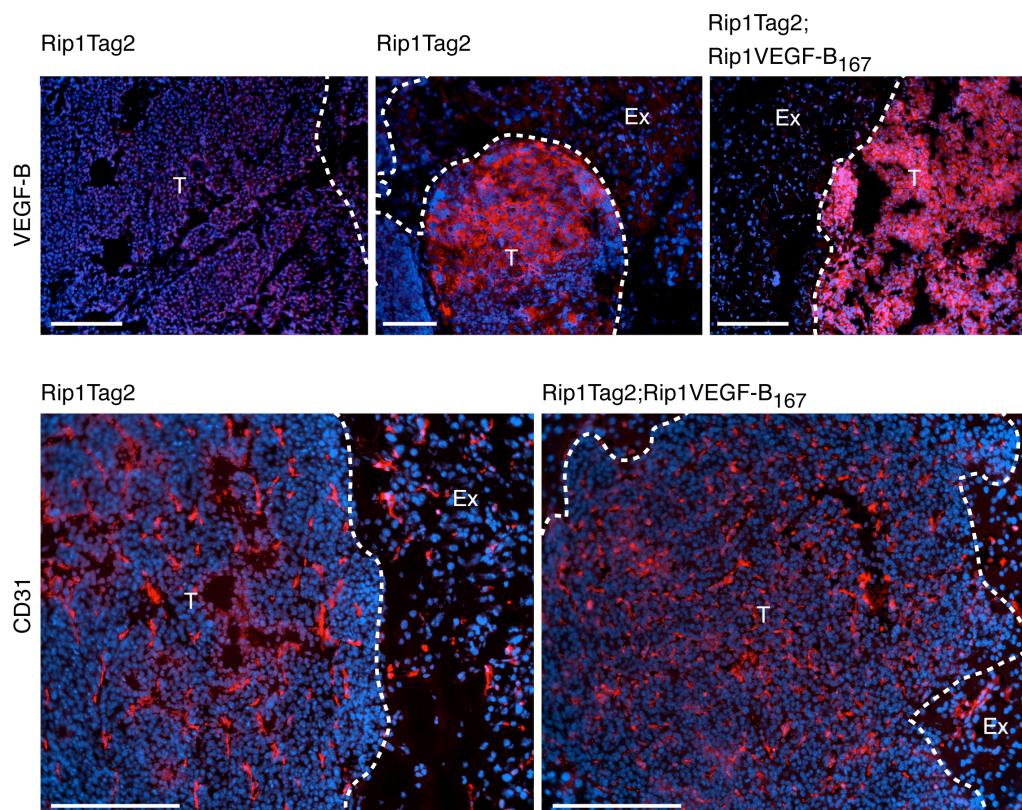


Figure 4. Tumoral expression of VEGF-B and tumor blood vasculature in control and Rip1Tag2; Rip1 VEGF-B₁₆₇ mice

Immunofluorescence analysis of twelve week-old Rip1Tag2 and Rip1Tag2;Rip1 VEGF-B₁₆₇ mice using anti-VEGF-B and anti-CD31 antibody. Note that some Rip1Tag2 control tumors upregulate expression of VEGF-B. Ex, exocrine tissue, T, tumor. Scale bars: 100 μ m.

Next, we reasoned that an increase in tumor angiogenesis might also accelerate tumor growth. However, Rip1Tag2;Rip1VEGF-B₁₆₇ mice did not die earlier than Rip1Tag2 control mice, suggesting that tumor growth was not significantly promoted in double transgenic mice. Moreover, quantitative analyses of the tumor burden unveiled that both the tumor incidence

and the tumor volume were reduced in Rip1Tag2;Rip1VEGF-B₁₆₇ compared to control mice, whereby only the reduction in tumor incidence was statistically significant ($p = 0.0452$, two-tailed Student's t test with Welch correction and $p = 0.0751$, two-tailed Student's t test, respectively; Table I). In contrast, neither tumor cell proliferation nor apoptosis were affected by transgenic expression of VEGF-B₁₆₇, which suggests that the enhancement of tumor angiogenesis upon transgenic expression of VEGF-B₁₆₇ had no direct effect on the cancer cells as such. The decrease in tumor incidence and tumor growth of Rip1Tag2;Rip1VEGF-B₁₆₇ mice cannot be explained so far. However, the analysis of tumor-bearing mice is still ongoing and the presented results have to be considered preliminary.

Table I. Tumor burden and tumor microvessel density in Rip1Tag2;Rip1VEGF-B₁₆₇ transgenic mice

	Rip1Tag2	Rip1Tag2;Rip1VEGF-B ₁₆₇	p value
Tumor incidence ^a	13.5 ± 6.5 (n = 81, N = 6)	6.3 ± 2.2 (n = 43, N = 15)	0.0452*
Tumor volume (mm ³) ^b	104.6 ± 66.7 (n = 81, N = 6)	50.8 ± 56.0 (n = 43, N = 15)	0.0751**
Proliferation rate of tumor cells (cells per field) ^c	85.9 ± 38.1 (n = 35, N = 4)	100.5 ± 50.7 (n = 34, N = 4)	0.1795**
Apoptotic tumor cells per field (cells per field) ^d	21.7 ± 14.4 (n = 34, N = 4)	19.92 ± 19.9 (n = 50, N = 6)	0.6545**
Tumor blood vessel density ^e	48.9 ± 15.4 (n = 38, N = 9)	60.9 ± 13.0 (n = 40, N = 7)	0.0004**
Tumors close to large blood vessels	59.5 % (n = 74, N = 3)	59.8 % (n = 261, N = 11)	

^aTumor incidence per mouse was determined macroscopically by counting all apparent pancreatic tumors with a minimal size of 1 mm in diameter. n = number of tumors, N = number of mice.

^bTumor volume per mouse (in mm³) was calculated from all macroscopically apparent pancreatic tumors with a minimal diameter of 1 mm, assuming a spherical shape of tumors. n = number of tumors, N = number of mice.

^cTumor cells in S phase per 40x microscopic magnification field as determined by BrdU incorporation. n = number of 40x fields, N = number of mice.

^dApoptotic tumor cells per 40x microscopic magnification field as determined by TUNEL staining. n = number of 40x fields, N = number of mice.

^eTumor blood vessel density was assessed by counting intra-tumoral CD31-positive vessels per 40x magnification field. n = number of 40x fields, N = number of mice.

*Two-tailed Student's t test with Welch correction; values represent mean ± SD.

**Two-tailed Student's t test; values represent mean ± SD.

Expression of VEGFB₁₆₇ does not affect tumor invasiveness in Rip1Tag2;Rip1VEGF-B₁₆₇ mice (preliminary data)

As a consequence of conflicting data it is not fully established whether β tumor cells express VEGFR-1 [206-208]. Despite this uncertainty, results from very recent studies demonstrating that VEGF-B-induced activation of VEGFR-1 might be involved in epithelial-to-mesenchymal transition of cancer cells motivated us to investigate such activity of VEGF-

B₁₆₇ in Rip1Tag2;Rip1VEGF-B₁₆₇ mice [203-205]. Therefore, we are currently assessing the malignant phenotype of Rip1Tag2;Rip1VEGF-B₁₆₇ and control tumors by histological grading upon hematoxylin and eosin staining. As shown in Table II, the preliminary statistical analyses indicate only minor changes in the ratio of benign versus malignant tumors. However, the still small number of control mice does not yet allow an appropriate and conclusive interpretation of these results.

Table II. Tumor grading of Rip1Tag2;Rip1VEGF-B₁₆₇ versus control mice

	Rip1Tag2 (n = 74, N = 3)	Rip1Tag2;Rip1VEGF-B ₁₆₇ (n = 261, N = 11)
Benign	27 %	21 %
Normal/Hyperplastic islets	25.7 %	16.1 %
Adenoma	1.3 %	5 %
Malignant	73 %	79 %
Carcinoma grade 1	12.2%	10.3 %
Carcinoma grade 2	55.4 %	67.8 %
Carcinoma grade 3	5.4 %	0.8 %

For each mouse, all islets and tumors found on one representative pancreatic section were graded into categories as indicated. All tumors of the respective genotype and category were pooled and normalized to the total number of tumors of the respective genotype.

In summary, the analysis of Rip1Tag2;Rip1VEGF-B₁₆₇ mice demonstrated that tumoral expression of VEGF-B₁₆₇ promotes tumor angiogenesis. However, no impact on the tumor cells themselves was observed to date, in particular, tumor volume, tumor incidence, and invasiveness were not increased during Rip1Tag2 tumorigenesis.

4.2.5. Discussion

We have generated Rip1VEGF-B₁₆₇ transgenic mice, which over-express human VEGF-B₁₆₇ specifically in β -cells of pancreatic islets of Langerhans. In comparison to age-matched control mice, which do not exhibit any detectable levels of VEGF-B₁₆₇ protein in islets, our observations indicate only a minor impact of VEGF-B₁₆₇ expression on the islet blood vasculature of transgenic mice. VEGF-B₁₆₇-expressing islets exhibited slightly more and dilated blood capillaries in the islet periphery, indicating a weak pro-angiogenic effect of VEGF-B₁₆₇. Also, transgenic islets were frequently observed to be located next to large blood vessels. However, as a result of the distinct endocrine pancreatic development, islets of Langerhans are known to be closely associated with the vascular system of the organ, and ongoing statistical analysis has yet to prove the significance of this finding. The observation that VEGF-B₁₆₇ did not critically influence blood vessel growth in transgenic islets is consistent with studies of VEGF-B-deficient mice, which demonstrated that this growth factor is not required for systemic angiogenesis under physiological conditions but is particularly involved in mediating pathological angiogenesis [193, 196-198]. Yet, it has to be mentioned that a previous study of RipVEGF-A₁₆₅ transgenic mice similarly reported no major qualitative or quantitative changes in islet vasculature induced by β -specific overexpression of VEGF-A₁₆₅ [148]. However, in an *in vitro* angiogenesis assay, isolated RipVEGF-A₁₆₅ transgenic islets promoted angiogenic responses in co-cultured endothelial cells, while wildtype islets did not induce such angiogenic effects. Thus, it is possible that *in vivo*, islets of Langerhans are not a permissible environment for the induction of pronounced angiogenesis even by potent angiogenic factors such as VEGF-A₁₆₅. Therefore, we are currently performing collagen gel assay experiments with islets from Rip1VEGF-B₁₆₇ mice to unveil a potentially latent angiogenic effect of VEGF-B₁₆₇ *in vitro*.

Using the Rip1Tag2 mouse model of pancreatic β -cell carcinogenesis, we have assessed the influence of tumoral overexpression of VEGF-B₁₆₇ on tumor angiogenesis, growth and progression. Rip1Tag2 transgenic mice express the SV40 large T antigen (Tag) under the control of the rat insulin gene promoter (Rip), which elicits the sequential development of β -cell tumors over a period of 12–14 weeks [124]. The tumor growth in Rip1Tag2 mice is critically dependent on an angiogenic switch occurring at about six weeks of age, which involves the onset of VEGF-A expression [189]. Of note, a previous study demonstrated that injection of a soluble VEGFR-1 into Rip1Tag2 mice repressed tumor growth, which might result from the concomitant sequestration of all three VEGFR-1 ligands, VEGF-A, PlGF, and VEGF-B [209]. During our analysis, we found that a small subset of control tumors expressed VEGF-B in a well-demarcated tumor area, indeed suggesting a role of this growth factor in Rip1Tag2 tumorigenesis. In contrast, all tumors of Rip1Tag2;Rip1VEGF-B₁₆₇ mice expressed high amounts of VEGF-B, enabling a comparative study of the two genotypes. First, we investigated the impact of VEGF-B₁₆₇ on tumor angiogenesis. Quantification of the tumor microvessel density using the blood endothelium-specific marker CD31 revealed a significant increase blood vessels per tumor area in Rip1Tag2;Rip1VEGF-B₁₆₇ mice when compared to age-matched control mice, strongly suggesting that VEGF-B₁₆₇ promotes tumor angiogenesis. This result is in line with a recent clinical study of oral squamous cell carcinoma, which correlated elevated VEGF-B expression with increased tumor microvessel density [95]. It was reported that one mechanism by which VEGF-B may support tumor neo-angiogenesis is the recruitment of

VEGFR-1-positive hematopoietic stem cells and pericytes [202]. Also, VEGF-A-induced angiogenesis might be modulated by the formation of VEGF-B/VEGF-A heterodimers in case both growth factors are produced in the same cell. Since VEGF-A is naturally upregulated during Rip1Tag2 tumorigenesis, such heterodimers might indeed be formed. The pericyte and hematopoietic stem cell recruitment as well as possible VEGF-B/VEGF-A heterodimerization are the subject of ongoing analyses of Rip1Tag2;Rip1VEGF-B₁₆₇ mice.

It has been demonstrated that an increase in tumor angiogenesis promotes tumor growth and thereby negatively influences the outcome of tumor-bearing animals as well as cancer patients (reviewed in [210]). However, double transgenic Rip1Tag2;Rip1VEGF-B₁₆₇ mice neither succumbed earlier to insulinoma nor exhibited increased tumor burden in comparison to control mice. Rather, both tumor incidence and tumor volume were reduced in Rip1Tag2;Rip1VEGF-B₁₆₇ mice. In contrast, tumor cell proliferation and apoptosis were unaffected by the expression of VEGF-B₁₆₇, which indicates that VEGF-B₁₆₇-mediated stimulation of angiogenesis had no effect on the tumor cells as such. Interestingly, a previous study of Rip1Tag2;Rip1VEGF-A₁₆₅ mice reported an accelerated induction of tumor angiogenesis and subsequently tumor growth and mortality, while the tumor microvessel density of fully developed tumors was not increased by the expression of VEGF-A₁₆₅ in comparison to control tumors. The observed phenotypic differences of Rip1Tag2;Rip1VEGF-B₁₆₇ and Rip1Tag2;Rip1VEGF-A₁₆₅ mice indicate that the two overexpressed growth factors trigger distinct signaling pathways. Thus, VEGF-B₁₆₇ may not only indirectly mediate angiogenesis by potentiating VEGF-A-signaling via VEGFR-2 but may induce intrinsic angiogenic signaling via VEGFR-1.

Based on our observations from single transgenic Rip1VEGF-B₁₆₇ mice we investigated whether we could detect any correlation with regard to the localization of Rip1Tag2;Rip1VEGF-B₁₆₇ tumors next to large blood vessels. However, no such relation was found when comparing double transgenic and control tumors. One possibility is that the Rip1Tag2;Rip1VEGF-B₁₆₇ tumors may have overgrown and incorporated such blood vessels. This hypothesis is currently being addressed by a quantitative analysis of intra-tumoral large blood vessels in double transgenic and control tumors.

Recently, several studies using pancreatic and colorectal cancer cell lines reported that VEGF-B stimulated tumor cell migration, invasion, and epithelial-to-mesenchymal (EMT) transition but not proliferation via activation of VEGFR-1 [203-205]. During EMT, cells progressively redistribute or down-regulate apical and basolateral epithelial-specific proteins, such as tight and adherens junction proteins, and re-express mesenchymal molecules, resulting in the abrogation of cell-cell contacts and the gain of motility (reviewed in [211]). Although still heavily debated, EMT may represent the *in vitro* correlate to invasiveness and metastasis. Since a subset of Rip1Tag2 control tumors expressed VEGF-B in specific areas that could represent invasive tumor edges, we investigated a potential effect of VEGFB₁₆₇ on the invasiveness of tumors *in vivo* and assessed the malignant phenotype of tumors of Rip1Tag2;Rip1VEGF-B₁₆₇ and control mice by histological grading. Thus far, we were not able to detect significant differences of tumor grades when comparing double transgenic and control tumors. However, the analysis is still ongoing and the numbers of analyzed mice is not yet sufficient to draw reliable conclusions. Yet, it has to be considered that expression of VEGFR-1 has not been verified yet in β -cells of islets and insulinomas *in vivo*, although it is commonly detected in islet and Rip1Tag2 tumor capillaries as well as in insulinoma cell lines [206-208].

Taken together, our preliminary data demonstrate that transgenic expression of VEGF-B₁₆₇ only moderately affects physiological angiogenesis, yet significantly promotes tumor angiogenesis. Our ongoing detailed analyses of Rip1Tag2;Rip1VEGF-B₁₆₇ mice will shed more light on the mechanisms of VEGF-B-mediated angiogenesis and its impact on tumor progression.

4.3. Generation of a Transgenic Mouse Model for the Study of VEGFR-2-specific Functions

Lucie Kopfstein¹, Pascal Lorentz¹, C. Dehio², Gerhard Christofori¹

¹Department of Clinical-Biological Sciences, Institute of Biochemistry and Genetics,
University of Basel, 4058 Basel, Switzerland

²Molecular Microbiology, Biozentrum, University of Basel, 4056 Basel, Switzerland

Running title: Generation of Rip1VEGF-E_{D1701} transgenic Mice

This work was supported by grants from the Swiss National Science Foundation, the Swiss Cancer League, the Swiss Bridge Award, the Krebsliga Beider Basel, the EU-FP6 framework programmes LYMPHANGIOGENOMICS LSHG-CT-2004-503573 and BRECOSM LSHC-CT-2004-503224, and Novartis Pharma Inc.

4.3.1. Abstract

Members of the vascular endothelial growth factor (VEGF) family and their receptors (VEGFR) are important regulators of blood and lymphatic vessel development. VEGFR-1 and VEGFR-2 are predominantly expressed on blood endothelium and mediate angiogenesis upon activation by their ligands. VEGF-A is the only known mammalian ligand for VEGFR-2 but binds and activates also VEGFR-1. The identification of the VEGFR-2-selective VEGF-E, a viral homolog of VEGF-A, has enabled the study of distinct biological functions of VEGFR-2. Here we report the generation of three independent transgenic mice expressing VEGF-E_{D1701} specifically in β -cells of pancreatic islets of Langerhans (Rip1VEGF-E_{D1701}). These mice represent a new tool for investigating the role of activated VEGFR-2 in blood vessels of adult animals. Moreover, Rip1VEGF-E_{D1701} mice are currently being crossed with Rip1Tag2 transgenic mice, a well characterized model of multistage β -cell tumorigenesis. Future studies of double-transgenic mice will further our understanding of the importance of VEGFR-2 signaling for tumor angiogenesis, tumor progression, and metastasis.

4.3.2. Introduction

Vascular endothelial growth factor receptor-2 (VEGFR-2/flk-1/KDR) is one of the three transmembrane VEGFR tyrosine kinases, which are involved in vasculogenesis, angiogenesis, and lymphangiogenesis. While in the adult, expression of VEGFR-3 (flt-4) is largely restricted to lymphatic endothelium, VEGFR-1 (flt-1) and VEGFR-2 are predominantly expressed on blood endothelial cells. However, VEGFR-2 is also expressed on other cells including lymphatic endothelial, hematopoietic stem, and tumor cells [212]. Furthermore, a soluble form of VEGFR-2 has been discovered in mouse and human serum [61]. VEGFR-2 is a high-affinity receptor for VEGF-A as well as the processed forms of VEGF-C and VEGF-D [47]. Studies of knockout mice suggest that during embryogenesis, VEGFR-2 is the main signal transducer of vasculogenesis and angiogenesis, whereas VEGFR-1 acts as a negative regulator [10, 13]. Also in the adult, VEGFR-2 is the major mediator of mitogenic and survival signals in endothelial cells and of VEGF-A-induced angiogenesis. While signaling via VEGFR-2 has been demonstrated to be crucial for the recruitment of hematopoietic precursor cells to the developing vasculature, its role has not yet been conclusively elucidated in the adult tissue [10, 47]. In contrast, distinct interactions between VEGFR-2 and NP-1, integrin $\alpha_v\beta_3$ and VE-cadherin have been shown to be critical for mediating angiogenesis, vascular permeability, and lymphangiogenesis [213-217]. Furthermore, several recent studies indicate that activation of VEGFR-2 also promotes lymphangiogenesis [217, 218].

During tumorigenesis, VEGF-A-mediated activation of VEGFR-2 significantly contributes to angiogenesis and thereby promotes tumor growth [90, 219]. Moreover, recent evidence suggests a primary role of VEGFR-2 in mediating VEGF-A-induced adhesion, migration, and invasion of tumor cells *in vitro*, in part via activation of integrins [220, 221]. However, since VEGF-A binds and activates both VEGFR-1 and VEGFR-2, the distinct contribution of VEGFR-2 signaling to observed biological effects was difficult to assess. The

discovery of VEGF-E, a viral homolog of VEGF-A and selective ligand for VEGFR-2, has enabled a more precise dissection of the role of this receptor during physiological and pathological angiogenesis. VEGF-E is the collective term for the five variants identified in the genome of the parapoxviruses Orf virus and Pseudocowpox virus, namely VEGF-E_{NZ-2}, VEGF-E_{NZ-7}, VEGF-E_{NZ-10}, VEGF-E_{D1701}, and VEGF-E_{VR634} [222-226]. Parapoxviruses infect sheep, goats, cattle, and humans, and induce skin lesions characterized by extensive vasodilation, dermal edema, and proliferation of endothelial cells [227-229]. Although VEGF-E variants show only 16 to 29% amino acid identity with VEGF-A₁₆₅, they display almost the same affinity for VEGFR-2 as VEGF-A₁₆₅. The variants VEGF-E_{NZ-2}, VEGF-E_{NZ-10}, and VEGF-E_{D1701} also bind NP-1, a co-receptor of VEGF-A, VEGF-B, and PlGF-2, which may be particularly important in mediating vascular permeability [223-225]. The ability of these VEGF-E variants to bind NP-1 is surprising given their lack of conservation of the heparin-binding domain implicated in the binding of VEGF-A, VEGF-B, and PlGF-2 to NP-1 [171, 216, 230]. Moreover, VEGF-E_{NZ-2} was reported to display heparin-binding activity, yet the amino acid stretch mediating this action is not yet identified [226]. Although differing in their amino acid sequence and receptor binding affinities, all VEGF-E variants possess similar activities as described for VEGF-A, such as induction of tissue-factor expression, chemotaxis, proliferation, and sprouting of cultured endothelial cells *in vitro* as well as induction of angiogenesis and vascular permeability *in vivo* [223-226].

The aim of the present study was to establish a transgenic mouse expressing VEGF-E under the control of the rat insulin promoter (Rip1), thereby targeting expression of the transgene to pancreatic islets of Langerhans. Future crossings of these mice with Rip1Tag2 transgenic mice, a well-characterized insulinoma model, will enable the study of the specific role of VEGFR-2 activation in tumor angiogenesis, including the recruitment of hematopoietic progenitor cells. Moreover, a potential involvement of VEGFR-2 in the promotion of tumor invasiveness and metastasis can be addressed.

4.3.3. Materials and Methods

Cloning of the Rip1VEGF-E_{D1701} construct

VEGF-E_{D1701} cDNA was amplified by PCR from the pCD379-VEGF-E_{D1701} vector construct kindly provided by Prof. C. Dehio (Division of Molecular Microbiology, Biozentrum, Basel, Switzerland) using the forward primer 5'- GCT CTA GAG CCA CCA TGA AGT TTC TCG TCG GC containing a 5'-XbaI restriction site (underlined) and the reverse primer 5'-CCC AAG CTT CTA GCG GCG TCT TCT GGG CGG containing a 5'-HindIII restriction site (underlined). PCR cycles were: 94°C, 2 min (x1); 94°C, 15 sec, 65°C, 30 sec, and 72°C, 45 sec (x30); and 72°C, 7 min (x1). PCR products were resolved on a 1% agarose gel and extracted with the QIAEXII Gel Extraction kit. Constructs were sequenced at Syngene Biotech (Schlieren, Switzerland), using the forward primer located in the Rip1 sequence: 5'-TAA TGG GAC AAACAG CAA AG and the reverse primer comprising the stop codon of VEGF-E 5'-CCC AAG CTT CTA GCG GCG TCT TCT GGG CGG.

Generation of Rip1VEGF-E_{D1701} transgenic mice

100 µg of the Rip1VEGF-E_{D1701} plasmid were digested with 10 µL BamHI in a total volume of 450 µL for five hours and resolved on a 0.8% agarose gel. The ~ 1.5 kb transgene construct was extracted from the gel and purified once with the GENE CLEAN SPIN kit (QBiogene, Luzern, Switzerland). The purified Rip1VEGF-E_{D1701} DNA fragment was used for generation of Rip1VEGF-E_{D1701} transgenic mice according to standard procedures at the Transgenic Mouse Core Facility TMCF, Biozentrum, Basel [147]. Screening for founders and of Rip1VEGF-E_{D1701} heterozygotes was performed by PCR using a forward primer located in the Rip1 sequence: 5'-TAA TGG GAC AAA CAG CAA AG and a reverse primer located in the VEGF-E sequence: 5'-CCA TGT TTT CGT GCT GTC CG), starting from standard toe or tail genomic DNA preparations. PCR cycles were: 94°C, 5 min (x1); 94°C, 30 sec, 55°C, 30 sec, and 72°C, 30 sec (x34); and 72°C, 7 min (x1).

RT-PCR analysis of of Rip1VEGF-E_{D1701} transgenic mice for VEGF-E expression

Pancreata were homogenized in TRIzol reagent for RNA isolation according to the manufacturer's protocol (Sigma Chemical Co., St. Louis, MO). 500 ng of total RNA was reverse transcribed using reverse transcriptase and random hexamers from Sigma Chemical Co., St. Louis, MO. The cDNA was screened for VEGF-E by temperature gradient PCR using the forward primer 5'- AGC CAA GGC CGA TGG TCT TTC and the reverse primer 5'-CCA TGT TTT CGT GCT GTC CG (both located in the VEGF-E sequence). PCR cycles were 94°C, 5 min (x1); 94°C, 30 sec, 54-66°C, 30 sec, and 72°C, 30 sec (x29); and 72°C, 7 min (x1).

4.3.4. Results

Generation of Rip1VEGF-E_{D1701} transgenic mice

To generate transgenic mice specifically expressing VEGF-E in β -cells of pancreatic islets of Langerhans, the cDNA encoding the 399 bp of full length VEGF-E_{D1701} deriving from Orf virus strain D1701 was amplified by PCR from the pCD379-VEGF-E_{D1701} vector construct. The VEGF-E_{D1701} cDNA was subsequently cloned between the 704 bp rat insulin II promoter and a 436 bp stretch containing SV40 small T intron and polyadenylation signal sequences of the Rip1 vector using XbaI and HindIII (Rip1; [124]) (Figure 1). The Rip1VEGF-E_{D1701} construct was tested for insertion of VEGF-E_{D1701} by restriction digests using XbaI/HindIII as well as with BamHI. Both digests revealed inserts of the expected size of approximately 400 bp and 1.5 kb, respectively. To exclude mutations, which might have been induced during PCR and cloning procedures, the Rip1VEGF-E_{D1701} construct was sequenced using primers encompassing the entire VEGF-E_{D1701} insert and a small stretch of the Rip1 sequence. Thereby, the appropriate insertion into the vector as well as the correct sequence of VEGF-E_{D1701} were verified.

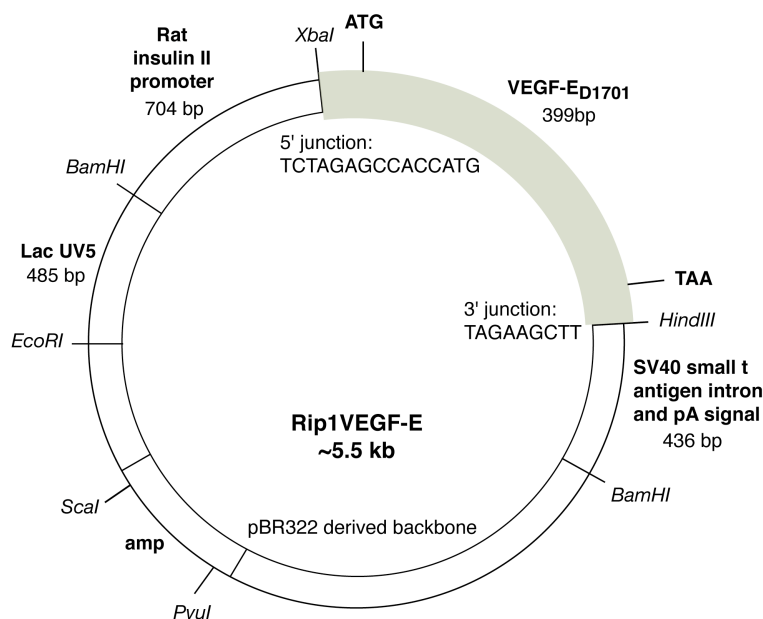


Figure 1. Map of the Rip1VEGF-E_{D1701} construct

For injection of the transgene into fertilized C57BL/6 oocytes, the Rip1VEGF-E_{D1701} construct was digested with BamHI. The insert comprising the rat insulin promoter (Rip1), the VEGF-E_{D1701} and the SV40 small T intron and polyadenylation signal sequences was used for generation of transgenic mice. However, only one Rip1VEGF-E_{D1701} founderline was obtained. To exclude transgene integration effects during future analyses we repeated oocyte injections, which resulted in four additional Rip1VEGF-E_{D1701} transgenic founders. All founderlines exhibited stable germline transmission and were healthy and fertile.

Analysis of transgenic VEGF-E_{D1701} expression

A first attempt to assess transgenic expression of VEGF-E by immunohistochemistry and immunofluorescence analysis with specific rabbit sera revealed unspecific binding of antibodies to β -cells of control mice (data not shown). Since no purified antibodies were commercially available, the five transgenic founderlines were tested for expression of VEGF-E by RT-PCR performed on pancreatic RNA. Considering the high ratio of endocrine to exocrine pancreas in young mice, pancreata were isolated from 3-4 week-old animals. As shown in Figure 2, the founderlines Rip1VEGF-E_{D1701}-3, Rip1VEGF-E_{D1701}-4, and Rip1VEGF-E_{D1701}-5 expressed VEGF-E in pancreata, whereas no VEGF-E mRNA could be detected in pancreata of Rip1VEGF-E_{D1701}-1 and Rip1VEGF-E_{D1701}-2 mice.

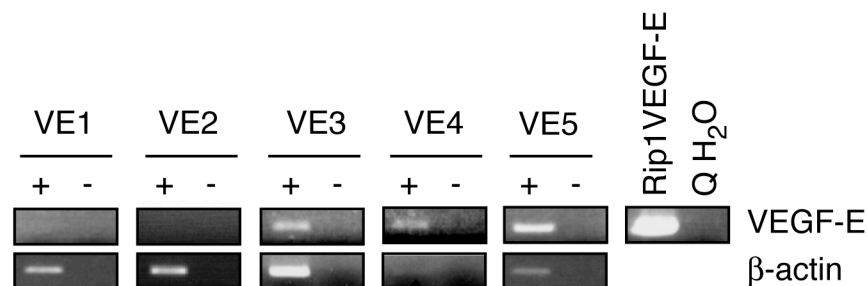


Figure 2. RT-PCR analysis of transgenic VEGF-E expression

Pancreatic RNA from the five Rip1VEGF-E_{D1701} founderlines was tested for expression of VEGF-E. Rip1VEGF-E_{D1701} plasmid served as positive, H₂O as negative control. β -actin primers were used to monitor quality of cDNA. VE1, founderline Rip1VEGF-E_{D1701}-1, VE2, founderline Rip1VEGF-E_{D1701}-2, VE3, founderline Rip1VEGF-E_{D1701}-3, VE4, founderline Rip1VEGF-E_{D1701}-4, VE5, founderline Rip1VEGF-E_{D1701}-5; + indicates with, - without reverse transcriptase.

The phenotypical characterization of the three expressing founderlines is currently ongoing. Furthermore, these mice are being crossed with Rip1Tag2 transgenic mice, a well-established mouse model of multistage β -cell carcinogenesis, and will be analyzed to dissect the specific role of activated VEGFR-2 in tumor angiogenesis and tumor progression [124].

4.3.5. Discussion

Here we report the establishment of Rip1VEGF-E_{D1701} transgenic mice, in which expression of the variant VEGF-E_{D1701} is targeted specifically to β -cells of pancreatic islets of Langerhans. Three independent healthy and fertile founderlines were generated exhibiting stable germline transmission as well as transgene expression in the pancreas, enabling the exclusion of transgene integration artifacts as cause of potential phenotypical observations.

Members of the vascular endothelial growth factor (VEGF) family and their receptors are important regulators of physiological and pathological angiogenesis. VEGFR-1 and VEGFR-2 are mainly involved in angiogenic processes, whereas VEGFR-3 is an important signal transducer during lymphangiogenesis [45]. Since VEGFR-2-deficient mice are embryonically lethal and VEGF-A as the only mammalian ligand for VEGFR-2 also activates VEGFR-1, the specific contribution of VEGFR-2 to VEGF-A-induced processes in adult animals has been difficult to assess. The discovery of the viral VEGF-E family members, which display selective affinity for VEGFR-2, has represented an important step towards elucidating distinct VEGFR-2-mediated signaling and biological effects. All VEGF-E variants characterized to date display almost the same affinity for VEGFR-2 as VEGF-A₁₆₅, and VEGF-E_{NZ-2}, VEGF-E_{NZ-10}, and VEGF-E_{D1701} can also bind the co-receptor NP-1 [223-226]. Although differing in their amino acid sequence and receptor binding affinities, all VEGF-E variants possess similar activities as described for VEGF-A, including induction of endothelial cell proliferation *in vitro* and angiogenesis *in vivo* (reviewed in [46]). Recent studies have demonstrated that VEGFR-1, which is a negative modulator during vascular development, becomes again important in pathological angiogenesis of the adult, such as occurring in cancer [179]. Although its importance is undisputed, the specific role of VEGFR-2 during tumor angiogenesis has only recently become clearer due to studies using VEGF-E [46, 67, 231]. Furthermore, VEGFR-2 has been shown to contribute to tumor cell migration and invasion *in vitro* and may therefore also be involved in metastasis *in vivo* [220, 221].

The generation of Rip1VEGF-E_{D1701} transgenic mice represents a new tool to study biological effects of activated VEGFR-2 in the adult vasculature. Furthermore, these mice are currently being crossed with Rip1Tag2 mice, a well-characterized model of poorly-metastatic β -cell carcinogenesis [124]. The analysis of double transgenic Rip1Tag2;Rip1VEGF-E_{D1701} mice will contribute to our understanding of the role of VEGFR-2 in tumor angiogenesis, tumor progression, and metastasis.

5. Conclusion and Outlook

The VEGF family of ligands and their receptors have emerged as central players of blood and lymphatic vessel development and play a critical role during malignancy. The objective of this study was to investigate and to compare side-by-side the biological effects elicited by the different VEGF family members *in vivo* under physiological conditions as well as during carcinogenesis. The here established transgenic mouse lines expressing either VEGF-B₁₆₇, PlGF-1, VEGF-E_{D1701}, VEGF-C156S or VEGF-D under the control of the same promoter represent valuable biological models that allow such comparative analysis of VEGFs and VEGFRs.

VEGF family members involved in lymphangiogenesis

The distinct phenotypes of transgenic mouse lines expressing either VEGF-C or VEGF-D suggest that although displaying the same receptor binding capacity for VEGFR-3 and -2, these growth factors exert different functions. In contrast, selective activation of VEGFR-3 by transgenic expression of VEGF-C156S results in the identical phenotype as described for VEGF-C. The observations presented in this thesis underline the value of these mouse models for the identification of distinct functions of VEGF-C, -C156S, and -D and may serve as basis for future *in vitro* and *in vivo* studies of lymphangiogenesis and metastasis employing these mouse lines. For instance, cultured primary endothelial cells derived from tumor-associated lymphatic vessels may serve to elucidate distinct molecular alterations as well as signaling pathways induced by VEGF-C, -C156S, and -D. Also, the hypothesis of lymphangioblast precursors that may directly contribute to the *de novo* formation of lymphatic vessels can be addressed *in vivo*. Furthermore, a potential molecular cross-talk between VEGFR-2 and -3 as well as its significance can be studied. Finally, these mice may also be used to test the efficacy of anti-metastatic therapies.

VEGF family members involved in angiogenesis

In the past ten years, the critical involvement of VEGF-A in normal as well as tumor angiogenesis has overshadowed the interest in elucidating the biological significance of the other ligands for VEGFR-1 and -2. The generation as well as ongoing characterization of transgenic mice expressing VEGF-B₁₆₇, PlGF-1, or VEGF-E_{D1701} under the Rip1 promoter may contribute to our understanding of the role of these growth factors under physiological conditions as well as during malignancy. At present, we have identified VEGF-B₁₆₇ and PlGF-1 as a promoter and inhibitor of tumor angiogenesis, respectively. Hence, although binding to the same receptor, these growth factors elicit opposing effects on the tumor blood vasculature, which might be considered when designing inhibitors of angiogenesis involving VEGFR-1. Whether VEGF-B₁₆₇ and PlGF-1 act predominantly via intrinsic activation of VEGFR-1 or whether they are only modulators of VEGF-A-mediated angiogenesis – possibly via heterodimerization with VEGF-A – will be one of many interesting issues that can be addressed with use of these mice. Also the ability of VEGF-B₁₆₇ and PlGF-1 to recruit VEGFR-1-positive hematopoietic stem cells, immune cells, and pericytes will be tested in the future. The phenotypical analysis of VEGF-E_{D1701}-expressing mice is currently underway and will help to elucidate the specific role of VEGFR-2 signaling during tumorigenesis.

6. References

1. Carmeliet, P. (2005). Angiogenesis in life, disease and medicine. *Nature* 438, 932-936.
2. Jain, R.K. (2003). Molecular regulation of vessel maturation. *Nat Med* 9, 685-693.
3. Bergers, G., and Song, S. (2005). The role of pericytes in blood-vessel formation and maintenance. *Neuro-oncol* 7, 452-464.
4. Landis, E.M., and Sage, L.E. (1971). Fluid movement rates through walls of single capillaries exposed to hypertonic solutions. *Am J Physiol* 221, 520-534.
5. Hong, Y.K., Shin, J.W., and Detmar, M. (2004). Development of the lymphatic vascular system: a mystery unravels. *Dev Dyn* 231, 462-473.
6. Alitalo, K., Tammela, T., and Petrova, T.V. (2005). Lymphangiogenesis in development and human disease. *Nature* 438, 946-953.
7. Robb, L., and Elefanty, A.G. (1998). The hemangioblast--an elusive cell captured in culture. *Bioessays* 20, 611-614.
8. Risau, W., and Flamme, I. (1995). Vasculogenesis. *Annu Rev Cell Dev Biol* 11, 73-91.
9. Risau, W. (1997). Mechanisms of angiogenesis. *Nature* 386, 671-674.
10. Shalaby, F., Rossant, J., Yamaguchi, T.P., Gertsenstein, M., Wu, X.F., Breitman, M.L., and Schuh, A.C. (1995). Failure of blood-island formation and vasculogenesis in Flk-1-deficient mice. *Nature* 376, 62-66.
11. Carmeliet, P., Ferreira, V., Breier, G., Pollefeyt, S., Kieckens, L., Gertsenstein, M., Fahrig, M., Vandenhoek, A., Harpal, K., Eberhardt, C., Declercq, C., Pawling, J., Moons, L., Collen, D., Risau, W., and Nagy, A. (1996). Abnormal blood vessel development and lethality in embryos lacking a single VEGF allele. *Nature* 380, 435-439.
12. Ferrara, N., Carver-Moore, K., Chen, H., Dowd, M., Lu, L., O'Shea, K.S., Powell-Braxton, L., Hillan, K.J., and Moore, M.W. (1996). Heterozygous embryonic lethality induced by targeted inactivation of the VEGF gene. *Nature* 380, 439-442.
13. Fong, G.H., Rossant, J., Gertsenstein, M., and Breitman, M.L. (1995). Role of the Flt-1 receptor tyrosine kinase in regulating the assembly of vascular endothelium. *Nature* 376, 66-70.
14. Hiratsuka, S., Minowa, O., Kuno, J., Noda, T., and Shibuya, M. (1998). Flt-1 lacking the tyrosine kinase domain is sufficient for normal development and angiogenesis in mice. *Proc Natl Acad Sci U S A* 95, 9349-9354.
15. Rossant, J., and Hirashima, M. (2003). Vascular development and patterning: making the right choices. *Curr Opin Genet Dev* 13, 408-412.
16. Dumont, D.J., Jussila, L., Taipale, J., Lymboussaki, A., Mustonen, T., Pajusola, K., Breitman, M., and Alitalo, K. (1998). Cardiovascular failure in mouse embryos deficient in VEGF receptor-3. *Science* 282, 946-949.
17. Lawson, N.D., Vogel, A.M., and Weinstein, B.M. (2002). sonic hedgehog and vascular endothelial growth factor act upstream of the Notch pathway during arterial endothelial differentiation. *Dev Cell* 3, 127-136.
18. Pola, R., Ling, L.E., Silver, M., Corbley, M.J., Kearney, M., Blake Pepinsky, R., Shapiro, R., Taylor, F.R., Baker, D.P., Asahara, T., and Isner, J.M. (2001). The morphogen Sonic hedgehog is an indirect angiogenic agent upregulating two families of angiogenic growth factors. *Nat Med* 7, 706-711.
19. Villa, N., Walker, L., Lindsell, C.E., Gasson, J., Iruela-Arispe, M.L., and Weinmaster, G. (2001). Vascular expression of Notch pathway receptors and ligands is restricted to arterial vessels. *Mech Dev* 108, 161-164.
20. Krebs, L.T., Xue, Y., Norton, C.R., Shutter, J.R., Maguire, M., Sundberg, J.P., Gallahan, D., Closson, V., Kitajewski, J., Callahan, R., Smith, G.H., Stark, K.L., and Gridley, T. (2000). Notch signaling is essential for vascular morphogenesis in mice. *Genes Dev* 14, 1343-1352.
21. Lawson, N.D., Scheer, N., Pham, V.N., Kim, C.H., Chitnis, A.B., Campos-Ortega, J.A., and Weinstein, B.M. (2001). Notch signaling is required for arterial-venous

- differentiation during embryonic vascular development. *Development* 128, 3675-3683.
22. Gale, N.W., and Yancopoulos, G.D. (1999). Growth factors acting via endothelial cell-specific receptor tyrosine kinases: VEGFs, angiopoietins, and ephrins in vascular development. *Genes Dev* 13, 1055-1066.
 23. Wang, H.U., Chen, Z.F., and Anderson, D.J. (1998). Molecular distinction and angiogenic interaction between embryonic arteries and veins revealed by ephrin-B2 and its receptor Eph-B4. *Cell* 93, 741-753.
 24. Gerety, S.S., Wang, H.U., Chen, Z.F., and Anderson, D.J. (1999). Symmetrical mutant phenotypes of the receptor EphB4 and its specific transmembrane ligand ephrin-B2 in cardiovascular development. *Mol Cell* 4, 403-414.
 25. Adams, R.H., Diella, F., Hennig, S., Helmbacher, F., Deutsch, U., and Klein, R. (2001). The cytoplasmic domain of the ligand ephrinB2 is required for vascular morphogenesis but not cranial neural crest migration. *Cell* 104, 57-69.
 26. Herzog, Y., Kalcheim, C., Kahane, N., Reshef, R., and Neufeld, G. (2001). Differential expression of neuropilin-1 and neuropilin-2 in arteries and veins. *Mech Dev* 109, 115-119.
 27. Herzog, Y., Guttmann-Raviv, N., and Neufeld, G. (2005). Segregation of arterial and venous markers in subpopulations of blood islands before vessel formation. *Dev Dyn* 232, 1047-1055.
 28. Hellstrom, M., Gerhardt, H., Kalen, M., Li, X., Eriksson, U., Wolburg, H., and Betsholtz, C. (2001). Lack of pericytes leads to endothelial hyperplasia and abnormal vascular morphogenesis. *J Cell Biol* 153, 543-553.
 29. Suri, C., Jones, P.F., Patan, S., Bartunkova, S., Maisonpierre, P.C., Davis, S., Sato, T.N., and Yancopoulos, G.D. (1996). Requisite role of angiopoietin-1, a ligand for the TIE2 receptor, during embryonic angiogenesis. *Cell* 87, 1171-1180.
 30. Maisonpierre, P.C., Suri, C., Jones, P.F., Bartunkova, S., Wiegand, S.J., Radziejewski, C., Compton, D., McClain, J., Aldrich, T.H., Papadopoulos, N., Daly, T.J., Davis, S., Sato, T.N., and Yancopoulos, G.D. (1997). Angiopoietin-2, a natural antagonist for Tie2 that disrupts in vivo angiogenesis. *Science* 277, 55-60.
 31. Wigle, J.T., and Oliver, G. (1999). Prox1 function is required for the development of the murine lymphatic system. *Cell* 98, 769-778.
 32. Karkkainen, M.J., Haiko, P., Sainio, K., Partanen, J., Taipale, J., Petrova, T.V., Jeltsch, M., Jackson, D.G., Talikka, M., Rauvala, H., Betsholtz, C., and Alitalo, K. (2004). Vascular endothelial growth factor C is required for sprouting of the first lymphatic vessels from embryonic veins. *Nat Immunol* 5, 74-80.
 33. Abtahian, F., Guerriero, A., Sebzda, E., Lu, M.M., Zhou, R., Mocsai, A., Myers, E.E., Huang, B., Jackson, D.G., Ferrari, V.A., Tybulewicz, V., Lowell, C.A., Lepore, J.J., Koretzky, G.A., and Kahn, M.L. (2003). Regulation of blood and lymphatic vascular separation by signaling proteins SLP-76 and Syk. *Science* 299, 247-251.
 34. Yuan, L., Moyon, D., Pardanaud, L., Breant, C., Karkkainen, M.J., Alitalo, K., and Eichmann, A. (2002). Abnormal lymphatic vessel development in neuropilin 2 mutant mice. *Development* 129, 4797-4806.
 35. Schneider, M., Othman-Hassan, K., Christ, B., and Wilting, J. (1999). Lymphangioblasts in the avian wing bud. *Dev Dyn* 216, 311-319.
 36. Salven, P., Mustjoki, S., Alitalo, R., Alitalo, K., and Rafii, S. (2003). VEGFR-3 and CD133 identify a population of CD34+ lymphatic/vascular endothelial precursor cells. *Blood* 101, 168-172.
 37. Kerjaschki, D., Huttary, N., Raab, I., Regele, H., Bojarski-Nagy, K., Bartel, G., Krober, S.M., Greinix, H., Rosenmaier, A., Karlhofer, F., Wick, N., and Mazal, P.R. (2006). Lymphatic endothelial progenitor cells contribute to de novo lymphangiogenesis in human renal transplants. *Nat Med* 12, 230-234.
 38. McDonald, N.Q., and Hendrickson, W.A. (1993). A structural superfamily of growth factors containing a cystine knot motif. *Cell* 73, 421-424.
 39. Leung, D.W., Cachianes, G., Kuang, W.J., Goeddel, D.V., and Ferrara, N. (1989). Vascular endothelial growth factor is a secreted angiogenic mitogen. *Science* 246, 1306-1309.

40. Olofsson, B., Pajusola, K., Kaipainen, A., von Euler, G., Joukov, V., Saksela, O., Orpana, A., Pettersson, R.F., Alitalo, K., and Eriksson, U. (1996). Vascular endothelial growth factor B, a novel growth factor for endothelial cells. *Proc Natl Acad Sci U S A* *93*, 2576-2581.
41. Joukov, V., Pajusola, K., Kaipainen, A., Chilov, D., Lahtinen, I., Kukk, E., Saksela, O., Kalkkinen, N., and Alitalo, K. (1996). A novel vascular endothelial growth factor, VEGF-C, is a ligand for the Flt4 (VEGFR-3) and KDR (VEGFR-2) receptor tyrosine kinases. *Embo J* *15*, 290-298.
42. Orlandini, M., Marconcini, L., Ferruzzi, R., and Oliviero, S. (1996). Identification of a c-fos-induced gene that is related to the platelet-derived growth factor/vascular endothelial growth factor family. *Proc Natl Acad Sci U S A* *93*, 11675-11680.
43. Maglione, D., Guerriero, V., Viglietto, G., Delli-Bovi, P., and Persico, M.G. (1991). Isolation of a human placenta cDNA coding for a protein related to the vascular permeability factor. *Proc Natl Acad Sci U S A* *88*, 9267-9271.
44. Autiero, M., Waltenberger, J., Communi, D., Kranz, A., Moons, L., Lambrechts, D., Kroll, J., Plaisance, S., De Mol, M., Bono, F., Kliche, S., Fellbrich, G., Ballmer-Hofer, K., Maglione, D., Mayr-Beyrle, U., Dewerchin, M., Dombrowski, S., Stanimirovic, D., Van Hummelen, P., Dehio, C., Hicklin, D.J., Persico, G., Herbert, J.M., Shibuya, M., Collen, D., Conway, E.M., and Carmeliet, P. (2003). Role of PIGF in the intra- and intermolecular cross talk between the VEGF receptors Flt1 and Flk1. *Nat Med* *9*, 936-943.
45. Tammela, T., Enholm, B., Alitalo, K., and Paavonen, K. (2005). The biology of vascular endothelial growth factors. *Cardiovasc Res* *65*, 550-563.
46. Shibuya, M. (2003). Vascular endothelial growth factor receptor-2: its unique signaling and specific ligand, VEGF-E. *Cancer Sci* *94*, 751-756.
47. Takahashi, H., and Shibuya, M. (2005). The vascular endothelial growth factor (VEGF)/VEGF receptor system and its role under physiological and pathological conditions. *Clin Sci (Lond)* *109*, 227-241.
48. Ferrara, N., Gerber, H.P., and LeCouter, J. (2003). The biology of VEGF and its receptors. *Nat Med* *9*, 669-676.
49. Woolard, J., Wang, W.Y., Bevan, H.S., Qiu, Y., Morbidelli, L., Pritchard-Jones, R.O., Cui, T.G., Sugiono, M., Waite, E., Perrin, R., Foster, R., Digby-Bell, J., Shields, J.D., Whittles, C.E., Mushens, R.E., Gillatt, D.A., Ziche, M., Harper, S.J., and Bates, D.O. (2004). VEGF165b, an inhibitory vascular endothelial growth factor splice variant: mechanism of action, in vivo effect on angiogenesis and endogenous protein expression. *Cancer Res* *64*, 7822-7835.
50. Plouet, J., Moro, F., Bertagnolli, S., Coldeboeuf, N., Mazarguil, H., Clamens, S., and Bayard, F. (1997). Extracellular cleavage of the vascular endothelial growth factor 189-amino acid form by urokinase is required for its mitogenic effect. *J Biol Chem* *272*, 13390-13396.
51. Olofsson, B., Pajusola, K., von Euler, G., Chilov, D., Alitalo, K., and Eriksson, U. (1996). Genomic organization of the mouse and human genes for vascular endothelial growth factor B (VEGF-B) and characterization of a second splice isoform. *J Biol Chem* *271*, 19310-19317.
52. Cao, Y., Chen, H., Zhou, L., Chiang, M.K., Anand-Apte, B., Weatherbee, J.A., Wang, Y., Fang, F., Flanagan, J.G., and Tsang, M.L. (1996). Heterodimers of placenta growth factor/vascular endothelial growth factor. Endothelial activity, tumor cell expression, and high affinity binding to Flk-1/KDR. *J Biol Chem* *271*, 3154-3162.
53. Achen, M.G., Jeltsch, M., Kukk, E., Makinen, T., Vitali, A., Wilks, A.F., Alitalo, K., and Stacker, S.A. (1998). Vascular endothelial growth factor D (VEGF-D) is a ligand for the tyrosine kinases VEGF receptor 2 (Flk1) and VEGF receptor 3 (Flt4). *Proc Natl Acad Sci U S A* *95*, 548-553.
54. Baldwin, M.E., Stacker, S.A., and Achen, M.G. (2002). Molecular control of lymphangiogenesis. *Bioessays* *24*, 1030-1040.
55. Joukov, V., Kumar, V., Sorsa, T., Arighi, E., Weich, H., Saksela, O., and Alitalo, K. (1998). A recombinant mutant vascular endothelial growth factor-C that has lost

- vascular endothelial growth factor receptor-2 binding, activation, and vascular permeability activities. *J Biol Chem* 273, 6599-6602.
56. Shibuya, M., Yamaguchi, S., Yamane, A., Ikeda, T., Tojo, A., Matsushime, H., and Sato, M. (1990). Nucleotide sequence and expression of a novel human receptor-type tyrosine kinase gene (flt) closely related to the fms family. *Oncogene* 5, 519-524.
 57. Terman, B.I., Carrion, M.E., Kovacs, E., Rasmussen, B.A., Eddy, R.L., and Shows, T.B. (1991). Identification of a new endothelial cell growth factor receptor tyrosine kinase. *Oncogene* 6, 1677-1683.
 58. Pajusola, K., Aprelikova, O., Korhonen, J., Kaipainen, A., Pertovaara, L., Alitalo, R., and Alitalo, K. (1992). FLT4 receptor tyrosine kinase contains seven immunoglobulin-like loops and is expressed in multiple human tissues and cell lines. *Cancer Res* 52, 5738-5743.
 59. Hughes, D.C. (2001). Alternative splicing of the human VEGFR-3/FLT4 gene as a consequence of an integrated human endogenous retrovirus. *J Mol Evol* 53, 77-79.
 60. Kendall, R.L., Wang, G., and Thomas, K.A. (1996). Identification of a natural soluble form of the vascular endothelial growth factor receptor, FLT-1, and its heterodimerization with KDR. *Biochem Biophys Res Commun* 226, 324-328.
 61. Ebos, J.M., Bocci, G., Man, S., Thorpe, P.E., Hicklin, D.J., Zhou, D., Jia, X., and Kerbel, R.S. (2004). A naturally occurring soluble form of vascular endothelial growth factor receptor 2 detected in mouse and human plasma. *Mol Cancer Res* 2, 315-326.
 62. Goldman, C.K., Kendall, R.L., Cabrera, G., Soroceanu, L., Heike, Y., Gillespie, G.Y., Siegal, G.P., Mao, X., Bett, A.J., Huckle, W.R., Thomas, K.A., and Curiel, D.T. (1998). Paracrine expression of a native soluble vascular endothelial growth factor receptor inhibits tumor growth, metastasis, and mortality rate. *Proc Natl Acad Sci U S A* 95, 8795-8800.
 63. Maynard, S.E., Min, J.Y., Merchan, J., Lim, K.H., Li, J., Mondal, S., Libermann, T.A., Morgan, J.P., Sellke, F.W., Stillman, I.E., Epstein, F.H., Sukhatme, V.P., and Karumanchi, S.A. (2003). Excess placental soluble fms-like tyrosine kinase 1 (sFlt1) may contribute to endothelial dysfunction, hypertension, and proteinuria in preeclampsia. *J Clin Invest* 111, 649-658.
 64. Davis-Smyth, T., Chen, H., Park, J., Presta, L.G., and Ferrara, N. (1996). The second immunoglobulin-like domain of the VEGF tyrosine kinase receptor Flt-1 determines ligand binding and may initiate a signal transduction cascade. *Embo J* 15, 4919-4927.
 65. Fuh, G., Garcia, K.C., and de Vos, A.M. (2000). The interaction of neuropilin-1 with vascular endothelial growth factor and its receptor flt-1. *J Biol Chem* 275, 26690-26695.
 66. Dias, S., Choy, M., Alitalo, K., and Rafii, S. (2002). Vascular endothelial growth factor (VEGF)-C signaling through FLT-4 (VEGFR-3) mediates leukemic cell proliferation, survival, and resistance to chemotherapy. *Blood* 99, 2179-2184.
 67. Shibuya, M., and Claesson-Welsh, L. (2006). Signal transduction by VEGF receptors in regulation of angiogenesis and lymphangiogenesis. *Exp Cell Res* 312, 549-560.
 68. Carmeliet, P., Moons, L., Luttun, A., Vincenti, V., Compernelle, V., De Mol, M., Wu, Y., Bono, F., Devy, L., Beck, H., Scholz, D., Acker, T., DiPalma, T., Dewerchin, M., Noel, A., Stalmans, I., Barra, A., Blacher, S., Vandendriessche, T., Ponten, A., Eriksson, U., Plate, K.H., Foidart, J.M., Schaper, W., Charnock-Jones, D.S., Hicklin, D.J., Herbert, J.M., Collen, D., and Persico, M.G. (2001). Synergism between vascular endothelial growth factor and placental growth factor contributes to angiogenesis and plasma extravasation in pathological conditions. *Nat Med* 7, 575-583.
 69. Kaplan, R.N., Riba, R.D., Zacharoulis, S., Bramley, A.H., Vincent, L., Costa, C., MacDonald, D.D., Jin, D.K., Shido, K., Kerns, S.A., Zhu, Z., Hicklin, D., Wu, Y., Port, J.L., Altorki, N., Port, E.R., Ruggiero, D., Shmelkov, S.V., Jensen, K.K., Rafii, S., and Lyden, D. (2005). VEGFR1-positive haematopoietic bone marrow progenitors initiate the pre-metastatic niche. *Nature* 438, 820-827.
 70. Bjorndahl, M.A., Cao, R., Burton, J.B., Brakenhielm, E., Religa, P., Galter, D., Wu, L., and Cao, Y. (2005). Vascular endothelial growth factor-a promotes peritumoral lymphangiogenesis and lymphatic metastasis. *Cancer Res* 65, 9261-9268.

71. Maruyama, K., Ii, M., Cursiefen, C., Jackson, D.G., Keino, H., Tomita, M., Van Rooijen, N., Takenaka, H., D'Amore, P.A., Stein-Streilein, J., Losordo, D.W., and Streilein, J.W. (2005). Inflammation-induced lymphangiogenesis in the cornea arises from CD11b-positive macrophages. *J Clin Invest* *115*, 2363-2372.
72. De Falco, S., Gigante, B., and Persico, M.G. (2002). Structure and function of placental growth factor. *Trends Cardiovasc Med* *12*, 241-246.
73. Klagsbrun, M., Takashima, S., and Mamluk, R. (2002). The role of neuropilin in vascular and tumor biology. *Adv Exp Med Biol* *515*, 33-48.
74. Miao, H.Q., Soker, S., Feiner, L., Alonso, J.L., Raper, J.A., and Klagsbrun, M. (1999). Neuropilin-1 mediates collapsin-1/semaphorin III inhibition of endothelial cell motility: functional competition of collapsin-1 and vascular endothelial growth factor-165. *J Cell Biol* *146*, 233-242.
75. Renzi, M.J., Feiner, L., Koppel, A.M., and Raper, J.A. (1999). A dominant negative receptor for specific secreted semaphorins is generated by deleting an extracellular domain from neuropilin-1. *J Neurosci* *19*, 7870-7880.
76. Mamluk, R., Gechtman, Z., Kutcher, M.E., Gasiunas, N., Gallagher, J., and Klagsbrun, M. (2002). Neuropilin-1 binds vascular endothelial growth factor 165, placenta growth factor-2, and heparin via its b1b2 domain. *J Biol Chem* *277*, 24818-24825.
77. Neufeld, G., Cohen, T., Shraga, N., Lange, T., Kessler, O., and Herzog, Y. (2002). The neuropilins: multifunctional semaphorin and VEGF receptors that modulate axon guidance and angiogenesis. *Trends Cardiovasc Med* *12*, 13-19.
78. Rossignol, M., Gagnon, M.L., and Klagsbrun, M. (2000). Genomic organization of human neuropilin-1 and neuropilin-2 genes: identification and distribution of splice variants and soluble isoforms. *Genomics* *70*, 211-222.
79. Soker, S., Takashima, S., Miao, H.Q., Neufeld, G., and Klagsbrun, M. (1998). Neuropilin-1 is expressed by endothelial and tumor cells as an isoform-specific receptor for vascular endothelial growth factor. *Cell* *92*, 735-745.
80. Soker, S., Miao, H.Q., Nomi, M., Takashima, S., and Klagsbrun, M. (2002). VEGF165 mediates formation of complexes containing VEGFR-2 and neuropilin-1 that enhance VEGF165-receptor binding. *J Cell Biochem* *85*, 357-368.
81. Kitsukawa, T., Shimono, A., Kawakami, A., Kondoh, H., and Fujisawa, H. (1995). Overexpression of a membrane protein, neuropilin, in chimeric mice causes anomalies in the cardiovascular system, nervous system and limbs. *Development* *121*, 4309-4318.
82. Kawasaki, T., Kitsukawa, T., Bekku, Y., Matsuda, Y., Sanbo, M., Yagi, T., and Fujisawa, H. (1999). A requirement for neuropilin-1 in embryonic vessel formation. *Development* *126*, 4895-4902.
83. Takashima, S., Kitakaze, M., Asakura, M., Asanuma, H., Sanada, S., Tashiro, F., Niwa, H., Miyazaki, J., Hirota, S., Kitamura, Y., Kitsukawa, T., Fujisawa, H., Klagsbrun, M., and Hori, M. (2002). Targeting of both mouse neuropilin-1 and neuropilin-2 genes severely impairs developmental yolk sac and embryonic angiogenesis. *Proc Natl Acad Sci U S A* *99*, 3657-3662.
84. Takagi, S., Kasuya, Y., Shimizu, M., Matsuura, T., Tsuboi, M., Kawakami, A., and Fujisawa, H. (1995). Expression of a cell adhesion molecule, neuropilin, in the developing chick nervous system. *Dev Biol* *170*, 207-222.
85. Shimizu, M., Murakami, Y., Suto, F., and Fujisawa, H. (2000). Determination of cell adhesion sites of neuropilin-1. *J Cell Biol* *148*, 1283-1293.
86. Jemal, A., Murray, T., Ward, E., Samuels, A., Tiwari, R.C., Ghafoor, A., Feuer, E.J., and Thun, M.J. (2005). Cancer statistics, 2005. *CA Cancer J Clin* *55*, 10-30.
87. Folkman, J. (2003). Fundamental concepts of the angiogenic process. *Curr Mol Med* *3*, 643-651.
88. Bergers, G., and Benjamin, L.E. (2003). Tumorigenesis and the angiogenic switch. *Nat Rev Cancer* *3*, 401-410.
89. Kopfstein, L., and Christofori, G. (2006). Metastasis: cell-autonomous mechanisms versus contributions by the tumor microenvironment. *Cell Mol Life Sci* *63*, 449-468.
90. Carmeliet, P., and Jain, R.K. (2000). Angiogenesis in cancer and other diseases. *Nature* *407*, 249-257.

91. Folberg, R., Hendrix, M.J., and Maniotis, A.J. (2000). Vasculogenic mimicry and tumor angiogenesis. *Am J Pathol* 156, 361-381.
92. Dvorak, H.F. (2002). Vascular permeability factor/vascular endothelial growth factor: a critical cytokine in tumor angiogenesis and a potential target for diagnosis and therapy. *J Clin Oncol* 20, 4368-4380.
93. Pugh, C.W., and Ratcliffe, P.J. (2003). Regulation of angiogenesis by hypoxia: role of the HIF system. *Nat Med* 9, 677-684.
94. Salven, P., Lymboussaki, A., Heikkila, P., Jaaskela-Saari, H., Enholm, B., Aase, K., von Euler, G., Eriksson, U., Alitalo, K., and Joensuu, H. (1998). Vascular endothelial growth factors VEGF-B and VEGF-C are expressed in human tumors. *Am J Pathol* 153, 103-108.
95. Shintani, S., Li, C., Ishikawa, T., Mihara, M., Nakashiro, K., and Hamakawa, H. (2004). Expression of vascular endothelial growth factor A, B, C, and D in oral squamous cell carcinoma. *Oral Oncol* 40, 13-20.
96. Donnini, S., Machein, M.R., Plate, K.H., and Weich, H.A. (1999). Expression and localization of placenta growth factor and PlGF receptors in human meningiomas. *J Pathol* 189, 66-71.
97. Takahashi, A., Sasaki, H., Kim, S.J., Kakizoe, T., Miyao, N., Sugimura, T., Terada, M., and Tsukamoto, T. (1999). Identification of receptor genes in renal cell carcinoma associated with angiogenesis by differential hybridization technique. *Biochem Biophys Res Commun* 257, 855-859.
98. Wei, S.C., Tsao, P.N., Yu, S.C., Shun, C.T., Tsai-Wu, J.J., Wu, C.H., Su, Y.N., Hsieh, F.J., and Wong, J.M. (2005). Placenta growth factor expression is correlated with survival of patients with colorectal cancer. *Gut* 54, 666-672.
99. Skobe, M., Hamberg, L.M., Hawighorst, T., Schirner, M., Wolf, G.L., Alitalo, K., and Detmar, M. (2001). Concurrent induction of lymphangiogenesis, angiogenesis, and macrophage recruitment by vascular endothelial growth factor-C in melanoma. *Am J Pathol* 159, 893-903.
100. Stacker, S.A., Caesar, C., Baldwin, M.E., Thornton, G.E., Williams, R.A., Prevo, R., Jackson, D.G., Nishikawa, S., Kubo, H., and Achen, M.G. (2001). VEGF-D promotes the metastatic spread of tumor cells via the lymphatics. *Nat Med* 7, 186-191.
101. Hiratsuka, S., Maru, Y., Okada, A., Seiki, M., Noda, T., and Shibuya, M. (2001). Involvement of Flt-1 tyrosine kinase (vascular endothelial growth factor receptor-1) in pathological angiogenesis. *Cancer Res* 61, 1207-1213.
102. Gerber, H.P., Condorelli, F., Park, J., and Ferrara, N. (1997). Differential transcriptional regulation of the two vascular endothelial growth factor receptor genes. Flt-1, but not Flk-1/KDR, is up-regulated by hypoxia. *J Biol Chem* 272, 23659-23667.
103. Partanen, T.A., Alitalo, K., and Miettinen, M. (1999). Lack of lymphatic vascular specificity of vascular endothelial growth factor receptor 3 in 185 vascular tumors. *Cancer* 86, 2406-2412.
104. Ferrara, N., and Kerbel, R.S. (2005). Angiogenesis as a therapeutic target. *Nature* 438, 967-974.
105. Gerber, H.P., Hillan, K.J., Ryan, A.M., Kowalski, J., Keller, G.A., Rangell, L., Wright, B.D., Radtke, F., Aguet, M., and Ferrara, N. (1999). VEGF is required for growth and survival in neonatal mice. *Development* 126, 1149-1159.
106. Inai, T., Mancuso, M., Hashizume, H., Baffert, F., Haskell, A., Baluk, P., Hu-Lowe, D.D., Shalinsky, D.R., Thurston, G., Yancopoulos, G.D., and McDonald, D.M. (2004). Inhibition of vascular endothelial growth factor (VEGF) signaling in cancer causes loss of endothelial fenestrations, regression of tumor vessels, and appearance of basement membrane ghosts. *Am J Pathol* 165, 35-52.
107. Kerbel, R., and Folkman, J. (2002). Clinical translation of angiogenesis inhibitors. *Nat Rev Cancer* 2, 727-739.
108. Sridhar, S.S., and Shepherd, F.A. (2003). Targeting angiogenesis: a review of angiogenesis inhibitors in the treatment of lung cancer. *Lung Cancer* 42 *Suppl 1*, S81-91.
109. Nathanson, S.D. (2003). Insights into the mechanisms of lymph node metastasis. *Cancer* 98, 413-423.

110. Pepper, M.S., Tille, J.C., Nisato, R., and Skobe, M. (2003). Lymphangiogenesis and tumor metastasis. *Cell Tissue Res* 314, 167-177.
111. Franchi, A., Gallo, O., Massi, D., Baroni, G., and Santucci, M. (2004). Tumor lymphangiogenesis in head and neck squamous cell carcinoma: a morphometric study with clinical correlations. *Cancer* 101, 973-978.
112. Dadras, S.S., Paul, T., Bertoncini, J., Brown, L.F., Muzikansky, A., Jackson, D.G., Ellwanger, U., Garbe, C., Mihm, M.C., and Detmar, M. (2003). Tumor lymphangiogenesis: a novel prognostic indicator for cutaneous melanoma metastasis and survival. *Am J Pathol* 162, 1951-1960.
113. Shida, A., Fujioka, S., Ishibashi, Y., Kobayashi, K., Nimura, H., Mitsumori, N., Suzuki, Y., Kawakami, M., Urashima, M., and Yanaga, K. (2005). Prognostic Significance of Vascular Endothelial Growth Factor D in Gastric Carcinoma. *World J Surg* 29, 1600-1607.
114. Kurahara, H., Takao, S., Maemura, K., Shinchi, H., Natsugoe, S., and Aikou, T. (2004). Impact of vascular endothelial growth factor-C and -D expression in human pancreatic cancer: its relationship to lymph node metastasis. *Clin Cancer Res* 10, 8413-8420.
115. Kawakami, M., Furuhashi, T., Kimura, Y., Yamaguchi, K., Hata, F., Sasaki, K., and Hirata, K. (2003). Expression analysis of vascular endothelial growth factors and their relationships to lymph node metastasis in human colorectal cancer. *J Exp Clin Cancer Res* 22, 229-237.
116. Kitadai, Y., Kodama, M., Cho, S., Kuroda, T., Ochiuni, T., Kimura, S., Tanaka, S., Matsumura, S., Yasui, W., and Chayama, K. (2005). Quantitative analysis of lymphangiogenic markers for predicting metastasis of human gastric carcinoma to lymph nodes. *Int J Cancer*.
117. Skobe, M., and Detmar, M. (2000). Structure, function, and molecular control of the skin lymphatic system. *J Invest Dermatol Symp Proc* 5, 14-19.
118. McColl, B.K., Stacker, S.A., and Achen, M.G. (2004). Molecular regulation of the VEGF family -- inducers of angiogenesis and lymphangiogenesis. *Apmis* 112, 463-480.
119. Orlandini, M., and Oliviero, S. (2001). In fibroblasts Vegf-D expression is induced by cell-cell contact mediated by cadherin-11. *J Biol Chem* 276, 6576-6581.
120. Orlandini, M., Semboloni, S., and Oliviero, S. (2003). Beta-catenin inversely regulates vascular endothelial growth factor-D mRNA stability. *J Biol Chem* 278, 44650-44656.
121. Nelson, W.J., and Nusse, R. (2004). Convergence of Wnt, beta-catenin, and cadherin pathways. *Science* 303, 1483-1487.
122. Roberts, N., Kloos, B., Cassella, M., Podgrabinska, S., Persaud, K., Wu, Y., Pytowski, B., and Skobe, M. (2006). Inhibition of VEGFR-3 activation with the antagonistic antibody more potently suppresses lymph node and distant metastases than inactivation of VEGFR-2. *Cancer Res* 66, 2650-2657.
123. Sleeman, J.P. (2000). The lymph node as a bridgehead in the metastatic dissemination of tumors. *Recent Results Cancer Res* 157, 55-81.
124. Hanahan, D. (1985). Heritable formation of pancreatic beta-cell tumours in transgenic mice expressing recombinant insulin/simian virus 40 oncogenes. *Nature* 315, 115-122.
125. Sachsenmeier, K.F., and Pipas, J.M. (2001). Inhibition of Rb and p53 is insufficient for SV40 T-antigen transformation. *Virology* 283, 40-48.
126. Christofori, G., Naik, P., and Hanahan, D. (1994). A second signal supplied by insulin-like growth factor II in oncogene-induced tumorigenesis. *Nature* 369, 414-418.
127. Folkman, J., Watson, K., Ingber, D., and Hanahan, D. (1989). Induction of angiogenesis during the transition from hyperplasia to neoplasia. *Nature* 339, 58-61.
128. Perl, A.K., Wilgenbus, P., Dahl, U., Semb, H., and Christofori, G. (1998). A causal role for E-cadherin in the transition from adenoma to carcinoma. *Nature* 392, 190-193.

129. Ohzato, H., Gotoh, M., Monden, M., Dono, K., Kanai, T., and Mori, T. (1991). Improvement in islet yield from a cold-preserved pancreas by pancreatic ductal collagenase distention at the time of harvesting. *Transplantation* 51, 566-570.
130. Djonov, V., Schmid, M., Tschanz, S.A., and Burri, P.H. (2000). Intussusceptive angiogenesis: its role in embryonic vascular network formation. *Circ Res* 86, 286-292.
131. Joukov, V., Sorsa, T., Kumar, V., Jeltsch, M., Claesson-Welsh, L., Cao, Y., Saksela, O., Kalkkinen, N., and Alitalo, K. (1997). Proteolytic processing regulates receptor specificity and activity of VEGF-C. *Embo J* 16, 3898-3911.
132. Stacker, S.A., Stenvers, K., Caesar, C., Vitali, A., Domagala, T., Nice, E., Roufail, S., Simpson, R.J., Moritz, R., Karpanen, T., Alitalo, K., and Achen, M.G. (1999). Biosynthesis of vascular endothelial growth factor-D involves proteolytic processing which generates non-covalent homodimers. *J Biol Chem* 274, 32127-32136.
133. Baldwin, M.E., Catimel, B., Nice, E.C., Roufail, S., Hall, N.E., Stenvers, K.L., Karkkainen, M.J., Alitalo, K., Stacker, S.A., and Achen, M.G. (2001). The specificity of receptor binding by vascular endothelial growth factor-d is different in mouse and man. *J Biol Chem* 276, 19166-19171.
134. Baldwin, M.E., Halford, M.M., Roufail, S., Williams, R.A., Hibbs, M.L., Grail, D., Kubo, H., Stacker, S.A., and Achen, M.G. (2005). Vascular endothelial growth factor D is dispensable for development of the lymphatic system. *Mol Cell Biol* 25, 2441-2449.
135. Veikkola, T., Jussila, L., Makinen, T., Karpanen, T., Jeltsch, M., Petrova, T.V., Kubo, H., Thurston, G., McDonald, D.M., Achen, M.G., Stacker, S.A., and Alitalo, K. (2001). Signalling via vascular endothelial growth factor receptor-3 is sufficient for lymphangiogenesis in transgenic mice. *Embo J* 20, 1223-1231.
136. Rissanen, T.T., Markkanen, J.E., Gruchala, M., Heikura, T., Puranen, A., Kettunen, M.I., Kholova, I., Kauppinen, R.A., Achen, M.G., Stacker, S.A., Alitalo, K., and Yla-Herttuala, S. (2003). VEGF-D is the strongest angiogenic and lymphangiogenic effector among VEGFs delivered into skeletal muscle via adenoviruses. *Circ Res* 92, 1098-1106.
137. Bhardwaj, S., Roy, H., Heikura, T., and Yla-Herttuala, S. (2005). VEGF-A, VEGF-D and VEGF-D induced intimal hyperplasia in carotid arteries. *Eur J Clin Invest* 35, 669-676.
138. Rutanen, J., Rissanen, T.T., Markkanen, J.E., Gruchala, M., Silvennoinen, P., Kivela, A., Hedman, A., Hedman, M., Heikura, T., Orden, M.R., Stacker, S.A., Achen, M.G., Hartikainen, J., and Yla-Herttuala, S. (2004). Adenoviral catheter-mediated intramyocardial gene transfer using the mature form of vascular endothelial growth factor-D induces transmural angiogenesis in porcine heart. *Circulation* 109, 1029-1035.
139. Yasuoka, H., Nakamura, Y., Zuo, H., Tang, W., Takamura, Y., Miyauchi, A., Nakamura, M., Mori, I., and Kakudo, K. (2005). VEGF-D expression and lymph vessels play an important role for lymph node metastasis in papillary thyroid carcinoma. *Mod Pathol* 18, 1127-1133.
140. White, J.D., Hewett, P.W., Kosuge, D., McCulloch, T., Enholm, B.C., Carmichael, J., and Murray, J.C. (2002). Vascular endothelial growth factor-D expression is an independent prognostic marker for survival in colorectal carcinoma. *Cancer Res* 62, 1669-1675.
141. Nakamura, Y., Yasuoka, H., Tsujimoto, M., Yang, Q., Imabun, S., Nakahara, M., Nakao, K., Nakamura, M., Mori, I., and Kakudo, K. (2003). Prognostic significance of vascular endothelial growth factor D in breast carcinoma with long-term follow-up. *Clin Cancer Res* 9, 716-721.
142. Yokoyama, Y., Charnock-Jones, D.S., Licence, D., Yanaihara, A., Hastings, J.M., Holland, C.M., Emoto, M., Umamoto, M., Sakamoto, T., Sato, S., Mizunuma, H., and Smith, S.K. (2003). Vascular endothelial growth factor-D is an independent prognostic factor in epithelial ovarian carcinoma. *Br J Cancer* 88, 237-244.
143. Nakamura, Y., Yasuoka, H., Tsujimoto, M., Yang, Q., Imabun, S., Nakahara, M., Nakao, K., Nakamura, M., Mori, I., and Kakudo, K. (2003). Flt-4-positive vessel

- density correlates with vascular endothelial growth factor-d expression, nodal status, and prognosis in breast cancer. *Clin Cancer Res* 9, 5313-5317.
144. Von Marschall, Z., Scholz, A., Stacker, S.A., Achen, M.G., Jackson, D.G., Alves, F., Schirner, M., Haberey, M., Thierauch, K.H., Wiedenmann, B., and Rosewicz, S. (2005). Vascular endothelial growth factor-D induces lymphangiogenesis and lymphatic metastasis in models of ductal pancreatic cancer. *Int J Oncol* 27, 669-679.
 145. Ishii, H., Yazawa, T., Sato, H., Suzuki, T., Ikeda, M., Hayashi, Y., Takanashi, Y., and Kitamura, H. (2004). Enhancement of pleural dissemination and lymph node metastasis of intrathoracic lung cancer cells by vascular endothelial growth factors (VEGFs). *Lung Cancer* 45, 325-337.
 146. Mandriota, S.J., Jussila, L., Jeltsch, M., Compagni, A., Baetens, D., Prevo, R., Banerji, S., Huarte, J., Montesano, R., Jackson, D.G., Orci, L., Alitalo, K., Christofori, G., and Pepper, M.S. (2001). Vascular endothelial growth factor-C-mediated lymphangiogenesis promotes tumour metastasis. *Embo J* 20, 672-682.
 147. Hogan B., B.R., Constantini F., Lacy E. (1994). *Manipulating the Mouse Embryo* (Cold Spring Harbor, NY: Cold Spring Harbor Laboratory Press).
 148. Gannon, G., Mandriota, S.J., Cui, L., Baetens, D., Pepper, M.S., and Christofori, G. (2002). Overexpression of vascular endothelial growth factor-A165 enhances tumor angiogenesis but not metastasis during beta-cell carcinogenesis. *Cancer Res* 62, 603-608.
 149. Wigle, J.T., Harvey, N., Detmar, M., Lagutina, I., Grosveld, G., Gunn, M.D., Jackson, D.G., and Oliver, G. (2002). An essential role for Prox1 in the induction of the lymphatic endothelial cell phenotype. *Embo J* 21, 1505-1513.
 150. Crnic, I., Strittmatter, K., Cavallaro, U., Kopfstein, L., Jussila, L., Alitalo, K., and Christofori, G. (2004). Loss of neural cell adhesion molecule induces tumor metastasis by up-regulating lymphangiogenesis. *Cancer Res* 64, 8630-8638.
 151. Wang, J., Kilic, G., Aydin, M., Burke, Z., Oliver, G., and Sosa-Pineda, B. (2005). Prox1 activity controls pancreas morphogenesis and participates in the production of "secondary transition" pancreatic endocrine cells. *Dev Biol* 286, 182-194.
 152. Weidner, N. (1998). Tumoural vascularity as a prognostic factor in cancer patients: the evidence continues to grow. *J Pathol* 184, 119-122.
 153. Joyce, J.A., Freeman, C., Meyer-Morse, N., Parish, C.R., and Hanahan, D. (2005). A functional heparan sulfate mimetic implicates both heparanase and heparan sulfate in tumor angiogenesis and invasion in a mouse model of multistage cancer. *Oncogene* 24, 4037-4051.
 154. Hirshberg, B., Cochran, C., Skarulis, M.C., Libutti, S.K., Alexander, H.R., Wood, B.J., Chang, R., Kleiner, D.E., and Gorden, P. (2005). Malignant insulinoma: spectrum of unusual clinical features. *Cancer* 104, 264-272.
 155. Cao, Y., Linden, P., Farnebo, J., Cao, R., Eriksson, A., Kumar, V., Qi, J.H., Claesson-Welsh, L., and Alitalo, K. (1998). Vascular endothelial growth factor C induces angiogenesis in vivo. *Proc Natl Acad Sci U S A* 95, 14389-14394.
 156. Witzenbichler, B., Asahara, T., Murohara, T., Silver, M., Spyridopoulos, I., Magner, M., Principe, N., Kearney, M., Hu, J.S., and Isner, J.M. (1998). Vascular endothelial growth factor-C (VEGF-C/VEGF-2) promotes angiogenesis in the setting of tissue ischemia. *Am J Pathol* 153, 381-394.
 157. Jeltsch, M., Kaipainen, A., Joukov, V., Meng, X., Lakso, M., Rauvala, H., Swartz, M., Fukumura, D., Jain, R.K., and Alitalo, K. (1997). Hyperplasia of lymphatic vessels in VEGF-C transgenic mice. *Science* 276, 1423-1425.
 158. Witmer, A.N., Dai, J., Weich, H.A., Vrensen, G.F., and Schlingemann, R.O. (2002). Expression of vascular endothelial growth factor receptors 1, 2, and 3 in quiescent endothelia. *J Histochem Cytochem* 50, 767-777.
 159. Saaristo, A., Veikkola, T., Tammela, T., Enholm, B., Karkkainen, M.J., Pajusola, K., Bueler, H., Yla-Herttuala, S., and Alitalo, K. (2002). Lymphangiogenic gene therapy with minimal blood vascular side effects. *J Exp Med* 196, 719-730.
 160. Dixelius, J., Makinen, T., Wirzenius, M., Karkkainen, M.J., Wernstedt, C., Alitalo, K., and Claesson-Welsh, L. (2003). Ligand-induced vascular endothelial growth factor receptor-3 (VEGFR-3) heterodimerization with VEGFR-2 in primary

- lymphatic endothelial cells regulates tyrosine phosphorylation sites. *J Biol Chem* 278, 40973-40979.
161. Kubo, H., Fujiwara, T., Jussila, L., Hashi, H., Ogawa, M., Shimizu, K., Awane, M., Sakai, Y., Takabayashi, A., Alitalo, K., Yamaoka, Y., and Nishikawa, S.I. (2000). Involvement of vascular endothelial growth factor receptor-3 in maintenance of integrity of endothelial cell lining during tumor angiogenesis. *Blood* 96, 546-553.
 162. Matsumura, K., Hirashima, M., Ogawa, M., Kubo, H., Hisatsune, H., Kondo, N., Nishikawa, S., and Chiba, T. (2003). Modulation of VEGFR-2-mediated endothelial-cell activity by VEGF-C/VEGFR-3. *Blood* 101, 1367-1374.
 163. Stacker, S.A., Williams, R.A., and Achen, M.G. (2004). Lymphangiogenic growth factors as markers of tumor metastasis. *Apmis* 112, 539-549.
 164. Regoli, M., Bertelli, E., Orazioli, D., Fonzi, L., and Bastianini, A. (2001). Pancreatic lymphatic system in rodents. *Anat Rec* 263, 155-160.
 165. Clarijs, R., Schalkwijk, L., Hofmann, U.B., Ruiten, D.J., and de Waal, R.M. (2002). Induction of vascular endothelial growth factor receptor-3 expression on tumor microvasculature as a new progression marker in human cutaneous melanoma. *Cancer Res* 62, 7059-7065.
 166. Persico, M.G., Vincenti, V., and DiPalma, T. (1999). Structure, expression and receptor-binding properties of placenta growth factor (PlGF). *Curr Top Microbiol Immunol* 237, 31-40.
 167. Maglione, D., Guerriero, V., Viglietto, G., Ferraro, M.G., Aprelikova, O., Alitalo, K., Del Vecchio, S., Lei, K.J., Chou, J.Y., and Persico, M.G. (1993). Two alternative mRNAs coding for the angiogenic factor, placenta growth factor (PlGF), are transcribed from a single gene of chromosome 14. *Oncogene* 8, 925-931.
 168. Cao, Y., Ji, W.R., Qi, P., and Rosin, A. (1997). Placenta growth factor: identification and characterization of a novel isoform generated by RNA alternative splicing. *Biochem Biophys Res Commun* 235, 493-498.
 169. Yang, W., Ahn, H., Hinrichs, M., Torry, R.J., and Torry, D.S. (2003). Evidence of a novel isoform of placenta growth factor (PlGF-4) expressed in human trophoblast and endothelial cells. *J Reprod Immunol* 60, 53-60.
 170. Park, J.E., Chen, H.H., Winer, J., Houck, K.A., and Ferrara, N. (1994). Placenta growth factor. Potentiation of vascular endothelial growth factor bioactivity, in vitro and in vivo, and high affinity binding to Flt-1 but not to Flk-1/KDR. *J Biol Chem* 269, 25646-25654.
 171. Migdal, M., Huppertz, B., Tessler, S., Comforti, A., Shibuya, M., Reich, R., Baumann, H., and Neufeld, G. (1998). Neuropilin-1 is a placenta growth factor-2 receptor. *J Biol Chem* 273, 22272-22278.
 172. DiPalma, T., Tucci, M., Russo, G., Maglione, D., Lago, C.T., Romano, A., Saccone, S., Della Valle, G., De Gregorio, L., Dragani, T.A., Viglietto, G., and Persico, M.G. (1996). The placenta growth factor gene of the mouse. *Mamm Genome* 7, 6-12.
 173. Sawano, A., Takahashi, T., Yamaguchi, S., Aonuma, M., and Shibuya, M. (1996). Flt-1 but not KDR/Flk-1 tyrosine kinase is a receptor for placenta growth factor, which is related to vascular endothelial growth factor. *Cell Growth Differ* 7, 213-221.
 174. Ziche, M., Maglione, D., Ribatti, D., Morbidelli, L., Lago, C.T., Battisti, M., Paoletti, I., Barra, A., Tucci, M., Parise, G., Vincenti, V., Granger, H.J., Viglietto, G., and Persico, M.G. (1997). Placenta growth factor-1 is chemotactic, mitogenic, and angiogenic. *Lab Invest* 76, 517-531.
 175. Clark, D.E., Smith, S.K., He, Y., Day, K.A., Licence, D.R., Corps, A.N., Lammoglia, R., and Charnock-Jones, D.S. (1998). A vascular endothelial growth factor antagonist is produced by the human placenta and released into the maternal circulation. *Biol Reprod* 59, 1540-1548.
 176. Roy, H., Bhardwaj, S., Babu, M., Jauhiainen, S., Herzig, K.H., Bellu, A.R., Haisma, H.J., Carmeliet, P., Alitalo, K., and Yla-Herttuala, S. (2005). Adenovirus-mediated gene transfer of placental growth factor to perivascular tissue induces angiogenesis via upregulation of the expression of endogenous vascular endothelial growth factor-A. *Hum Gene Ther* 16, 1422-1428.

177. Landgren, E., Schiller, P., Cao, Y., and Claesson-Welsh, L. (1998). Placenta growth factor stimulates MAP kinase and mitogenicity but not phospholipase C-gamma and migration of endothelial cells expressing Flt 1. *Oncogene* *16*, 359-367.
178. Eriksson, A., Cao, R., Pawliuk, R., Berg, S.M., Tsang, M., Zhou, D., Fleet, C., Tritsarlis, K., Dissing, S., Leboulch, P., and Cao, Y. (2002). Placenta growth factor-1 antagonizes VEGF-induced angiogenesis and tumor growth by the formation of functionally inactive PlGF-1/VEGF heterodimers. *Cancer Cell* *1*, 99-108.
179. Lutun, A., Tjwa, M., Moons, L., Wu, Y., Angelillo-Scherrer, A., Liao, F., Nagy, J.A., Hooper, A., Priller, J., De Klerck, B., Compernelle, V., Daci, E., Bohlen, P., Dewerchin, M., Herbert, J.M., Fava, R., Matthys, P., Carmeliet, G., Collen, D., Dvorak, H.F., Hicklin, D.J., and Carmeliet, P. (2002). Revascularization of ischemic tissues by PlGF treatment, and inhibition of tumor angiogenesis, arthritis and atherosclerosis by anti-Flt1. *Nat Med* *8*, 831-840.
180. Odorisio, T., Schietroma, C., Zaccaria, M.L., Cianfarani, F., Tiveron, C., Tatangelo, L., Failla, C.M., and Zambruno, G. (2002). Mice overexpressing placenta growth factor exhibit increased vascularization and vessel permeability. *J Cell Sci* *115*, 2559-2567.
181. Oura, H., Bertoncini, J., Velasco, P., Brown, L.F., Carmeliet, P., and Detmar, M. (2003). A critical role of placental growth factor in the induction of inflammation and edema formation. *Blood* *101*, 560-567.
182. Lacal, P.M., Failla, C.M., Pagani, E., Odorisio, T., Schietroma, C., Falcinelli, S., Zambruno, G., and D'Atri, S. (2000). Human melanoma cells secrete and respond to placenta growth factor and vascular endothelial growth factor. *J Invest Dermatol* *115*, 1000-1007.
183. Nomura, M., Yamagishi, S., Harada, S., Yamashima, T., Yamashita, J., and Yamamoto, H. (1998). Placenta growth factor (PlGF) mRNA expression in brain tumors. *J Neurooncol* *40*, 123-130.
184. Hatva, E., Bohling, T., Jaaskelainen, J., Persico, M.G., Haltia, M., and Alitalo, K. (1996). Vascular growth factors and receptors in capillary hemangioblastomas and hemangiopericytomas. *Am J Pathol* *148*, 763-775.
185. Parr, C., Watkins, G., Boulton, M., Cai, J., and Jiang, W.G. (2005). Placenta growth factor is over-expressed and has prognostic value in human breast cancer. *Eur J Cancer* *41*, 2819-2827.
186. Zhang, L., Chen, J., Ke, Y., Mansel, R.E., and Jiang, W.G. (2005). Expression of Placenta growth factor (PlGF) in non-small cell lung cancer (NSCLC) and the clinical and prognostic significance. *World J Surg Oncol* *3*, 68.
187. Chen, C.N., Hsieh, F.J., Cheng, Y.M., Cheng, W.F., Su, Y.N., Chang, K.J., and Lee, P.H. (2004). The significance of placenta growth factor in angiogenesis and clinical outcome of human gastric cancer. *Cancer Lett* *213*, 73-82.
188. Lindahl, P., Johansson, B.R., Leveen, P., and Betsholtz, C. (1997). Pericyte loss and microaneurysm formation in PDGF-B-deficient mice. *Science* *277*, 242-245.
189. Inoue, M., Hager, J.H., Ferrara, N., Gerber, H.P., and Hanahan, D. (2002). VEGF-A has a critical, nonredundant role in angiogenic switching and pancreatic beta cell carcinogenesis. *Cancer Cell* *1*, 193-202.
190. Grimmond, S., Lagercrantz, J., Drinkwater, C., Silins, G., Townson, S., Pollock, P., Gotley, D., Carson, E., Rakar, S., Nordenskjold, M., Ward, L., Hayward, N., and Weber, G. (1996). Cloning and characterization of a novel human gene related to vascular endothelial growth factor. *Genome Res* *6*, 124-131.
191. Olofsson, B., Jeltsch, M., Eriksson, U., and Alitalo, K. (1999). Current biology of VEGF-B and VEGF-C. *Curr Opin Biotechnol* *10*, 528-535.
192. Lagercrantz, J., Larsson, C., Grimmond, S., Fredriksson, M., Weber, G., and Piehl, F. (1996). Expression of the VEGF-related factor gene in pre- and postnatal mouse. *Biochem Biophys Res Commun* *220*, 147-152.
193. Bellomo, D., Headrick, J.P., Silins, G.U., Paterson, C.A., Thomas, P.S., Gartside, M., Mould, A., Cahill, M.M., Tonks, I.D., Grimmond, S.M., Townson, S., Wells, C., Little, M., Cummings, M.C., Hayward, N.K., and Kay, G.F. (2000). Mice lacking the vascular endothelial growth factor-B gene (*Vegfb*) have smaller hearts, dysfunctional

- coronary vasculature, and impaired recovery from cardiac ischemia. *Circ Res* 86, E29-35.
194. Aase, K., von Euler, G., Li, X., Ponten, A., Thoren, P., Cao, R., Cao, Y., Olofsson, B., Gebre-Medhin, S., Pekny, M., Alitalo, K., Betsholtz, C., and Eriksson, U. (2001). Vascular endothelial growth factor-B-deficient mice display an atrial conduction defect. *Circulation* 104, 358-364.
 195. Sun, Y., Jin, K., Childs, J.T., Xie, L., Mao, X.O., and Greenberg, D.A. (2006). Vascular endothelial growth factor-B (VEGFB) stimulates neurogenesis: evidence from knockout mice and growth factor administration. *Dev Biol* 289, 329-335.
 196. Sun, Y., Jin, K., Childs, J.T., Xie, L., Mao, X.O., and Greenberg, D.A. (2004). Increased severity of cerebral ischemic injury in vascular endothelial growth factor-B-deficient mice. *J Cereb Blood Flow Metab* 24, 1146-1152.
 197. Mould, A.W., Tonks, I.D., Cahill, M.M., Pettit, A.R., Thomas, R., Hayward, N.K., and Kay, G.F. (2003). Vegfb gene knockout mice display reduced pathology and synovial angiogenesis in both antigen-induced and collagen-induced models of arthritis. *Arthritis Rheum* 48, 2660-2669.
 198. Wanstall, J.C., Gambino, A., Jeffery, T.K., Cahill, M.M., Bellomo, D., Hayward, N.K., and Kay, G.F. (2002). Vascular endothelial growth factor-B-deficient mice show impaired development of hypoxic pulmonary hypertension. *Cardiovasc Res* 55, 361-368.
 199. Silvestre, J.S., Tamarat, R., Ebrahimian, T.G., Le-Roux, A., Clergue, M., Emmanuel, F., Duriez, M., Schwartz, B., Branellec, D., and Levy, B.I. (2003). Vascular endothelial growth factor-B promotes in vivo angiogenesis. *Circ Res* 93, 114-123.
 200. Mould, A.W., Greco, S.A., Cahill, M.M., Tonks, I.D., Bellomo, D., Patterson, C., Zournazi, A., Nash, A., Scotney, P., Hayward, N.K., and Kay, G.F. (2005). Transgenic overexpression of vascular endothelial growth factor-B isoforms by endothelial cells potentiates postnatal vessel growth in vivo and in vitro. *Circ Res* 97, e60-70.
 201. Gunningham, S.P., Currie, M.J., Han, C., Turner, K., Scott, P.A., Robinson, B.A., Harris, A.L., and Fox, S.B. (2001). Vascular endothelial growth factor-B and vascular endothelial growth factor-C expression in renal cell carcinomas: regulation by the von Hippel-Lindau gene and hypoxia. *Cancer Res* 61, 3206-3211.
 202. Lyden, D., Hattori, K., Dias, S., Costa, C., Blaikie, P., Butros, L., Chadburn, A., Heissig, B., Marks, W., Witte, L., Wu, Y., Hicklin, D., Zhu, Z., Hackett, N.R., Crystal, R.G., Moore, M.A., Hajar, K.A., Manova, K., Benezra, R., and Rafii, S. (2001). Impaired recruitment of bone-marrow-derived endothelial and hematopoietic precursor cells blocks tumor angiogenesis and growth. *Nat Med* 7, 1194-1201.
 203. Wey, J.S., Fan, F., Gray, M.J., Bauer, T.W., McCarty, M.F., Somcio, R., Liu, W., Evans, D.B., Wu, Y., Hicklin, D.J., and Ellis, L.M. (2005). Vascular endothelial growth factor receptor-1 promotes migration and invasion in pancreatic carcinoma cell lines. *Cancer* 104, 427-438.
 204. Fan, F., Wey, J.S., McCarty, M.F., Belcheva, A., Liu, W., Bauer, T.W., Somcio, R.J., Wu, Y., Hooper, A., Hicklin, D.J., and Ellis, L.M. (2005). Expression and function of vascular endothelial growth factor receptor-1 on human colorectal cancer cells. *Oncogene* 24, 2647-2653.
 205. Yang, A.D., Camp, E.R., Fan, F., Shen, L., Gray, M.J., Liu, W., Somcio, R., Bauer, T.W., Wu, Y., Hicklin, D.J., and Ellis, L.M. (2006). Vascular endothelial growth factor receptor-1 activation mediates epithelial to mesenchymal transition in human pancreatic carcinoma cells. *Cancer Res* 66, 46-51.
 206. Oberg, C., Waltenberger, J., Claesson-Welsh, L., and Welsh, M. (1994). Expression of protein tyrosine kinases in islet cells: possible role of the Flk-1 receptor for beta-cell maturation from duct cells. *Growth Factors* 10, 115-126.
 207. Gorden, D.L., Mandriota, S.J., Montesano, R., Orci, L., and Pepper, M.S. (1997). Vascular endothelial growth factor is increased in devascularized rat islets of Langerhans in vitro. *Transplantation* 63, 436-443.
 208. Christofori, G., Naik, P., and Hanahan, D. (1995). Vascular endothelial growth factor and its receptors, flt-1 and flk-1, are expressed in normal pancreatic islets and throughout islet cell tumorigenesis. *Mol Endocrinol* 9, 1760-1770.

209. Compagni, A., Wilgenbus, P., Impagnatiello, M.A., Cotten, M., and Christofori, G. (2000). Fibroblast growth factors are required for efficient tumor angiogenesis. *Cancer Res* 60, 7163-7169.
210. Folkman, J. (2002). Role of angiogenesis in tumor growth and metastasis. *Semin Oncol* 29, 15-18.
211. Thiery, J.P. (2002). Epithelial-mesenchymal transitions in tumour progression. *Nat Rev Cancer* 2, 442-454.
212. Katoh, O., Tauchi, H., Kawaishi, K., Kimura, A., and Satow, Y. (1995). Expression of the vascular endothelial growth factor (VEGF) receptor gene, KDR, in hematopoietic cells and inhibitory effect of VEGF on apoptotic cell death caused by ionizing radiation. *Cancer Res* 55, 5687-5692.
213. Soldi, R., Mitola, S., Strasly, M., Defilippi, P., Tarone, G., and Bussolino, F. (1999). Role of alphavbeta3 integrin in the activation of vascular endothelial growth factor receptor-2. *Embo J* 18, 882-892.
214. Hutchings, H., Ortega, N., and Plouet, J. (2003). Extracellular matrix-bound vascular endothelial growth factor promotes endothelial cell adhesion, migration, and survival through integrin ligation. *Faseb J* 17, 1520-1522.
215. Carmeliet, P., Lampugnani, M.G., Moons, L., Breviario, F., Compernelle, V., Bono, F., Balconi, G., Spagnuolo, R., Oostuyse, B., Dewerchin, M., Zanetti, A., Angellilo, A., Mattot, V., Nuyens, D., Lutgens, E., Clotman, F., de Ruiter, M.C., Gittenberger-de Groot, A., Poelmann, R., Lupu, F., Herbert, J.M., Collen, D., and Dejana, E. (1999). Targeted deficiency or cytosolic truncation of the VE-cadherin gene in mice impairs VEGF-mediated endothelial survival and angiogenesis. *Cell* 98, 147-157.
216. Whitaker, G.B., Limberg, B.J., and Rosenbaum, J.S. (2001). Vascular endothelial growth factor receptor-2 and neuropilin-1 form a receptor complex that is responsible for the differential signaling potency of VEGF(165) and VEGF(121). *J Biol Chem* 276, 25520-25531.
217. Hong, Y.K., Lange-Asschenfeldt, B., Velasco, P., Hirakawa, S., Kunstfeld, R., Brown, L.F., Bohlen, P., Senger, D.R., and Detmar, M. (2004). VEGF-A promotes tissue repair-associated lymphatic vessel formation via VEGFR-2 and the alpha1beta1 and alpha2beta1 integrins. *Faseb J* 18, 1111-1113.
218. Nagy, J.A., Vasile, E., Feng, D., Sundberg, C., Brown, L.F., Detmar, M.J., Lawitts, J.A., Benjamin, L., Tan, X., Manseau, E.J., Dvorak, A.M., and Dvorak, H.F. (2002). Vascular permeability factor/vascular endothelial growth factor induces lymphangiogenesis as well as angiogenesis. *J Exp Med* 196, 1497-1506.
219. Jain, R.K. (2002). Tumor angiogenesis and accessibility: role of vascular endothelial growth factor. *Semin Oncol* 29, 3-9.
220. Lacal, P.M., Ruffini, F., Pagani, E., and D'Atri, S. (2005). An autocrine loop directed by the vascular endothelial growth factor promotes invasiveness of human melanoma cells. *Int J Oncol* 27, 1625-1632.
221. Byzova, T.V., Goldman, C.K., Pampori, N., Thomas, K.A., Bett, A., Shattil, S.J., and Plow, E.F. (2000). A mechanism for modulation of cellular responses to VEGF: activation of the integrins. *Mol Cell* 6, 851-860.
222. Lyttle, D.J., Fraser, K.M., Fleming, S.B., Mercer, A.A., and Robinson, A.J. (1994). Homologs of vascular endothelial growth factor are encoded by the poxvirus orf virus. *J Virol* 68, 84-92.
223. Ogawa, S., Oku, A., Sawano, A., Yamaguchi, S., Yazaki, Y., and Shibuya, M. (1998). A novel type of vascular endothelial growth factor, VEGF-E (NZ-7 VEGF), preferentially utilizes KDR/Flk-1 receptor and carries a potent mitotic activity without heparin-binding domain. *J Biol Chem* 273, 31273-31282.
224. Wise, L.M., Veikkola, T., Mercer, A.A., Savory, L.J., Fleming, S.B., Caesar, C., Vitali, A., Makinen, T., Alitalo, K., and Stacker, S.A. (1999). Vascular endothelial growth factor (VEGF)-like protein from orf virus NZ2 binds to VEGFR2 and neuropilin-1. *Proc Natl Acad Sci U S A* 96, 3071-3076.
225. Meyer, M., Clauss, M., Lepple-Wienhues, A., Waltenberger, J., Augustin, H.G., Ziche, M., Lanz, C., Buttner, M., Rziha, H.J., and Dehio, C. (1999). A novel vascular endothelial growth factor encoded by Orf virus, VEGF-E, mediates angiogenesis via

- signalling through VEGFR-2 (KDR) but not VEGFR-1 (Flt-1) receptor tyrosine kinases. *Embo J* 18, 363-374.
226. Wise, L.M., Ueda, N., Dryden, N.H., Fleming, S.B., Caesar, C., Roufail, S., Achen, M.G., Stacker, S.A., and Mercer, A.A. (2003). Viral vascular endothelial growth factors vary extensively in amino acid sequence, receptor-binding specificities, and the ability to induce vascular permeability yet are uniformly active mitogens. *J Biol Chem* 278, 38004-38014.
227. Haig, D.M., and Mercer, A.A. (1998). Ovine diseases. *Orf. Vet Res* 29, 311-326.
228. Mercer, A., Fleming, S., Robinson, A., Nettleton, P., and Reid, H. (1997). Molecular genetic analyses of parapoxviruses pathogenic for humans. *Arch Virol Suppl* 13, 25-34.
229. Groves, R.W., Wilson-Jones, E., and MacDonald, D.M. (1991). Human orf and milkers' nodule: a clinicopathologic study. *J Am Acad Dermatol* 25, 706-711.
230. Makinen, T., Olofsson, B., Karpanen, T., Hellman, U., Soker, S., Klagsbrun, M., Eriksson, U., and Alitalo, K. (1999). Differential binding of vascular endothelial growth factor B splice and proteolytic isoforms to neuropilin-1. *J Biol Chem* 274, 21217-21222.
231. Heil, M., Mitnacht-Krauss, R., Issbrucker, K., van den Heuvel, J., Dehio, C., Schaper, W., Clauss, M., and Weich, H.A. (2003). An engineered heparin-binding form of VEGF-E (hbVEGF-E). Biological effects in vitro and mobilization of precursor cells. *Angiogenesis* 6, 201-211.

7. Curriculum Vitae

Name	Lucie Kopfstein
Date and place of birth	November 17, 1976, Brandýs nad Labem, Czech Republic
Nationality	Swiss, Czech
Education	
2003-present	MD PhD thesis research at the Institute of Biochemistry and Genetics, University of Basel, research group of Prof. Gerhard Christofori
2002	Three-year MD PhD Program Fellowship of the Swiss National Science Foundation (SNF) (150'000 CHF)
1999	Medical thesis at the Institute of Clinical Pathology and Molecular Biology, University Medical Center of Geneva, research group of Prof. Bettina Borisch „Mutational analysis of Bcl-10, a gene involved in t(1;14)(p22;q32) associated with MALT-B-cell Non Hodgkin Lymphomas“. MD degree at the University of Basel in 2005.
1996-2002	MD studies at the Medical Faculties of the University of Basel (1996-98 and 1999-2002) and the University of Geneva (1998-99). Graduation at the University of Basel 2002.
1989-1996	Stiftsschule Einsiedeln SZ, Matura Typus B
1983-1989	Elementary School, Freienbach and Pfäffikon SZ

8. Conferences

Oral presentations

- 2005 Gordon Research Conference on Angiogenesis and Microcirculation, Salve Regina University, Newport, RI, USA
- 12th Annual European Cancer Center Symposium on Clinical and Experimental Oncology (EuCC), University Hospital Basel, Basel, Switzerland

Poster presentations

- 2005 MVA Ascona, Tumor-Host Interaction and Angiogenesis: Basic Mechanisms and Therapeutic Perspectives, Monte Verità, Ascona, Switzerland
- 2004 MD PhD Meeting Leuenberg, Hölstein, Switzerland

9. Publications

Kopfstein L, Veikkola T, Djonov VG, Baeriswyl V, Schomber T, Strittmatter K, Stacker S, Achen MG, Alitalo K, Christofori G (2006) Vascular endothelial growth factor-D-mediated lymphangiogenesis promotes lymph node and lung metastasis. (submitted)

Kopfstein L and Christofori G (2006) Metastasis: cell-autonomous mechanisms versus contributions by the tumor microenvironment. *Cell Mol Life Sci* 63: 449-468.

Crnic I, Strittmatter K, Cavallaro U, Kopfstein L, Jussila L, Alitalo K and Christofori G (2004) Loss of neural cell adhesion molecule induces tumor metastasis by up-regulating lymphangiogenesis. *Cancer Res* 64: 8630-8638.

10. Acknowledgements

I would like to thank my supervisor Gerhard Christofori for giving me the possibility to join his lab of “real” scientists. I am grateful for his support and confidence as well as for giving me the opportunity to participate in international conferences, which allowed me to get more insight into the world of research. Furthermore, I thank all the former and present lab colleagues for their friendly help and company. I explicitly thank:

- Ivana Crnic for accompanying me on my first steps in the mouse world and introducing various staining techniques to me.
- Miguel Cabrita, who showed me how to turn on the computer in the first place and how to fix my Mac and printer problems later on – his patience is unsurpassed! I thank him also for teaching me the basics of cloning and for reading my paper and review drafts.
- Tibor Schomber, my one-year bench-neighbor, who extended my biological understanding and german colloquial language. Thanks for your scientific input and entertaining company.
- Karin Strittmatter, who always found the time to help me out whenever I was badly organized. I will miss her calm and cordial support (particularly in the near future!).
- Ursula Schmieder for genotyping my mice and Helena Antoniadis for cutting innumerable slides for me.
- Pascal Lorentz, who analyzed the Rip1VEGF-C156S mice in more detail and helped Karin and me with the Rip1VEGF-B₁₆₇ mice.
- Roland Jost for taking care of my hundreds of mice and being a great company in the mousehouse.
- Angie Kren and Fabienne Jaeggi, for sharing “the good and the bad times”, cigarettes, voodoo and much more!

Finally I thank Thomas for his patience and love and my parents for their unconditional support over the last *almost* 30 years. Miluji vás!

11. Declaration of Independence

I declare that I wrote this thesis “The role of distinct VEGF family members in Rip1Tag2 tumorigenesis” with the help indicated and only handed it in to the faculty of science of the University of Basel and to no other faculty and no other university.